The gut commensal microbiome remotely regulates mammary tissue mast cells to induce metastatic dissemination of HR^+ breast cancer

Tzu-Yu (Alkaid) Feng
Taoyuan, Taiwan

M.S. National Taiwan University 2015

A Dissertation presented to the Graduate Faculty of the University of Virginia in Candidacy for the Degree of Doctor of Philosophy

Department of Microbiology, Immunology and Cancer Biology

University of Virginia
July, 2022

Acknowledgement

I feel incredibly fortunate to receive doctoral training at University of Virginia. I cannot be more grateful to be immersed in such a resourceful environment provided by Biomedical Sciences Graduate Program and Department of Microbiology, Immunology, Cancer Biology and within School of Medicine. I would like to thank the Carter Immunology Center, Comprehensive Cancer Center, and TransUniversity Microbiome Initiative for providing funding and extensive training environment for me to become a scientist in the field of cancer immunology. During my graduate study, I was extremely lucky to receive thoughtful advice and brilliant insights from my dissertation committee: Dr. Andrew C. Dudley (chairperson), Dr. Amy H. Bouton, Dr. Timothy N.J. Bullock, and Dr. Daniel Gioeli. I deeply appreciate the time and effort they put into our committee meetings.

Most importantly, I would like to thank my mentor, Dr. Melanie R. Rutkowski for supporting me in the past years. She has not only taught me critical thinking, but also showed me the resilience, diligence, kindness, and wisdom on a daily basis. I am deeply grateful for having the opportunity to perform research in the Rutkowski lab. She is a scientific mentor, a life coach, and a role model for me. I will miss our meetings and discussions a lot.

I am extremely lucky to have great support from the former and current lab members. Especially, I would like to thank Francesca N. Azar for her intellectual and technical inputs in my study. Most importantly, her priceless friendship always made those difficult times much easier. Dr. Claire Buchta Rosean and Raegan R. Bostic guided me to learn the techniques of performing animal studies. Without the great foundation they established, I would never have the chance to achieve the mast cell study. Mitchell T. McGinty, Audrey M. Putelo, and Sree H. Kolli have supported me through those 20- to 40-mice experiments. I was incredibly lucky to work with these fantastic and brilliant people. I have learned a lot from these people and am very grateful for that. I will miss those days when we worked together.

I would also want to thank friends and collaborators outside of the Rutkowski lab. Dr. Sally Dreger and Dr. Stephen Robinson greatly helped us investigate the clinical relevance of our findings; Dr. Maureen Carey and Dr. Eugene Ke helped me perform biostatistical analysis; Dr. Sanja Arandjelovic gave us her constructive and critical thoughts on the mast cell study; Dr. James McCann, Dr. Luca Musante, and Dr. Uta Erdbruegger provided resources and advice for our EV study; Keena Tomas kindly taught me to establish mammary organoid culture system; Jamie L. Null, Dr. Yu-Hsin (Eva) Chu, Dr. Jessica Hung, and Philip V. Seegren kindly shared valued resources and knowledge. Their instructions and assistance greatly helped me achieve better science.

Lastly, I would like to thank my friends and family who supported me along the way. Specifically, all the Taiwanese and Germany friends I met through Taiwanese Graduate Student Association really made Charlottesville as my second home. Last but not least, I would also like to thank Ms. Ming-Chin (Maggie) Chen for her continuous support. She has treated me like her own daughter. Her encouragement and trust were the initiations of my great journey at UVa. I am so grateful to have all of these people in my life!

Table of Contents

Table of Figures and Tables

Abstract

Metastatic breast cancer is a treatable but uncurable disease. Around 75% of patients with metastatic breast cancer were diagnosed with hormone-receptor positive (HR^+) breast tumors, highlighting the need to further define the factors that enable metastatic dissemination of HR^+ breast cancer cells. According to the recent epidemiological results, HR^+ breast cancer patients experienced heterogeneous outcomes, despite receiving comparable treatments. These data raise the possibility that tumor-independent factors influence metastatic capacity of HR^+ tumor cells.

Our recently published study revealed that commensal dysbiosis, defined as an inflammatory gut microbiome with low biodiversity, established prior to breast tumor initiation enhances dissemination of HR^+ tumor cells. Our study demonstrated that the gut commensal microbiome is a host-intrinsic factor that influences the metastatic behavior of mammary tumor cells. However, the cellular and molecular mechanisms underlying dysbiosis-induced tumor dissemination remain unknown.

In this dissertation, we sought to identify how cellular changes in mammary tissues that arise in response to gut commensal dysbiosis enhance dissemination of HR^+ breast tumor cells. Utilizing multiplex flow cytometry and histological approaches, we determined that gut commensal dysbiosis increases the abundance and profibrogenicity of mast cells in normal mammary tissues. Coupling pharmacological inhibitors and adoptive transfer approaches, we demonstrated that mammary tissue-associated mast cells from non-tumor-bearing dysbiotic mice are sufficient to induce HR^+ tumor dissemination. The collagen levels in adjacent mammary tissues from HR^+ breast cancer patients are positively correlated with mast cell density and tumor recurrence, supporting the idea that mast cell-mediated fibrosis in mammary tissues contributes to poor outcomes in HR^+ breast cancer patients. This study illuminates how crosstalk occurring between the gut microbiome and mammary tissue lead to preconditioning of tissue-associated mast cells to increase HR^+ tumor dissemination. These findings will allow for an in-depth knowledge of the role of commensal microbiome in the early dissemination of HR^+ breast tumor cells with the ultimate goal of developing therapeutic strategies to reduce metastasis in HR^+ breast cancer patients.

Chapter 1: Introduction

1.1 Metastatic breast cancer-disease overview

1.1.1 Epidemiology

Breast cancer is the second most common cause of cancer-related mortality for women in the United States[1]. It is estimated that 44,130 people (43,600 women and 530 men) died from breast cancer in 2021[1]; the majority of cancer-related death was caused by metastasis to distal organs, such as bones, liver, lung, and brain[2]. Breast cancers are classified into four molecular subtypes based on expression of hormone-receptors (HR; estrogen-receptor and progesterone-receptor) and human epidermal growth factor receptor 2 (HER2). HR^+ (ER- and/or PR-positive) breast cancer accounts for approximately 60% of total breast cancers and can be sub-categorized into luminal A and luminal B, based on HER2 expression (Luminal A: HR-positive and HER2-negative; Luminal B: HR-positive and HER2-positive). Hormone receptor negative subtypes are further subcategorized into HR-negative/HER2-positive ($HER2^+$) breast cancer, which represents around 20% of breast cancer patients while triple-negative breast cancer (TNBC, ER-, PR, and HER2-negative) constitutes around 20% of breast cancer cases. Therapeutic treatment strategies are based upon the molecular profile of breast tumors, due to the discovery of therapeutic vulnerabilities for $HER2^+$ and HR^+ subtypes[3]. In clinical settings, HR^+ breast cancer patients are likely to benefit from adjuvant or neoadjuvant hormone therapies; $HER2^+$ breast cancer patients are more likely to respond HER2-targeted therapies. Unlike HR^+ and $HER2^+$ breast cancer, no targeted therapies for TNBC exist. Because of this, patients are generally treated with untargeted systemic chemotherapies, reducing the efficacy of treatment for this breast cancer subtype[4].

Despite targeted therapies for HR^+ breast cancer, it is not a guarantee that treatment will improve patient outcomes[4]. The 4-year survival rate among HR^+ breast cancer patients is estimated to be around 90%, $HER2^+$ at 82.7%, and TNBC at 77%[5]. Although patients with HR^+ breast tumors typically have more favorable outcomes, the epidemiological data from the SEER study indicates that most metastatic breast cancer patients were previously diagnosed with HR^+ tumors (61.2% $HR^+/HER2^-$ and 14.8% $HR^+/HER2^+$)[6]. These epidemiological results highlight the need to optimize current diagnostic and therapeutic strategies for the prevention of metastatic breast cancer.

1.1.2 Limitation of current prognostic strategies

Metastatic dissemination of breast tumor cells begins during early stages of disease progression[7], even prior to diagnosis[8]. Nodal metastasis is one of the most reliable prognostic indicators for risk of recurrence. However, nodal metastasis is not sufficient to predict risk for metastasis beyond 10 years post-diagnosis. Recurrence rates for patients, regardless of lymph node involvement, are similar after 10 years post diagnosis[9]. This indicates the necessity to identify additional prognostic markers for predicting metastatic risk in patients with HR^+ breast tumors. Liquid biopsies and the detection of circulating tumor cells[10] and cell-free tumor-associated DNA/miRNA[11] have emerged as novel alternative biomarkers, both demonstrating accurate prediction for risk of metastatic disease. One area which could yield novel and more reliable indicators of metastasis risk is to understand why some patients develop metastatic disease whereas others do not[12].

1.1.3 Tissue microenvironment may be the key of understanding the heterogeneity of outcomes for HR$^+$ breast cancer

According to the TAILORx trial, HR$^+$ breast cancer patients with similar breast cancer subtypes and disease burden and who have received similar treatments still experience heterogeneous outcomes[13]. This suggests that the tumor size and the current understanding of tumor molecular subtypes do not fully decipher the aggressiveness of cancer cells. Tumor cells do not exist in isolation, but reside in a complex tissue microenvironment that regulates growth, egress, and metastatic dissemination. Multiple studies have demonstrated that differences in the tumor microenvironment affect breast cancer outcomes. However, a growing body of evidence indicates that transcriptomic changes, such as lipid metabolism genes and epigenetic changes favoring tumor progression or metastasis are also present in the adjacent mammary tissues[14], even prior to breast cancer diagnosis[15]. An alternative possibility suggested by these transcriptomic results is that tumor-independent host-intrinsic changes in the adjacent tissue exist that facilitate the progression of breast cancer. More importantly, it also raises an interesting hypothesis that heterogeneity in the mammary tissue microenvironment contributes to variable outcomes for patients diagnosed with HR$^+$ breast cancer.

Immune cells play a crucial role in the regulation of tumor progression. It is becoming clear that the tissue and systemic microenvironment can greatly influence the plasticity and the function of immune cells. For example, an adoptive transfer experiment of innate lymphoid cells (ILCs) revealed that retinoic acid-receptor-related orphan receptor (ROR)γt-dependent ILCs phenotypically adapt to the local tissue environment they

invade[16]. By co-injecting ILCs and B16 melanoma, Nussbaum *et al.* demonstrated that splenic (ROR)γt-dependent ILCs can suppress the growth of B16 melanoma, whereas intestinal (ROR)γt-dependent ILCs fail to restrain the tumor growth[16]. Anti-tumor immunity can also be changed due to physiological conditions, such as obesity. Increased levels of leptin, an adipose cell-derived protein, enhances expression of programmed cell death protein-1 (PD-1) on T cells, leading to T cell dysfunction in the tumor microenvironment of mammary- or melanoma tumor-bearing mice[17]. Both leptin and PD-1 ligation facilitate STAT3 signaling in cytotoxic T cells, resulting in increased fatty acid oxidation and decreased glycolysis[18]. As a result, the leptin/PD-1/STAT3 axis-induced cytotoxic T cell dysfunction reduces infiltration of tumors with T cells, decreases interferon-γ and granzyme B production, and reduces T cell-mediated tumor control[18]. This is because increased PD-1 expression on T cells is associated with better response to anti-PD-1 therapy. Leptin-induced PD-1 may explain why obesity is associated with better outcomes upon anti-PD-1 therapy in melanoma, colorectal cancer, and non-small cell lung cancer[17, 19, 20]. These data support the idea that host-intrinsic factor(s) may contribute to heterogeneous outcomes in cancer patients. Importantly, mounting evidence suggests the changes in the mammary tissue compartment before[15] or during[14, 21] breast cancer diagnosis influence the metastatic behavior of breast tumor cells. These studies support our hypothesis that pre-existing changes in the mammary tissue environment can influence the outcomes of breast cancer. Furthermore, we hypothesize that identifying how cellular or molecular changes arise in the mammary tissues prior to tumor diagnosis could pave the way towards uncovering more accurate prognostic markers for predicting risk for HR^+ breast tumor metastasis.

1.2 Microbiota: a new player in the field of cancer biology

There are trillions of bacteria, viruses, fungi, archaea, and protozoa that reside in and on the body. The numbers of microbes are approximately equal to that of human cells[22], underscoring the close relationship that we have with our commensal cohabitants. Bacteria account for the majority of commensal microorganisms residing at our barrier surfaces, with the gut having the greatest biomass of commensals. The gut microbiome composition can be regulated by multiple endogenous and exogenous factors, including maternal factors[23], delivery method[24], host genetics[25, 26], environmental exposures[27-29], diet[30, 31], host immune activity[32], and medicine[33, 34]. In the past two decades, transcriptomic, proteomic, and metabolomic techniques have greatly expanded our knowledge of microbial genes and their products. Although the majority of the microbial functions remain unclear, it has been demonstrated that the microbiome critically affects multiple aspects of host physiology, including education and function of the immune system[35], host metabolism[36], neurodevelopment[37], and behavior[38]. Of relevance to breast cancer, some commensal bacteria can remove the glucuronide moiety from conjugated estrogen, resulting in increased the reabsorption of estrogen into circulation and resulting in enhanced risk of estrogen-dependent malignancies, such as HR^+ breast cancer[39]. Indeed, short-term use of the broad-spectrum antibiotic ampicillin leads to increased estrogen excretion in feces of women[40-42]. These studies suggest that short-term use of certain antibiotics may decrease the risk of HR^+ breast cancer by facilitating the excretion of estrogen, however, the long-term effect of antibiotics treatment on breast cancer remains controversial.

Increased inflammation in mammary tissues is observed in animals with pro-inflammatory microbiota, also known as commensal dysbiosis. Dysbiosis is caused by use of antibiotics[43], age[44], poor diet[45], and a variety of other factors. For breast cancer, increased inflammation is positively associated with increased tumorigenesis and enhanced tumor growth[46] . Using fecal microbiota transplantation (FMT), we have shown that a dysbiotic microflora is sufficient to increase the dissemination of HR^+ breast tumor cells in animals, and that this occurred due to increased inflammation systemically and within the tissue environment[43, 47]. These studies demonstrate that gut commensal microbiota distally regulate the invasiveness of HR^+ breast cancer through regulation of immune homeostasis of the mammary tissue microenvironment.

1.2.1 Gut commensal microbiota as a cornerstone of host immunity

Unlike conventionally raised specific pathogen-free (SPF) mice, germ-free (GF) mice do not have detectable microorganisms in or on their body. By comparing the immunological phenotype in SPF mice, researchers found that GF mice have multiple immune defects, including reduced numbers of intestinal T cells[48], impaired T cell differentiation at the intestinal mucosa[48], decreased production of immunoglobulin A (IgA) in the gut[49, 50], and increased immunoglobulin E (IgE) in serum and intestine[51]. Many of these defects can be rescued by transferring a fecal microbiota from mice or humans, highlighting the importance of gut microbiome in modulating the host immunity[52] .

Short-chain fatty acids (SCFAs), products of bacterial fermentation of indigestible polysaccharides, are one category of microbiome-derived metabolites in regulating the homeostasis of host immunity. The majority of microbiome-derived SCFAs are acetate, propionate, and butyrate in an approximately molar ratio of 3:1:1, respectively[53]. Following their production, SCFAs are transported into the portal circulation via colonocytes resulting in the regulation of host immunity. For instance, Furusawa *et al.* showed that bacterial-derived butyrate is sufficient to induce colonic regulatory T cells (Treg) via promoting the H3 acetylation of *Foxp3*[54] (Figure 1.1). Later, Park *et al*. further demonstrated that the activity of histone deacetylase (HDAC) in T cells can be inhibited by exogenous SCFAs, resulting in mTOR-S6K pathway-dependent differentiation of type 1 T helper cells (Th1), type 17 T helper cells (Th17), and Tregs[55] (Figure 1.1). Microbiome-derived SCFAs do not only impact T cell homeostasis, but also influence innate immunity. For instance, it is reported that the butyrate-GPR109a axis reduces pro-inflammatory properties in colonic macrophages and dendritic cells[56].

Microbe-associated molecular patterns (MAMPs) from gut commensals are also involved in maintaining host immune functions. Polysaccharide A (PSA) from *Bacteroides fragilis*, a prevalent component in mammalian intestinal microbiota, can directly interact with host immune cells via toll-like receptor 2 (TLR2). Round *et al.* showed that the direct interaction between *B. fragilis*-derived PSA and TLR2 on Tregs promotes immune tolerance[57] (Figure 1.1). Later, Dasgupta *et al.* further demonstrated that PSA can indirectly induces Tregs in the lamina propria[58]. Mechanistically this occurred due to PSA-activated plasmacytoid dendritic cells (pDC) inducing IL-10-expressing T regs[58]. Using 2,4,6-

trinitrobenzenesulfonic acid-induced colitis, Dasgupta *et al.* observed that the PSA/pDC/Treg axis is sufficient to restrain intestinal inflammation in animals[58] (Figure 1.1).

Importantly, the gut commensal microbiome can influence hematopoiesis and immune responses beyond the gastrointestinal tract. Germ free mice have diminished hematopoietic stem and progenitor cells (HSPCs) within the bone marrow, which can be restored by systemic administration of the nucleotide-binding oligomerization domain-containing protein 1 (NOD-1) agonist, γ-d-glutamyl-meso-diaminopimelic acid (iE-DAP)[59] (Figure 1.1). As expected, the diminished HSPC pool results in systemically reduced myeloid cells in the spleens and livers of GF animals[60]. The diminished abundance of monocytes, macrophages, and neutrophils in GF mice can be rescued by orally administering cecal slurries from SPF mice or MAMPs from heat-killed *Escherichia coli* strain Nissle; therefore, improving the resistance to the infection of *Listeria monocytogenes* in GF animals[60]. Furthermore, Balmer *et al.* demonstrated that the gut microbiome facilitates acute infection-induced "emergent granulopoiesis" in bone marrow through toll-like receptor (TLR) signaling[61]. Although it is not fully clear how the gut microbiome systemically regulates the immune system, these aforementioned results suggest that the microbiome-derived MAMPs translocate from the gut to systemic tissues, directly modulating immune cells at steady state and during disease. Indeed, commensal-derived microbial components have been detected in breast[62, 63], ovary[63], lung[63, 64], and mesenteric lymph node[65] tissues from humans. In the setting of cancer, tumor-induced inflammation and anti-tumor therapies are linked to increased intestinal permeability[66],

which can further enhance microbial translocation from the intestinal lumen to systemic tissues[67]. Inoculating animals with fluorescently-labeled microbes through oral administration will be a compelling strategy to investigate the dynamic interactions between immune cells and translocated microorganisms at systemic sites before and during cancer progression.

Unsurprisingly, the findings that commensal microorganisms regulate immune homeostasis and host immunity have ignited a great interest in the field of caner immunology. I will discuss the major findings of how gut commensal microbiome-derived factors influence tumors and anti-tumor therapies in the section of 1.2.2.

1.2.2 Gut microbiome-derived metabolites modulate tumor progression and anti-tumor immunity

1.2.2.1 SCFAs

Because microbiome-derived SCFAs influence innate and adaptive immunity, the question remains as to whether measuring the concentration of SCFAs could be used as a prognostic marker for clinical outcomes. Fecal SCFAs are swiftly absorbed by colonocytes in a concentration-dependent manner, potentiating changes to tumor-associated immune cells in distal tissue sites. Recently, Nomura *et al.* measured the concentrations of SCFAs in feces and plasma from 52 patients with melanoma, head-and-neck carcinoma, gastrointestinal carcinoma, renal cell carcinoma, urothelial carcinoma, lung carcinoma, or sarcoma[68]. All the samples were collected prior to anti-

PD-1 treatment. Although the sample size was small for each tumor type, Nomura and colleagues found that certain SCFAs in the plasma and feces correlated with longer progression-free survival[68]. Interestingly, the patients who responded to PD-1 blockade therapy had higher concentrations of the SCFAs acetate, propionate, butyrate, and valerate in their feces whereas propionate and isovaleric acid were elevated in the plasma[68]. The positive correlation between SCFA concentration and therapeutic efficacy of PD-1 blockade therapy may be due to the ability of SCFAs to inhibit HDAC signaling, which increases PD-L1 and PD-L2 expression on tumor cells[69]. On the other hand, the increased levels of butyrate and propionate are associated with resistance to blockade of CTLA4 for patients with metastatic melanoma due to increased proportions of Tregs in peripheral blood and subsequent reduced accumulation of effector and memory T cells[70]. Together, these clinical results suggest that the influence of SCFAs on the efficacy of immune checkpoint blockade is context-dependent.

Accumulating data suggest that SCFAs reduce aggressiveness of HR^- breast tumors, but little is known as to the effects of SCFAs on HR^+ breast cancer outcomes. In a transgenic model of HER2 breast cancer, the levels of plasma SCFAs negatively associate with the development of spontaneous mammary tumors[71]. By overexpressing the SCFA receptors FFAR2 and FFAR3 on the mesenchymal-like TNBC breast cancer cell line MDA-MB-231 and epithelial-like breast cancer cell line MCF7, Thirunavukkarasan *et al.* found that signaling via FFAR2 and FFAR3 significantly inhibits the invasiveness of MDA-MB-231 in vitro, whereas no effects were observed in the less invasive MCF7 cell line[72]. These studies suggest that SCFAs have the ability to directly regulate tumor cell invasiveness

and growth for TNBC breast tumor cell lines. Considering the direct and indirect impact of SCFAs on tumor invasiveness and the paradoxical protective effects that dietary fiber has in breast cancer[73], it would be interesting to test whether SCFAs affect anti-tumor immunity.

1.2.2.2 Bile acids

Bile acids are amphipathic products of cholesterol metabolism and function as physiological detergents[74]. Primary bile acids synthesized by hepatocytes are cholic and chenodeoxycholic acid, which are predominately conjugated to glycine or taurine. Whereas most bile acids in humans are glycine-conjugated bile acids, in mice, the majority are taurine-conjugated. After synthesis, primary bile acids are transported into the intestinal duct, where gut commensal bacteria convert the primary bile acids into secondary bile acids, such as deoxycholic acid and lithocholic acid. In the upper small intestine, bile acids emulsify fats facilitating the absorption of hydrophobic nutrients after which 95% of bile acids are reabsorbed, and transported back into enterohepatic circulation and peripheral blood after participating in the process of lipid digestion[74].

The positive correlation of breast cancer risk and metabolic disorders[75] is usually associated with dysregulated bile acid homeostasis[76], suggesting that the bile acids regulate breast tumor progression and outcomes. Currently, the influence of bile acids remains controversial. In a small breast cancer cohort (N=67), Tang *et al.* demonstrated that higher levels of intratumoral glycochenodeoxycholic acid (GCDC) associated with

longer survival and signaling pathways that inhibit tumor growth[77]. The authors also showed that the treatment with high concentrations of GCDC (100 μmol/L) inhibited proliferation of the human HR^+ breast cancer cell line MCF7 *in vitro*[77]. However, an earlier study demonstrated that GCDC stimulated MCF7 proliferation at the same concentration[78]. Notably, the growth of MCF7 was not affected by 10 or 50 μmol/L of GCDC, which is closer to the biological concentration of intratumoral GCDC (1.8 μmol/L). Besides GCDC, the role of chenodexoycholic acid (CDCA) for HR^+ breast cancer is also controversial. Whereas Alasmael *et al.* demonstrated that CDCA induced apoptosis and autophagy in MCF7[79], Journe *et al.* found that CDCA did not affect viability of MCF7 or cell proliferation in similar conditions[80]. Interestingly, Journe *et al.* showed that CDCA can induce the proliferation of MCF7 in the presence of estrogen[80]. Similarly, a positive correlation between intratumoral bile acid receptor farnesoid X receptor (FXR) and estrogen receptor (ER)/luminal markers in patients was found, suggesting that the effects of estrogen signaling and bile acid signaling may be linked.

In addition to the direct impact of bile acids on tumor cell viability and proliferation, emerging evidence suggests that the microbiome/bile acid/FXR axis can also affect anti-tumor immunity. For instance, increased levels of CDCA in vancomycin-treated mice enhance recruitment of tumoricidal natural killer T (NKT) cells in a CXCL16/CXCR6-dependent manner for hepatocellular carcinoma[81] (Figure 1.1). Vancomycin targets gram-positive bacteria such as *Clostridium*, which are involved in the conversion of primary bile acids (ex: CDCA) into secondary bile acids (ex: lithocholic acid)[82]. The accumulation of CDCA induced CXCL16 in liver sinusoidal endothelial cells induced the

recruitment of CXCR6$^+$ NKT cells[81]. Additionally, bile acid/FXR signaling can enhance the expression of either anti-inflammatory or pro-inflammatory mediators from dendritic cells (DC), monocytes, macrophages, myeloid-derived suppressor cells (MDSC), B cells, and T cells[83], all of which infiltrate normal and malignant mammary tissues[84, 85]. Indeed, multiple bile acids were detected in breast tumors and the adjacent mammary tissue of patients diagnosed with HR$^+$ breast cancer, HER2$^+$ breast cancer, or TNBC[77]. These studies underscore the possibility that bile acid/FXR signaling can shape the immune microenvironment in breast tumors and the adjacent mammary tissues.

1.2.2.3 Inosine

Inosine, a primary metabolite of adenosine, regulates immune responses through interacting with adenosine receptors A_1, A_{2A}, A_{2B}, and A_3. Because these receptors are widely expressed by all immune cells, inosine modulates immune responses in multiple inflammatory diseases and contexts[77]. The commensal bacterium *Bifidobacterium pseudolongum* is one source of inosine. Using spontaneous and implantable colon cancer models, Marger *et al.* found that inosine produced by *B. pseudolongum* improves efficacy of anti-CTLA4 antibody. Although *B. pseudolongum* does not influence tumor growth on its own, it does induce the differentiation of CD4 T cells and CD8 T cells[86]. Together with anti-CTLA4 antibody, the inoculation of *B. pseudolongum* increases IFN-γ-producing effector T cells in the spleen and intestine, augmenting the efficacy of CTLA4-blockade[86]. Similarly, Wang *et al.* found that inosine is an alternative carbon source for T cell metabolism in a glucose restricted environment to support T cell proliferation and

functional activity[87]. These mechanistic studies highlight the importance of the gut microbiome for anti-tumor immunity.

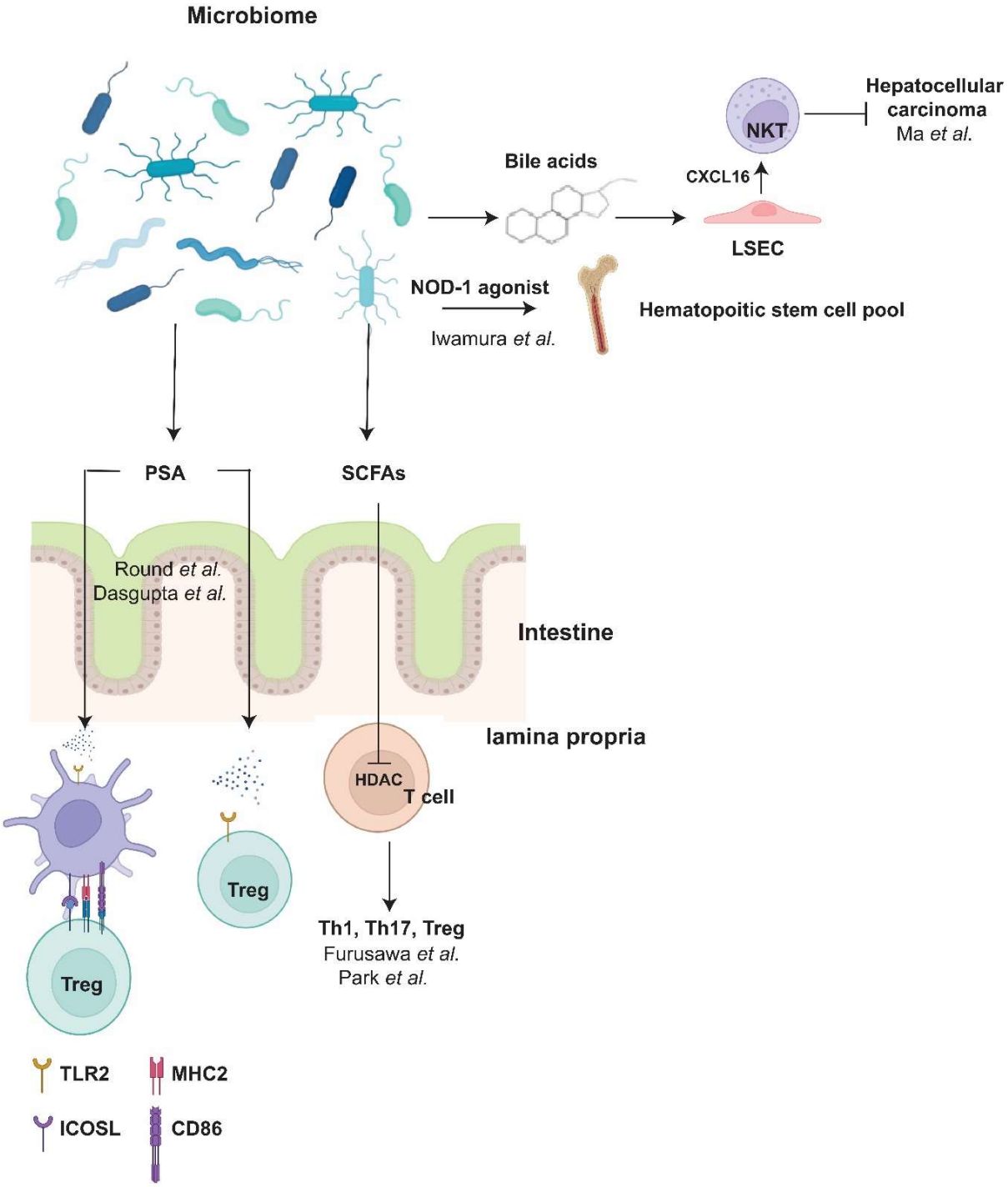
Microbiome
Bile acids
NKT
Hepatocellular carcinoma
Ma et al.
CXCL16
LSEC
NOD-1 agonist
Iwamura et al.
Hematopoitic stem cell pool
PSA
SCFAs
Round et al.
Dasgupta et al.
Intestine
lamina propria
HDAC
T cell
Treg
Treg
Th1, Th17, Treg
Furusawa et al.
Park et al.
TLR2
MHC2
ICOSL
CD86

Figure 1.1 Microbiome systemically modulates homeostasis of host immunity through metabolites or microbe-associated molecular patterns (MAMPs)

Gut commensal microbiota serves as a source of bile acids, SCFAs, and MAMPs. SCFAs influence the differentiation of T helper type 1 (Th1) cells, T helper type 17 (Th17) cells, and Tregs in lamina propria. Gut microbiome-mediated bile acid metabolism regulates the recruitment of natural killer T cells (NTKs) into liver influencing anti-hepatocellular carcinoma activity. *Bacteroides fragilis*-derived polysaccharide A (PSA), a type of MAMPs, promotes intestinal Tregs through direct interactions with toll-like receptor 2 (TLR2) on CD4 T cells or indirect stimulation of dendritic cell (DC)-mediated induction of Treg. Beyond the intestinal tract and the adjacent organs, the gut commensal microbiome can also modulate the pool of hematopoietic stem cells in the bone marrow through nucleotide-binding oligomerization domain-containing protein 1 (NOD-1) signaling.

1.3 The current understanding of the role of mast cells in breast cancer

Mast cells are evolutionarily conserved innate immune cells found in connective tissues throughout the body, such as perivascular sites, brain, smooth muscle, peritoneal cavity, gastrointestinal tract, and respiratory tract[88]. Mast cells are known for initiating inflammatory responses during allergic diseases. Although mast cells are often neglected in cancer research due to their low abundance in the tissue and tumor microenvironment, it has become clear that in cancer and non-cancer settings, mast cells are pivotal regulators of immune function. In this section, I will discuss the current understanding of mast cell biology and their roles in breast cancer.

1.3.1 Introduction of mast cells

1.3.1.1 Development of mast cells

Non-tissue residing mast cells develop from hematopoietic progenitor populations in the bone marrow[89] where precursor populations are recruited to distal sites via chemokine gradients into the tissue[90], undergo division[89, 91], followed by maturation and activation by tissue microenvironmental factors. On the other hand, tissue-resident mast cells are derived from yolk sac progenitors[92-94]. Tissue mast cells are long-lived[95-97] and can be replenished from precursors residing in the tissue[93, 98]. However, very little is known how progenitor tissue-residing mast cells are matured. For bone marrow-derived mast cells, progenitors differentiate from common myeloid progenitors (CMP), a process that is tightly controlled by CCAAT/enhancer binding protein α (C/EBPα), GATA-binding factor 2 (GATA-2), GATA-binding factor 3 (GATA-3), Hes-1, and melanocyte Inducing

Transcription Factor (MITF)[89]. The downregulation of C/EBPα in granulocyte-monocyte progenitors (GMP) along with upregulation of GATA-2, GATA-3, and Hes-1 allow GMP to differentiate into bipotent progenitors, which have the potential to become mast cell and basophils. The subsequent upregulation of MITF and further downregulation of C/EBPα lead to the commitment of progenitors into mast cells.

Yolk sac-derived mast cell progenitors enter into connective tissues (ex: adipose tissue and skin) during early embryonic development and are self-maintained at steady state in mice, whereas bone marrow-derived mast cell progenitors constantly travel through the circulatory system to seed peripheral tissues[93]. Although bone marrow-derived mast cell progenitors are continually replenished during adulthood, yolk sac-derived mast cell progenitors are not dispensable. Kitamura *et al.* showed that the adoptive transfer of bone marrow cells from a wild-type mouse into a mast cell deficient recipient replenishes cecal mast cells while only partially restoring skin-residing mast cells.[99] Mirroring this finding, Li *et al.* elucidated that the origin of mast cell progenitors in the gut of adult mice is bone marrow, whereas progenitors in the skin are derived from both yolk sac and bone marrow progenitor populations[93]. These studies suggest that mast cell progenitors from both origins are equally necessary to maintain tissue mast cell-pools into adulthood, similar to the ontogeny of tissue macrophages. Unlike other granulocytes, mature mast cells are long-lived immune cells that can survive for up to 12 weeks in the murine ear[100]. Human mast cells from adult skin showed proliferative ability in response to stem cell factor (SCF) stimulation *in vitro*[101], however, it remains undetermined whether mature mast cells maintain proliferative ability *in vivo*.

1.3.1.2 Subtypes of mast cells

A tremendous amount of work has been done to identify subtypes of mast cells in animals and humans, where the classification of mast cell subsets is based on the anatomical location and/or the protein contents in the secretory granules. In mice, the most well characterized subtypes of mast cells are connective-tissue mast cell (CTMC) and mucosal mast cell (MMC). CTMCs are found in skin, peritoneal cavity, and the gastrointestinal tract, whereas MMCs usually populate at mucosal sites. CTMCs have granules that contain heparin, histamine, tryptase, and chymase, whereas the granule contents of MMCs are mainly comprised of chymase, have low levels of histamine and undetectable levels of heparin[102]. In humans, mast cells are classified into MC_T (mast cells containing mainly tryptase) and MC_{TC} (mast cells containing both tryptase and chymase)[102]. MC_T reside in the external mucosa of the gastrointestinal and respiratory tracts, whereas MC_{TC} are usually found in the submucosa and perivascular tissues[103, 104]. Distinct tissue tropisms give rise to distinct functional attributes, with MC_T critically regulating the immune responses while MC_{TC} are involved in tissue repair[103, 104]. Although human and murine mast cells share multiple protein signatures[105], mast cells from each species also produce a distinct repertoire of proteases[102] and respond differently in the presence of the mast cell stabilizer cromolyn[106]. Host-intrinsic and/or tissue microenvironment-driven variations can also contribute to phenotypical differences in mast cells[106, 107]. Together, including the aforementioned factors when evaluating the physiological roles of mast cell may help to deconvolute the heterogeneous effects of mast cells.

1.3.2 Do mast cells influence the outcomes of breast cancer?

Mast cells are known to initiate allergic disorders and anti-pathogen responses, but whether and how the mast cells influence outcomes of cancer patients is less characterized. Nevertheless, mechanistic studies of mast cell-driven physiological changes in allergic disorders and anti-pathogen responses have provided a foundation to disentangle mechanistically how mast cells affect cancer progression. From those studies, we have learned that mast cells store a variety of cytokines, chemokines, growth factors, proteases, histamine, and lipid-derived mediators such as prostaglandins, leukotrienes, and platelet activating factor in their cytoplasmic granules[108], all of which can be released in response to high affinity IgE receptor (FcεRI) crosslinking[109] or microbe-associated molecular pattern (MAMP) stimulation[110]. The release of mast cell granules into the extracellular space impacts a wide range of biological processes, including fibrosis, immune cell activation/recruitment, and/or angiogenesis[111], ultimately influencing the aggressiveness of tumors. In the following sections, I will discuss the how mast cells influence breast cancer outcomes.

1.3.2.1 The abundance or transcriptomic signatures of mast cells are associated with variable outcomes

Toluidine blue staining, Alcian blue staining, and immunological staining for mast cell markers, including tryptase, chymase, and cKit, are well-established and convenient tools to quantify the mast cells in the tumor-draining lymph nodes, peri-, and intra-tumoral locations of clinical specimens derived from surgeries. With the above-mentioned

histological approaches, researchers have attempted to associate mast cell abundance with breast cancer outcomes. In 1979, Bowers H. and colleagues reported that numbers of mast cells within tumor-draining lymph nodes positively correlated with survival, using a cohort of 43 breast cancer patients[112]. In the recent two decades however, studies with larger samples sizes have reported that the numbers of mast cells in the intratumoral/peritumoral compartments associate with various prognoses across all subtypes of human breast cancer[113].

Although the histological approaches are convenient tools for enumerating and mapping mast cells from archival patient samples, there are several limitations that have likely led to divergent observations: 1) the mast cell population is relatively small within the breast tissue microenvironment. Histological studies can only cover a small portion of the tissues, especially when utilizing archival or tumor-adjacent tissues, diminishing the reliability and validity of the results; 2) Unlike tryptase or chymase, ckit can also be highly expressed by various cell types[114], diminishing the confidence that studies utilizing cKit as a bona-fide mast cell marker are only enumerating mast cells; 3) Mast cells are phenotypically and functionally heterogeneous. Using one or two markers is unlikely to detect all of the mast cells in the tissues. Although metachromatic stains, such as toluidine blue and Alcian blue can detect mast cells without the limitation of a finite repertoire of markers, those stains fail to detect degranulated mast cells[115] and fail to encapsulate the possibility that mast cells with distinct functions can have opposing effects on tumor outcomes; 4) Tissue sectioning can cause the degranulation of mast cells leading to underestimated numbers of mast cells[115].

Indeed, applying bulk transcriptomic technologies allows researchers to detect mast cells with a larger repertoire of markers. CIBERSORT is a machine learning algorithm able to deconvolute individual immune cell signatures from bulk tissue sequences, with a capability of resolving individual immune cell populations in samples with low signal/noise ratios (e.g. poorly immune infiltrated tumors) [116]. For the signature matrix, a reference atlas of known cell signatures is required for deconvolution, such as the human cell atlas[117] or other sorted and analyzed reference datasets. CIBERSORT[116] has been employed to identify the association of clinical outcomes of solid tumors with 22 immune cell subsets, including mast cells[118]. Using CIBERSORT, numerous studies identified that the signatures of IgE-activated mast cells are associated with poor survival in HR^{+}[119], $HER2^{+}$[119-121], and TNBC breast cancer[119, 122]. Interestingly, for TNBC breast cancer, some researchers have identified that high signatures of mast cells associate with pathological complete responses (pCR)[121]. Although CIBERSORT provides a powerful platform to study the role of mast cells, there are limitations of this tool that may obscure the true association of mast cells with breast cancer outcomes. Firstly, the genomic signatures of mast cells used as a reference for the CIBERSORT program were derived from a microarray analysis of resting or IgE-activated cord blood-derived mast cells[123]. Besides IgE, mast cells can also be activated by various stimuli that can be enriched in the microenvironment of the tumor and the surrounding tissues, such as prostaglandin E2[124], adenosine[125], and IL-33[126]. Recently, the findings that normal or malignant mammary tissues have distinct microbial populations[63] raises the additional possibility that mammary tissue-associated mast cells can also be activated by microbial associated molecular patterns. Mast cells activated via an IgE-independent mechanism likely

express different signatures as compared to IgE-stimulated mast cells. Therefore, using CIBERSORT on bulk sequenced samples is likely to provide inadequate coverage of the genome, coverage that is required to uncover unique or tumor-associated signatures of mast cells that correspond with favorable or non-favorable outcomes. Secondly, mast cell signatures, such as cKit and FcεRIα, greatly overlap with other innate immune cells[105, 123], as mentioned previously. Investigating mast cell signatures from bulk-sequencing data[113] from patients likely may not provide the resolution required to accurately decipher how mast cells affect breast cancer outcomes. Considering that mast cells are rare immune subsets within tissues, if it is accessible, the use of flow cytometry could provide a more accurate representation of true mast cell counts in whole disassociated tissues. However, using this approach on biopsies and resected tumor/normal tissues may not be feasible.

1.3.2.2 The potential molecular mechanisms of mast cell-driven metastasis in breast cancer

The majority of clinical observations have linked transcriptomic signatures of activated mast cells with pro-metastatic signatures and poor survival[113], while pan-analysis of mast cell abundance resulted in more heterogeneous observations[127]. These results suggest that qualitative changes in mast cells may have a direct effect on tumor growth, the immune environment, or metastasis. Indeed, the granule contents released by activated mast cells can lead to pro-metastatic phenotypes, including fibrosis, increased angiogenesis, and immune suppression. These mechanisms are discussed below.

It has been well established that mast cells store a wide range of pro-fibrogenic or pro-angiogiogenic mediators within their granules, such as platelet-derived growth factor (PDGF), tryptase, chymase, IL-1β, IL-13, IL-4, IL-6, CCL2, CCL5, fibroblast growth factor (FGF), vascular endothelial growth factor (VEGF) and TGF-β1[128,129, 130] (Figure 1.2). Among the mentioned mediators, tryptase has been associated with stromal changes and poor outcomes in breast cancer patients[113, 127]. It has been shown that tryptase activates fibroblasts and endothelial cells through interactions with proteinase activated receptor (PAR)-2 on the stomal cells. Blocking tryptase signaling with the tryptase inhibitor APC-366 reduces tryptase-induced proliferation of endothelial progenitor cells[131] and the activation of fibroblasts[132]. Indeed, breast tumors have significantly increased tryptase$^+$ mast cells and α-smooth muscle actin (SMA)$^+$ activated fibroblasts as compared to normal breast tissues[133]. Serum levels of tryptase and tryptase$^+$ mast cells positively correlate with CD34 expression on endothelial cells and increased microvascular density in human breast tumors[134]. Of note, breast cancer patients with enriched tryptase$^+$ mast cells in the primary tumor have increased risk of developing brain metastasis[135]. Together, these data raise the possibility that mast cell-derived tryptase promotes breast tumor metastasis through regulation of fibrosis and angiogenesis.

In addition to the direct influence on stromal cells, several studies have demonstrated that mast cells shape the innate immune landscape of tumors, leading to a pro-tumor and immune suppressive microenvironment. For instance, mast cells recruit myeloid-derived suppressor cells (MDSCs) via CCL2/CCR2 signaling, leading to subsequent recruitment of regulatory Tregs and immunosuppression in the tumor environment in a murine model

of hepatocarcinoma[136]. In B16 melanoma, mast cells synergize with MDSCs, exacerbating lung metastases[137]. MDSCs in the peripheral blood from metastatic breast cancer (MBC) patients are negatively correlated with survival[138], underlining the necessity of investigating the interactions between mast cell/MDSCs in MBC patients.

In addition to MDSCs, mast cells also regulate the recruitment and differentiation of M2-like macrophages, well-known mediators of tumor invasiveness[139]. In the *gp130^{FF}* mice, a spontaneous model of murine gastric cancer, IL-33-activated mast cells recruit M2-like macrophages into tumors through CCL2, CCL3, and CCL4, culminating in the subsequent outgrowth of tumors[126] (Figure 1.2). It has also been reported that IL-13 from IL-33-activated mast cells induces the differentiation of regulatory M2 macrophages[140] (Figure 1.2). IL-33 is enriched in tumors and the adjacent mammary tissues from patients with HR$^+$ breast tumor, suggesting that IL-33-activated mast cell may play a role in establishing pro-invasion immune environment in humans[141].

Most current studies have related mast cells residing in tumor or tumor-draining lymph nodes to the outcomes of breast cancer. What remains largely unknown is whether mast cells in adjacent mammary tissues also affect tumor outcomes, given their ability to orchestrate structural and immunological changes to the tissue environment. Mast cell-mediated stromal rearrangement is required for the development of mammary ducts during mammary tissue development, suggesting that mast cells are involved in the maintenance of mammary tissue homeostasis[84]. Like other immune cell subsets, the

surrounding tissue microenvironment can reciprocally influence the activity and function of mast cells[142]. Recently, accumulating studies have revealed that the transcriptomic changes favoring tumor progression occur in the mammary tissues[14], even prior to the diagnosis of breast cancer[15]. These data suggest that an altered tissue microenvironment may induce functional changes to mammary tissue-associated mast cells which can have negative consequences during the early stages of tumor progression.

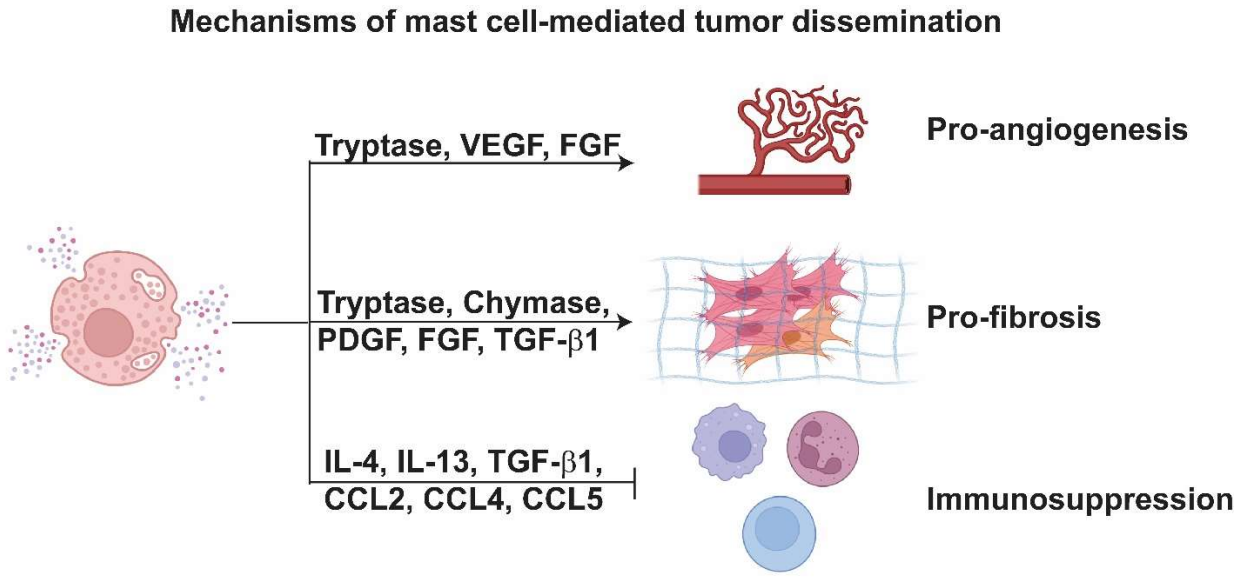

Figure 1.2 The mast cell is a cellular source of various mediators involved in angiogenesis, fibrosis, and immunosuppression.

Increased angiogenesis, enhanced fibrosis, and enriched accumulation of regulatory immune cells can increase tumor growth and dissemination. Mast cells store abundant mediators that stimulate pro-metastatic phenotypes in tumor cells. Pro-angiogenesis mediators: tryptase, vascular endothelial growth factor (VEGF), and fibroblast growth factor (FGF); Pro-fibrosis mediators: tryptase, chymase, platelet-derived growth factor (PDGF), FGF, and transforming growth factor-beta 1 (TGF-β1); Mediators that induce the differentiation or recruitment of regulatory immune cells: interleukin-4 (IL-4), interleukin-13 (IL-13), TGF-β1, CCL2, CCL4, and CCL5.

1.4 Overview of this dissertation

Considering the heterogenous outcomes for HR^+ breast cancer, and that early dissemination requires crosstalk between the adjacent tissue and tumor, it is likely that biological differences exist in *normal mammary tissue* prior to cancer detection that enhance long-term susceptibility to metastatic disease. For example, when mammary tissue inflammation driven by CCL2[143] or PGE_2[144], macrophage infiltration[145, 146], and fibrosis[147, 148] precedes breast cancer, risk for metastatic disease is significantly increased in patients that are eventually diagnosed with HR^+ disease. However, it is not well understood whether normal or benign-adjacent mammary tissue directly contributes to HR^+ tumor dissemination. In alignment with this hypothesis, we demonstrated that commensal dysbiosis induced chemokines CCL2 and CXCL10 in normal mammary tissues. Importantly, when dysbiosis was induced prior to tumor initiation, HR^+ tumors disseminated more readily into the blood, distal lymph nodes, and to the lungs. These results supported the idea that the gut commensal microbiome is a host-intrinsic modulator of HR^+ breast cancer outcomes. In this dissertation, the goal of my studies was to identify the cellular and molecular drivers in the normal non-tumor-bearing or tumor-adjacent mammary tissue environment that enhance metastatic dissemination of HR^+ tumors. The central hypothesis is that commensal dysbiosis increases the pro-metastatic potential of mammary tissues, resulting in chemokine and cellular changes that facilitate egress of tumor cells from the mammary tissue environment.

In Chapter 1, I provided an introduction highlighting the complex interplay between metastatic breast cancer, the gut microbiome, and mast cells. In Chapter 2, I will discuss

the evidence that pre-existing commensal dysbiosis phenotypically changes mammary tissue-associated mast cells, resulting in fibroblast activation in the mammary tissues, enhanced collagen accumulation, and subsequent early dissemination of HR^+ breast tumors. In Chapter 3, I will integrate findings from my graduate work with observations from others to explore the potential mechanisms of how commensal dysbiosis distally regulates the pro-metastatic immune environment in mammary tissues leading to enhanced invasiveness of HR^+ tumor cells. I will also discuss the relevance of these findings in the context of aging. Finally, I will summarize my findings on mast cells and breast cancer in the context to what is known in the literature, establishing a new model in which the gut microbiome distally modulates mast cell phenotype to promote or facilitate metastatic breast cancer.

Chapter 2: Reciprocal interactions between the gut microbiome and mammary tissue mast cells promote metastatic dissemination of HR$^+$ breast tumors

2.1 Forward

This work is in press at *Cancer Immunology Research*, accepted July 13th 2022, with me as the first author. The text and figures were adapted from the publication for Chapter 2. Below is the full citation.

Tzu-Yu Feng[1], Francesca N. Azar[1], Sally A. Dreger[2], Claire Buchta Rosean[1], Mitchell T. McGinty[1], Audrey M. Putelo[1], Sree H. Kolli[1], Maureen A. Carey[1,3], Stephanie Greenfield[1], Wesley J. Fowler[2], Stephen D. Robinson[2,4], Melanie R. Rutkowski[1*]

1 Department of Microbiology, Immunology, and Cancer Biology, University of Virginia, VA, USA

2 Gut Microbes and Health Programme, Quadram Institute Bioscience, Norwich Research Park, Norwich, UK

3 Division of Infectious Diseases and International Health, Department of Medicine, University of Virginia, VA, USA

4 School of Biological Sciences, University of East Anglia, Norwich Research Park, Norwich, UK

* Corresponding Author

2.2 Abstract

Establishing commensal dysbiosis, defined as an inflammatory gut microbiome with low biodiversity, prior to breast tumor initiation, enhances early dissemination of hormone-receptor positive (HR^+) mammary tumor cells. Here, we sought to determine whether cellular changes occurring in normal mammary tissues, prior to tumor initiation and in response to dysbiosis, enhance dissemination of HR^+ tumors. Commensal dysbiosis increased both the frequency and profibrogenicity of mast cells in the normal non-tumor-bearing mammary tissues, a phenotypic change that persisted after tumor implantation. Pharmacological and adoptive transfer approaches demonstrated that pro-fibrogenic mammary tissue mast cells from dysbiotic animals were sufficient to enhance dissemination of HR^+ tumor cells. Using archival HR^+ patient samples, we determined that enhanced collagen levels in tumor-adjacent mammary tissue positively correlated with mast cell abundance and HR^+ breast cancer recurrence. Together, these data demonstrate that mast cells programmed by commensal dysbiosis activate mammary tissue fibroblasts and orchestrate early dissemination of HR^+ breast tumors.

2.3 Significance

The role of mammary tissue-associated mast cells during breast cancer is poorly defined. Here, we establish that prior to tumor initiation, gut commensal dysbiosis distally programs mammary tissue mast cells to activate tissue-resident fibroblasts and facilitate metastatic dissemination of HR^+ tumors. These findings uncover a novel gut microbiome-innate immune cell axis that exists in normal mammary tissue that increases susceptibility to early metastatic spread of HR^+ tumors.

2.4 Introduction

Despite successful first-line treatments, a substantial population of hormone-receptor positive (HR^+: estrogen- and/or progesterone-receptor$^+$, $HER2^-$) breast cancer patients develop metastasis and succumb to the disease. According to the Surveillance, Epidemiology and End Results (SEER) database, HR^+ breast cancer is the most common molecular subtype (73.1%) of the metastatic breast cancer population in the US[149]. Well-established treatment strategies have significantly increased long-term survival of women diagnosed with HR^+ breast cancer, but accurate prediction of patient recurrence remains a significant barrier to reducing the mortality associated with metastatic breast cancer.

Using a novel murine model of HR^+ breast cancer[150-152], we recently demonstrated that gut commensal dysbiosis (an inflammatory gut microbiome with low biodiversity) established prior to breast tumor initiation enhances metastatic dissemination of HR^+ tumors despite primary tumor growth remaining unchanged[153]. This was one of the first studies to demonstrate that the gut microbiome acts as a host-intrinsic mediator of breast tumor metastasis, and further suggest that the negative consequence of having gut dysbiosis to breast cancer progression is established prior to tumor diagnosis. Sequencing of the gut microbiome from treatment-naïve patients recently diagnosed with breast cancer similarly demonstrated that differences in the gut microbiome affected tumor aggressiveness, prognosis, and therapy response[154], supporting the notion that the gut microbiome can systemically and negatively impact breast cancer outcomes.

The mechanism by which changes in the gut microbiome impact breast tumor metastasis remains unknown. Dysbiosis can trigger systemic inflammation which is associated with increased metastatic recurrence in breast cancer patients[155]. We previously found that dysbiosis elevated levels of CCL2 in mammary tissue prior to tumor initiation. When increased levels of CCL2 precede breast cancer, there is an increased risk of developing breast cancer[156] or metastatic disease after diagnosis[143]. Considering the heterogenous outcomes for HR^+ breast cancer and in light of our recent findings, we hypothesized that commensal dysbiosis changes the immunological tone of the normal non-tumor-bearing mammary tissue, and that the cellular and molecular changes that arise in response to dysbiosis enhance early metastatic spread when a tumor is present. Here, we sought to address this hypothesis by investigating how commensal dysbiosis-induced mammary tissue inflammation influences dissemination of HR^+ tumor cells.

Mast cells are evolutionarily conserved innate immune cells that exhibit a diverse range of effector functions in multiple physiological and disease-associated settings. Mast cells mediate stromal rearrangement needed for the development of mammary ducts during mammary tissue development and homeostasis[84], suggesting a role for the maintenance of mammary tissue homeostasis. Although the role of mast cells in mammary gland development and homeostasis are well-known, their role during breast tumor progression and outcomes remains controversial[127, 157]. Studies exist demonstrating both positive and negative associations between mast cells and breast cancer outcomes[158]. Mechanistically, the reasons for differences in observed outcomes have remained unclear. Majorini *et al.* demonstrated that tumor-associated mast cells can directly modulate the

phenotype of tumor cells towards a more luminal phenotype, directly stimulating estrogen receptor expression and risk of relapse[159]. Our colleagues McKee *et al.* further demonstrated that antibiotic treatment enhances mast cell accumulation into mammary tumors, increasing tumor fibrosis and growth kinetics[160], suggesting that modulation of the gut microbiome could dictate mast cell-mediated differences in breast cancer outcomes. Despite this, it remains unknown what endogenous factors affect mast cell phenotypes in the mammary tissue environment or whether mammary tissue-associated mast cells have a long-term and direct impact on breast cancer metastasis.

In this study, we demonstrate that commensal dysbiosis enhances accumulation of mast cells in the mammary tissue of non-tumor-bearing mice, and that this occurs in response to elevated mammary tissue CCL2 levels. In the presence of a tumor, pre-existing commensal dysbiosis results in tissue-infiltrating mast cells becoming pro-fibrogenic, culminating in increased tissue collagen levels and the promotion of early metastatic dissemination of HR^+ tumors. We confirm that increased mast cell abundance correlates with high collagen levels in breast tissues of women diagnosed with HR^+ breast cancer and risk for recurrence. To our knowledge, this is the first study revealing that commensal microbiome-mediated recruitment and phenotypic changes of mammary tissue-associated mast cells in normal non-tumor-bearing mammary tissue influence the metastatic spread of HR^+ tumor cells.

2.5 Results

Commensal dysbiosis drives accumulation of mast cells in normal non-tumor-bearing mammary tissues.

Previously, we demonstrated that the gut microbiome was a distal host-intrinsic mediator of breast tumor metastasis. When commensal dysbiosis was established prior to breast tumor initiation, metastatic dissemination of HR^+ tumors to the axillary lymph node, blood, and lungs were significantly increased[43]. Importantly, dissemination of HR^+ tumor cells did not occur due to differences in tumor growth, as tumor volumes were unchanged in response to dysbiosis[43]. Using the model highlighted in Figure 2.1A to initiate commensal dysbiosis, metagenomic 16S rDNA sequencing from feces of mice at the day of tumor initiation (day 0) indicated a substantial difference in beta (inter-individual differences) and a reduction in alpha (intra-individual commensal richness) diversity of the microbiome from mice treated with antibiotics when compared to vehicle-treated mice (Figure 2.2A-B), confirming that commensal dysbiosis was established prior to tumor initiation, as we previously reported[43]. Twelve days after the day 0 analysis, differences in the microbiome between dysbiotic and non-dysbiotic mice diminished, with reduced differences between dysbiotic and non-dysbiotic mice in both beta and alpha diversity, regardless of tumor status (Figure 2.2A-B). The significant departure in microbiome composition at day 0 relative to observed differences at day 12 led us to hypothesize that microenvironmental changes arising in response to dysbiosis in non-tumor-bearing animals prime the mammary tissue to enhance metastatic dissemination. We further hypothesized that inflammatory differences in the mammary tissue environment initiated by differences in the microbiome prior to tumor initiation persisted in the presence of a tumor.

In support of our hypothesis, we previously demonstrated that gut commensal dysbiosis elevates chemokines CCL2 and CXCL10 in normal non-tumor-bearing mammary tissues, both of which remain elevated in adjacent mammary tissues during HR^+ tumor progression[153]. To determine the cellular changes in the mammary tissue that accompany commensal dysbiosis, the immune cell composition was investigated in the normal and adjacent tissues from non-tumor-bearing mice with or without commensal dysbiosis. Commensal dysbiosis was established with antibiotics prior to analysis of mammary tissues and mice were synchronized into estrus to normalize cellular changes occurring in response to the estrus cycle (Figure 2.1A), as previously described[153]. Macrophages and myeloid cells in the mammary gland increase risk of metastatic breast cancer[145, 146], and can be recruited in response to CCL2[161] and CXCL10[162]. Commensal dysbiosis alone did not increase myeloid populations in the mammary gland of non-tumor-bearing mice (Figure 2.3A), despite our previous finding that dysbiosis enhanced the accumulation of myeloid cells in adjacent mammary tissue and tumors during early and advanced stages of HR^+ cancer[43]. Although CD4 T cells were slightly elevated in mammary tissues of non-tumor-bearing dysbiotic mice, the differences were not statistically significant and did not persist during tumor progression (Figure 2.3B). Similarly, no significant changes in the number of CD8 T cells, NK and NKT cells, double negative T cells were observed at any point prior to or during tumor progression (Figure 2.3B-C).

Mast cells are highly responsive to the microenvironment in which they reside, and in other non-cancer disease models have been shown to induce fibrosis[111] and inflammation[163], both of which are relevant to the changes that occur in the mammary

tissue of tumor-bearing mice with pre-existing commensal dysbiosis[43]. We used flow cytometry to evaluate mast cells, using the gating schematic outlined in Figure 2.3D. We found that mast cell numbers were significantly increased in non-tumor-bearing normal mammary tissues in response to commensal dysbiosis (Figure 2.1B). Importantly, changes in mast cell numbers mirrored the changes in mammary tissue levels of CCL2 and CXCL10. Specifically, mast cell numbers remained elevated in the adjacent mammary tissues of dysbiotic mice after tumor implantation (Figure 2.1C-D). We confirmed these results by also quantitating mast cells in adjacent mammary tissues of tumor-bearing dysbiotic or non-dysbiotic mice using histochemistry and toluidine blue staining (Figure 2.1E and 2.1F). Tryptase, a serine protease predominantly produced by mast cells, serves as a specific mast cell marker in both animal and human studies[115]. In line with increased mast cell numbers observed in adjacent mammary tissues in tumor-bearing mice, significantly enhanced protein levels of tryptase were detected in mammary tissue lysates of adjacent mammary tissues from dysbiotic tumor-bearing mice when compared to levels in non-dysbiotic mice (Figures 2.3E-F). Mice bearing the highly metastatic PyMT tumor model[164] also had increased mast cell abundance in the adjacent mammary tissue in response to commensal dysbiosis (Figure 2.1G- H), suggesting that the observed changes in mast cell numbers are not tumor model-specific. Interestingly, despite observing numeric changes of mast cells in adjacent mammary tissues of dysbiotic tumor-bearing mice, there were no differences in the numbers of tumor-associated mast cells between dysbiotic or non-dysbiotic mice at the 12-day temporal point (Figure 2.3G).

The lung is a major reservoir of mast cells[165], and a major site for breast tumor metastasis[149]. To evaluate the effects of dysbiosis on mast cell abundance in lungs of tumor-bearing mice, flow cytometry was used to enumerate mast cells. Interestingly, the abundance of mast cells was increased both in response to dysbiosis and a tumor (Figure 2.3H). These results indicate that commensal dysbiosis increases the abundance of mast cells in lungs of mice with mammary tumors, but not in the tumors of mice with commensal dysbiosis.

We have previously shown that fecal microbiota transplantation (FMT) of a dysbiotic microbiome enhances metastatic dissemination of HR^+ breast tumors[43]. As an additional readout of dysbiosis-induced mast cell expansion, we next tested whether FMT with a dysbiotic microbiome also enhances numbers of mast cells in the mammary tissues of tumor-bearing mice. To do this, cecal contents from dysbiotic and non-dysbiotic donor mice were orally gavaged into antibiotic-sterilized recipient mice for 3 consecutive days (Figure 2.3I). After allowing a week for the transplanted microbiome to engraft in the recipient mice, flow cytometry was used to analyze normal non-tumor-bearing mammary tissues. Similar to animals with dysbiosis, mice receiving an FMT of a dysbiotic microbiome had significantly greater numbers of mast cells in mammary tissues, compared to those that received an FMT of a non-dysbiotic microbiome (Figure 2.3J). Tumor cells were implanted into the mammary tissue after the engraftment period, and adjacent mammary tissues were analyzed 12 days post tumor-initiation using flow cytometry (Figure 2.3K). Mice transplanted with a dysbiotic microflora had significantly increased mast cell numbers in tumors compared to those that received a non-dysbiotic

microbiome (Figure 2.3K). These results indicate that commensal dysbiosis is sufficient to enhance mast cells in mammary tissues during HR^+ tumor progression.

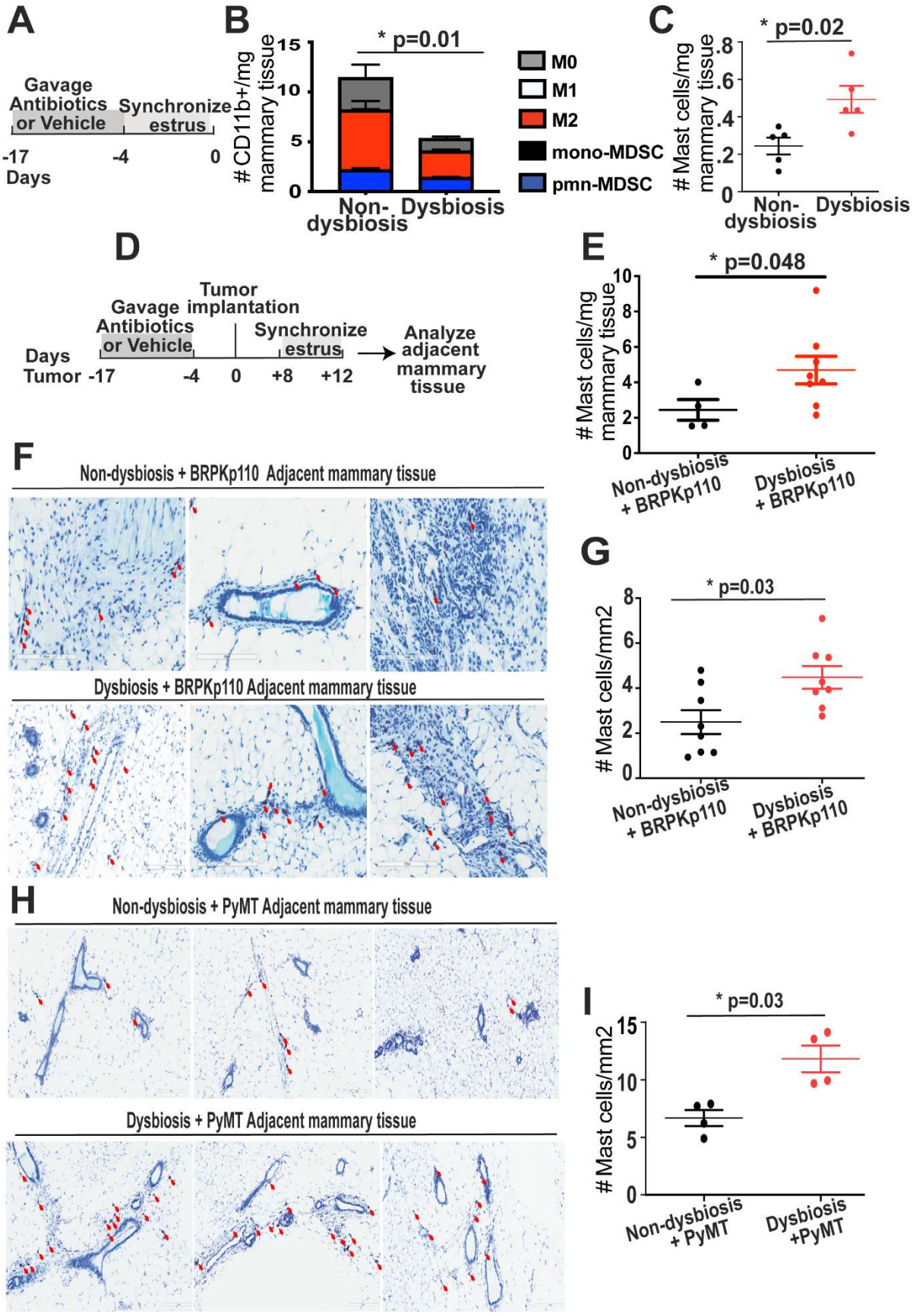
A
Gavage Antibiotics or Vehicle
Synchronize estrus
-17
-4
0
Days
B
CD11b+/mg mammary tissue
* p=0.01
M0
M1
M2
mono-MDSC
pmn-MDSC
Non-dysbiosis
Dysbiosis
C
Mast cells/mg mammary tissue
* p=0.02
Non-dysbiosis
Dysbiosis
D
Tumor Gavage Antibiotics or Vehicle
Tumor implantation
Synchronize estrus
Analyze adjacent mammary tissue
Days
Tumor -17
-4
0
+8
+12
E
Mast cells/mg mammary tissue
* p=0.048
Non-dysbiosis + BRPKp110
Dysbiosis + BRPKp110
F
Non-dysbiosis + BRPKp110 Adjacent mammary tissue
Dysbiosis + BRPKp110 Adjacent mammary tissue
G
Mast cells/mm2
* p=0.03
Non-dysbiosis + BRPKp110
Dysbiosis + BRPKp110
H
Non-dysbiosis + PyMT Adjacent mammary tissue
Dysbiosis + PyMT Adjacent mammary tissue
I
Mast cells/mm2
* p=0.03
Non-dysbiosis + PyMT
Dysbiosis +PyMT

Figure 2.1

Mast cells accumulate in the mammary tissues of mice with commensal dysbiosis. **A,** Experimental scheme for **B**. C57BL/6 mice were orally gavaged daily with a broad-spectrum cocktail of antibiotics or an equal volume of water as a vehicle control for 14 days. Gavage was ceased for 4 days prior to sample collection. A modified Whitten effect was used to synchronize estrus prior to sample collection. **B,** Mast cells (live, singlet, $CD45^{+}Lin^{-}cKit^{+}Fc\varepsilon RI\alpha^{+}$) were quantitated in normal non-tumor-bearing mammary tissues at day 0 using flow cytometry. **C,** Experimental scheme for **D-H**. Mammary tumor cells were orthotopically injected into the 4^{th} mammary fat pad of mice with or without commensal dysbiosis. Twelve days post tumor initiation, adjacent mammary tissues were evaluated. Mice were synchronized in estrus prior to sample collection. **D to F** 12 days after BRPKp110 tumor implantation, mast cells in the adjacent mammary tissues were enumerated using flow cytometry **(D)** or by toluidine blue staining of formalin-fixed and parrafin embedded whole mammary glands **(E and F)**. **G,** Representative images of adjacent mammary tissues isolated from mice bearing the aggressive HR^{+} tumor PyMT 12 days post tumor implantation stained with toluidine blue. **H,** Quantification of mast cells in the adjacent mammary tissues from PyMT-bearing mice 12 days post tumor implantation. For **E**-**H**, Mast cells were enumerated by blindly counting within one whole mount section of adjacent mammary tissue stained with toluidine blue. Total mast cell numbers were quantitated by normalizing to the entire mammary tissue area. Mast cells are marked with red arrows. Representative of two independent experiments with 4-5 mice/group. For dot plots, each symbol represents an individual mouse, and statistical significance was determined by two-tailed Mann-Whitney *U* test.

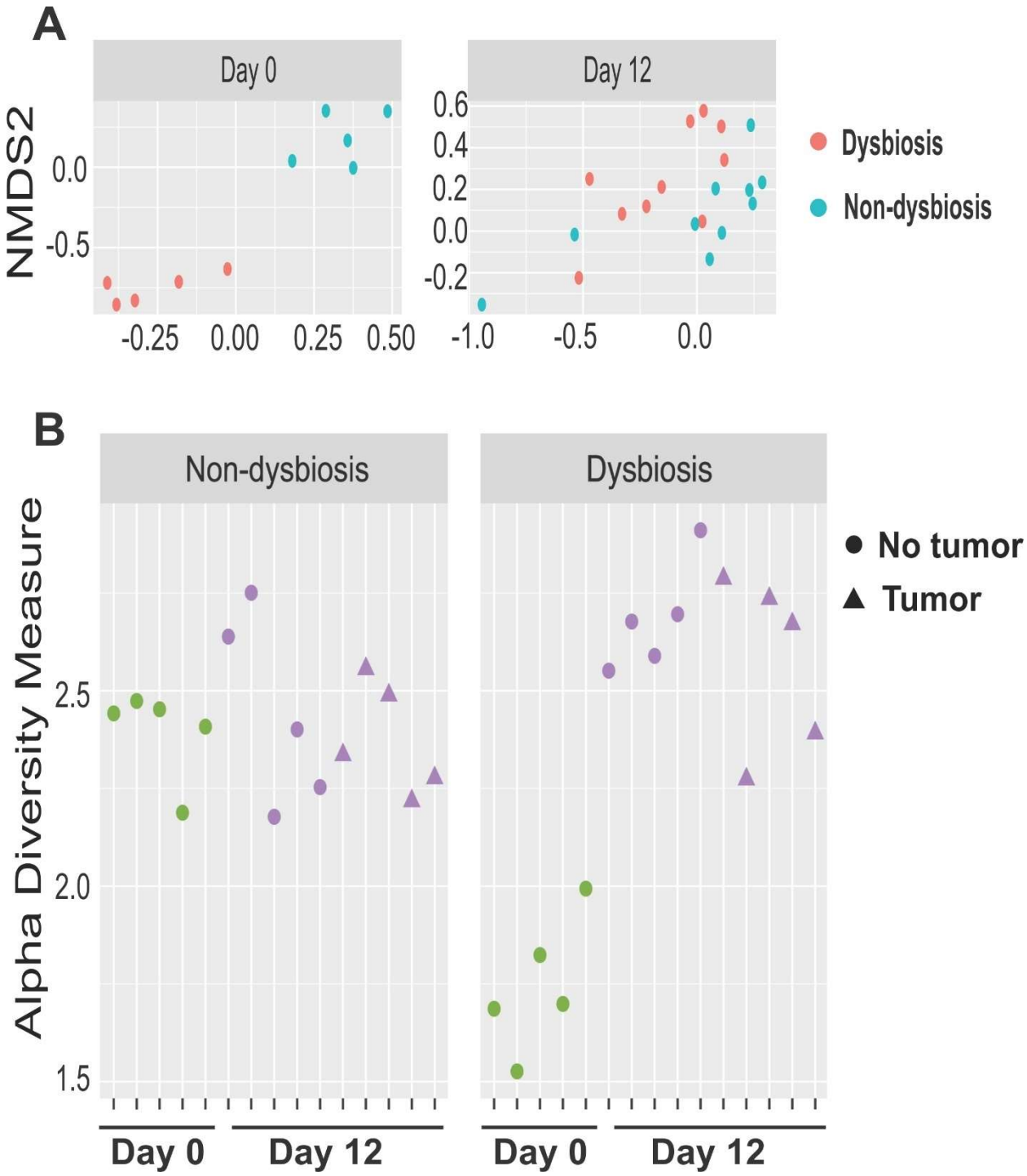
A
Day 0
Day 12
NMDS2
0.0
-0.5
-0.25
0.00
0.25
0.50
0.6
0.4
0.2
0.0
-0.2
-1.0
-0.5
0.0
Dysbiosis
Non-dysbiosis
B
Non-dysbiosis
Dysbiosis
Alpha Diversity Measure
2.5
2.0
1.5
Day 0
Day 12
Day 0
Day 12
No tumor
Tumor

Figure 2.2

Antibiotic-induced differences in the gut commensal microbiome diminish over time and independently of tumor initiation.

A and B, Fecal samples were collected from non-tumor-bearing non-dysbiotic or dysbiotic mice at day 0 as depicted in Fig. 2.1A or 12 days post BRPKp110 implantation as compared to samples from non-tumor bearing counterparts (see the experimental layout in Fig. 2.1C) 16S rDNA analysis of the fecal microbiome from each group was performed. Beta diversity **(A)** measures the diversity of commensal microorganisms between non-dysbiotic and dysbiotic groups of mice at day 0- or 12-days post tumor initiation. Data are visualized using Non-metric Multi-Dimensional Scaling (NMDS) plot with Bray-Curtis Dissimilarity Distances. Alpha diversity **(B)** is a measure of species richness within each group. Data are visualized by using the Shannon Diversity Index. Each symbol represents an individual mouse.

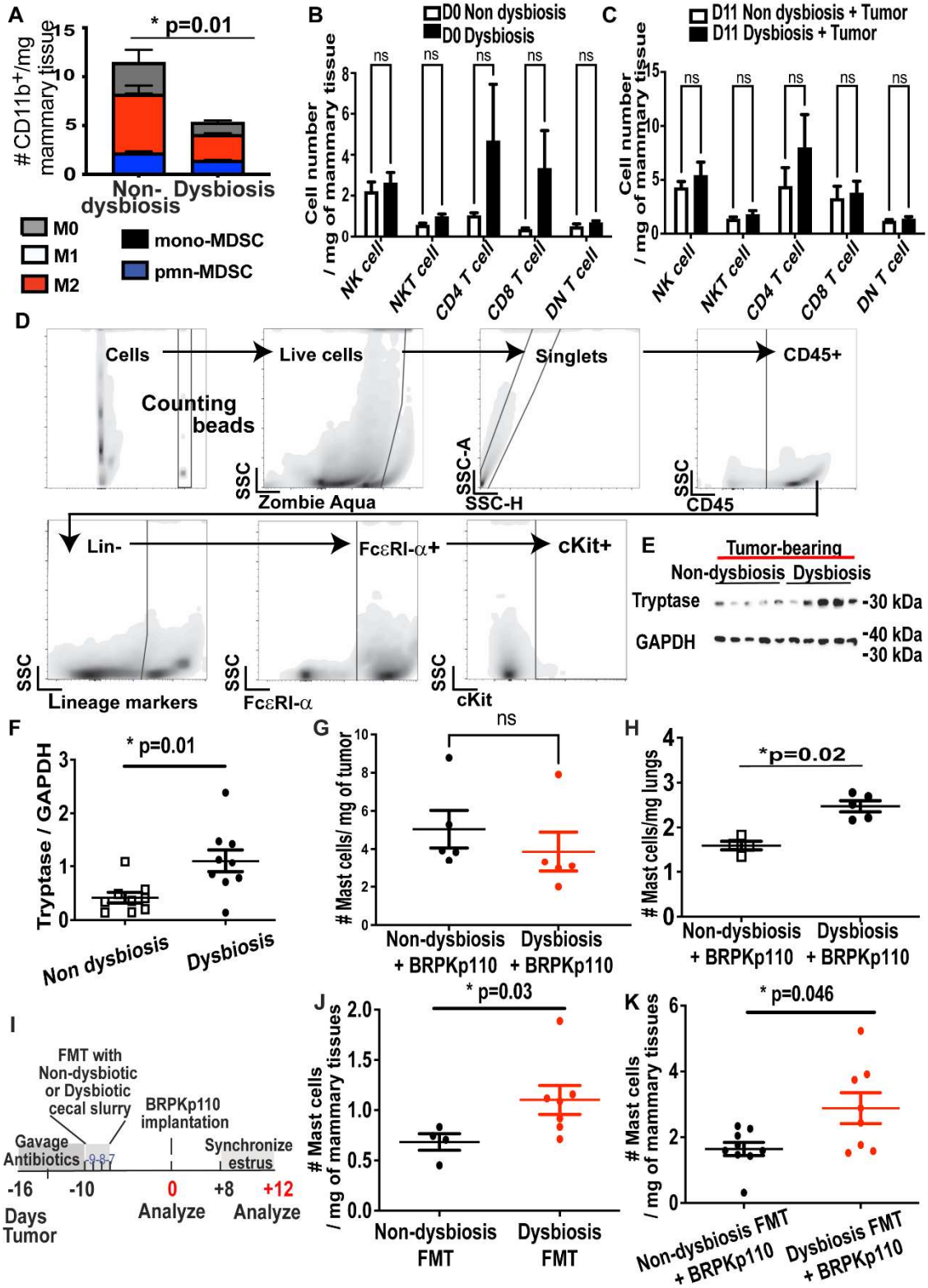
A
* p=0.01
# CD11b+/mg mammary tissue
Non-dysbiosis
Dysbiosis
M0
M1
M2
mono-MDSC
pmn-MDSC
B
D0 Non dysbiosis
D0 Dysbiosis
Cell number / mg of mammary tissue
ns
NK cell
NKT cell
CD4 T cell
CD8 T cell
DN T cell
C
D11 Non dysbiosis + Tumor
D11 Dysbiosis + Tumor
D
Cells
Live cells
Singlets
CD45+
Counting beads
SSC
Zombie Aqua
SSC-A
SSC-H
CD45
Lin-
FcεRI-α+
cKit+
Lineage markers
cKit
E
Tumor-bearing
Non-dysbiosis
Dysbiosis
Tryptase
GAPDH
-30 kDa
-40 kDa
F
* p=0.01
Tryptase / GAPDH
Non dysbiosis
Dysbiosis
G
Mast cells/ mg of tumor
Non-dysbiosis + BRPKp110
Dysbiosis + BRPKp110
H
*p=0.02
Mast cells/mg lungs
I
FMT with Non-dysbiotic or Dysbiotic cecal slurry
BRPKp110 implantation
Gavage Antibiotics
Synchronize estrus
-16
-10
0
+8
+12
Days Tumor
Analyze
Analyze
J
* p=0.03
# Mast cells / mg of mammary tissues
Non-dysbiosis FMT
Dysbiosis FMT
K
* p=0.046
# Mast cells / mg of mammary tissues
Non-dysbiosis FMT + BRPKp110
Dysbiosis FMT + BRPKp110

Figure 2.3

Mast cells accumulate in the mammary tissue in response to commensal dysbiosis and HR$^+$ mammary tumors.

A-C, C57BL/6 mice were treated as described in Figure 2.1A. **A**, On day 0, myeloid cells were quantitated from disassociated normal non-tumor-bearing mammary tissues. All populations were gated on live, singlet, CD45$^+$CD11b$^+$ cells. Numbers represent absolute numbers of cells quantitated using counting beads. M0 macrophages = F4/80$^+$CD86$^-$ CD206$^-$. M1 macrophages = F4/80$^+$CD86$^+$CD206$^-$. M2 macrophages = F4/80$^+$CD86$^-$ CD206$^+$. Monocytic MDSC = Ly6C^{hi}Ly6G$^-$. Polymorphonuclear MDSC = Ly6C^{mid}Ly6G$^+$. **B**, On day 0, T cells and NK cells were enumerated in mammary tissues of dysbiotic and non-dysbiotic mice. **C,** Quantitation of T cells and NK cells from adjacent mammary tissues of tumor-bearing dysbiotic and non-dysbiotic mice 12 days after tumor initiation. For both A and B, all populations were gated on live, singlet, and CD45+. NK cells = CD3$^-$, NK1.1$^+$; NKT cells = CD3$^+$, NK1.1$^+$; CD4 T cells = CD3$^+$, NK1.1$^-$, CD4$^+$; CD8 T cells = CD3$^+$, CD8α^+, NK1.1$^-$; double negative (DN) T cells = CD3$^+$, NK1.1$^-$, CD4$^-$, CD8α^-. **D,** Gating strategy for identifying mast cells. Using flow cytometry, mast cells were identified as CD45$^+$ Lin$^-$ FCεRIα^+ cKit$^+$ cells. **E and F,** Immunoblot of the mast cell marker tryptase and GAPDH, as a loading control **(E)**. Protein levels of tryptase were quantified by ImageJ and normalized to GAPDH **(F)**. **G-H,** Quantification of mast cells in tumors **(G)** or lungs **(H)** from BRPKp110 tumor-bearing mice 12 days post tumor initiation. Numbers of mast cells were normalized to tissue weight. **I-K**, quantitation of mast cells in mammary tissues of mice receiving a fecal microbiome transplant of dysbiotic or a non-dysbiotic microbiome. **I,** Experimental scheme for fecal microbiota transplantation. C57BL/6 mice were orally gavaged for 7 days with a broad-spectrum cocktail of antibiotics. Immediately following the cessation of antibiotics, mice were orally gavaged for three consecutive days with cecal slurries collected from non-dysbiotic or dysbiotic mice collected at day 0, as depicted in Fig. 2.1A. Mice were rested for 7 days to allow for engraftment of transplanted microbial populations, after which mammary tissues were either analyzed for mast cells **(J)** or BRPKp110 tumors were initiated. **J-K,** Utilizing flow cytometry, the abundance of mast cells in normal non-tumor-bearing **(J)** or adjacent mammary tissues 12 days-post tumor initiation **(K)** were enumerated. Numbers represent mast cells/milligram of mammary tissue. Each symbol represents an individual mouse, and statistical significance was determined by two-tailed Mann-Whitney *U* test.

Mast cells promote early dissemination of HR$^+$ mammary tumor cells.

We next asked whether mast cell activation influences the dissemination of HR$^+$ breast tumor cells. To prevent mast cell activation, mice were orally gavaged with the mast cell stabilizer ketotifen fumarate (10 mg/kg) once daily from days 1 to 5 following implantation of the poorly-metastatic HR$^+$ tumor line BRPKp110 into the mammary fat pad (Figure 2.4A). Ketotifen treatment significantly reduced dysbiosis-mediated tumor dissemination into the lungs at advanced stages of tumor progression (Figure 2.4B and 2.5A). Importantly, ketotifen treatment did not affect the primary BRPKp110 tumor growth (Figure 2.5B). Ketotifen treatment also significantly reduced the lung dissemination of the highly-metastatic HR$^+$ breast tumor cell line PyMT (Figure 2.4C and 2.5C). Because the treatment with ketotifen reduced the PyMT primary tumor volumes (Figure 2.5D), the numbers of PyMT tumor cells in the lungs were normalized to final tumor burden (Figure 2.4C) to account for variation in tumor growth. Interestingly, ketotifen treatment also reduced tumor dissemination in non-dysbiotic mice bearing PyMT tumors (Figure 2.4C), raising the possibility that mast cell-mediated tumor dissemination could also be influenced by tumor-intrinsic factors. Importantly, treatment of mice with cromolyn, another mast cell stabilizer (Figure 2.5E) also significantly reduced dissemination of BRPKp110 tumor cells into the lungs of dysbiotic mice (Figure 2.5F-G), suggesting that the observed differences in tumor burden were not a consequence of off-target effects of either inhibitor. Altogether, these data suggest that mast cell activation contributes to dysbiosis-induced metastatic dissemination of HR$^+$ breast tumors.

Next, we tested the ability of mast cells derived from mammary tissue of dysbiotic animals to induce metastatic dissemination. Mast cells were sorted from mammary tissues of non-tumor-bearing dysbiotic and non-dysbiotic mice. Equal numbers of sorted mast cells were orthotopically transferred into the left inguinal mammary fat pad of mast cell-deficient *Kit*$^{w\text{-}sh/w\text{-}sh}$ mice (Sash mice)[166]. The following day, BRPKp110 tumor cells were injected into the same mammary fat pad that received mast cells (Figure 2.4D). Using flow cytometry, we confirmed that equivalent numbers of mast cells remained in the mammary tissues of Sash mice 12 days following tumor initiation regardless of whether they were derived from mammary tissues of dysbiotic or non-dysbiotic mice (Figure 2.4E). These results indicated that both groups of sorted mast cells were equally capable of engrafting into the mammary tissue of Sash mice. Sash mice that received mast cells sorted from mammary tissues of dysbiotic mice had significantly increased dissemination of tumor cells into the blood and to the axillary lymph nodes (Figure 2.4F-H), compared to the Sash mice receiving mast cells from mammary tissues of non-dysbiotic mice (Figure 2.4F-H). To test whether dysbiosis alone can affect tumor dissemination in the absence of mast cells, Sash mice or wild-type C57BL/6 mice were given a fecal transplant with a dysbiotic microbiome using the strategy outlined in Figure 2.5H. Although dysbiotic Sash mice showed comparable tumor growth compared to wild-type mice (Figure 2.5I), dissemination of tumor cells into the blood was significantly reduced compared to wild-type mice transplanted with the same dysbiotic microbiome (Figure 2.5J-K). Collectively, these data indicate that mast cells are required for dysbiosis-induced metastatic dissemination of HR^{+} tumors. Furthermore, these results suggest that mammary tissue mast cells are functionally changed in response to commensal dysbiosis, and that the

dysbiosis-induced functional changes that occur prior to tumor initiation increase dissemination of HR^+ tumor cells.

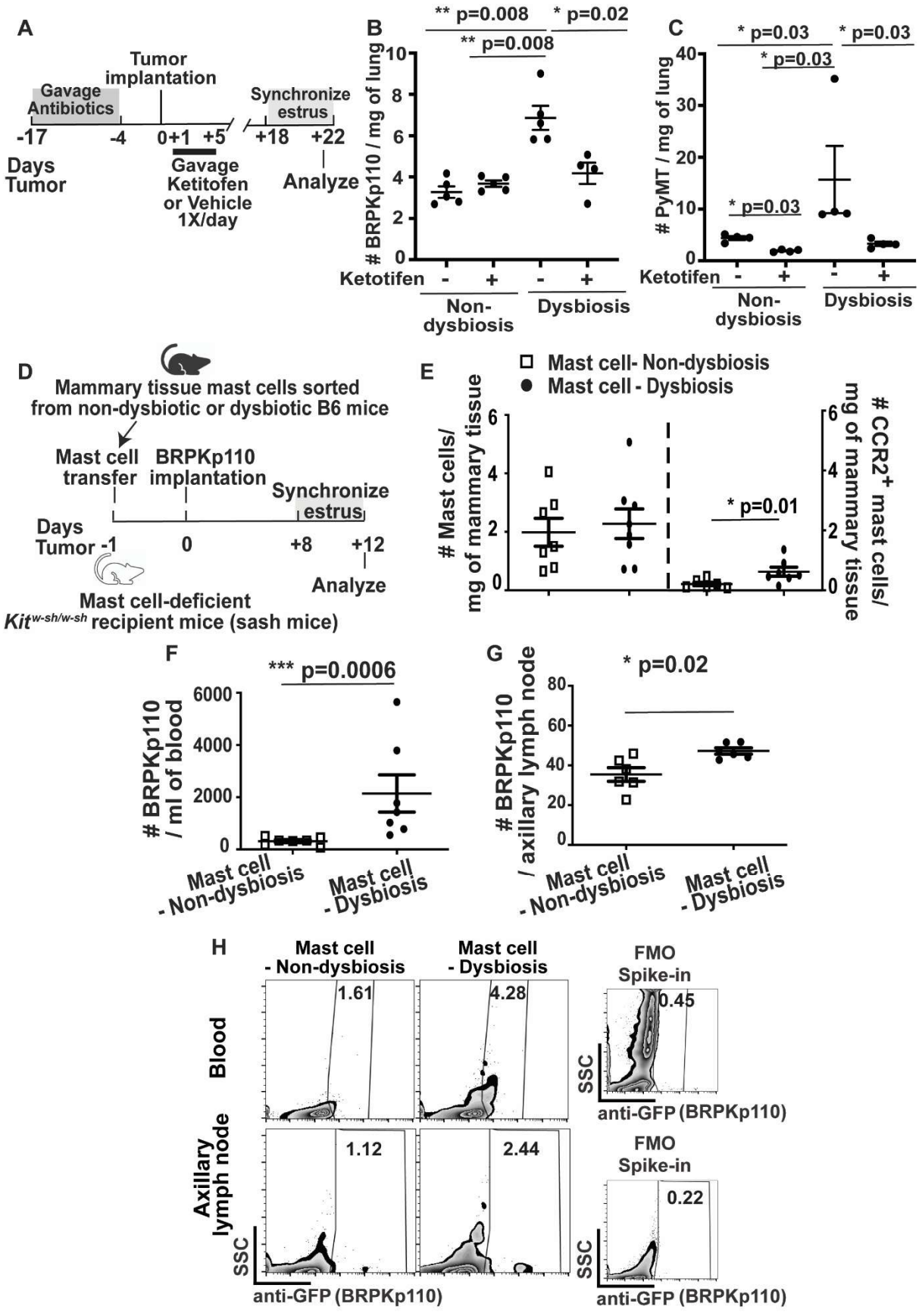
A
Tumor implantation
Gavage Antibiotics
Synchronize estrus
-17
-4
0+1
+5
+18
+22
Days Tumor
Gavage Ketitofen or Vehicle 1X/day
Analyze
B
** p=0.008
* p=0.02
** p=0.008
# BRPKp110 / mg of lung
Ketotifen
Non-dysbiosis
Dysbiosis
C
* p=0.03
* p=0.03
* p=0.03
* p=0.03
# PyMT / mg of lung
Ketotifen
Non-dysbiosis
Dysbiosis
D
Mammary tissue mast cells sorted from non-dysbiotic or dysbiotic B6 mice
Mast cell transfer
BRPKp110 implantation
Synchronize estrus
Days Tumor -1
0
+8
+12
Analyze
Mast cell-deficient Kit w-sh/w-sh recipient mice (sash mice)
E
Mast cell- Non-dysbiosis
Mast cell - Dysbiosis
Mast cells/ mg of mammary tissue
* p=0.01
# CCR2+ mast cells/ mg of mammary tissue
F
*** p=0.0006
# BRPKp110 / ml of blood
Mast cell - Non-dysbiosis
Mast cell - Dysbiosis
G
* p=0.02
# BRPKp110 / axillary lymph node
Mast cell - Non-dysbiosis
Mast cell - Dysbiosis
H
Mast cell - Non-dysbiosis
Mast cell - Dysbiosis
FMO Spike-in
Blood
1.61
4.28
0.45
SSC
anti-GFP (BRPKp110)
Axillary lymph node
1.12
2.44
0.22
SSC
anti-GFP (BRPKp110)

Figure 2.4

Mast cells promote dissemination of HR$^+$ tumor cells in response to commensal dysbiosis.

A, Experimental scheme for ketotifen treatment in **B** and **C**. Tumor-bearing dysbiotic or non-dysbiotic mice were gavaged with ketotifen or vehicle daily starting 1-day post tumor initiation and continuing to day 5 post-tumor. Mice were evaluated 22 days post tumor initiation. **B and C,** Lungs from mice bearing advanced BRPKp110 or PyMT tumors were evaluated for disseminated GFP$^+$ BRPKp110 **(B)** or luciferase$^+$ PyMT **(C)** tumor cells 22 days post tumor initiation using flow cytometry. Numbers of disseminated PyMT were normalized to the final tumor volumes. **D,** Experimental scheme for **E-H**. Equal numbers of mast cells sorted from normal non-tumor-bearing mammary tissues of non-dysbiotic or dysbiotic C57BL/6 mice at day 0, followed by transfer into the inguinal mammary fat pad of mast cell-deficient *Kit$^{w\text{-}sh/w\text{-}sh}$* mice. After 18 hours post transfer, BRPKp110 tumor cells were injected into the same mammary fat pad of *Kit$^{w\text{-}sh/w\text{-}sh}$* recipient mice that received the mast cell transfer. Twelve days post tumor implantation, adjacent mammary tissues were evaluated for transferred mast cells whereas blood and distal axillary lymph nodes were evaluated for disseminated GRP$^+$ tumor cells. **E,** Flow cytometry was utilized to quantitate absolute numbers of mast cells and CCR2$^+$ mast cells remaining post-transfer from the adjacent mammary tissues of tumor-bearing *Kit$^{w\text{-}sh/w\text{-}sh}$* mice. Numbers represent mast cells/milligram of mammary tissue. **F-H,** Dissemination of GFP$^+$ BRPKp110 tumor cells was quantitated from the peripheral blood **(F)**, and tumor-draining axillary lymph nodes **(G)** by flow cytometry 12 days post tumor initiation in *Kit$^{w\text{-}sh/w\text{-}sh}$* mice. **H,** Representative density flow cytometry plots showing GFP$^+$ BRPKp110 tumor cells in the peripheral blood and tumor-draining axillary lymph nodes of *Kit$^{w\text{-}sh/w\text{-}sh}$* mice. FMO spike-in represents a gating control of blood or lymph nodes spiked with BRPKp110 tumor cells, minus the anti-GFP antibody. Numbers represent the percentage of gated GFP$^+$ tumor cells of CD45 negative cells. Cumulative of two independent experiments with 3 mice/group. Each symbol represents an individual mouse, and statistical significance was determined by two-tailed Mann-Whitney *U* test.

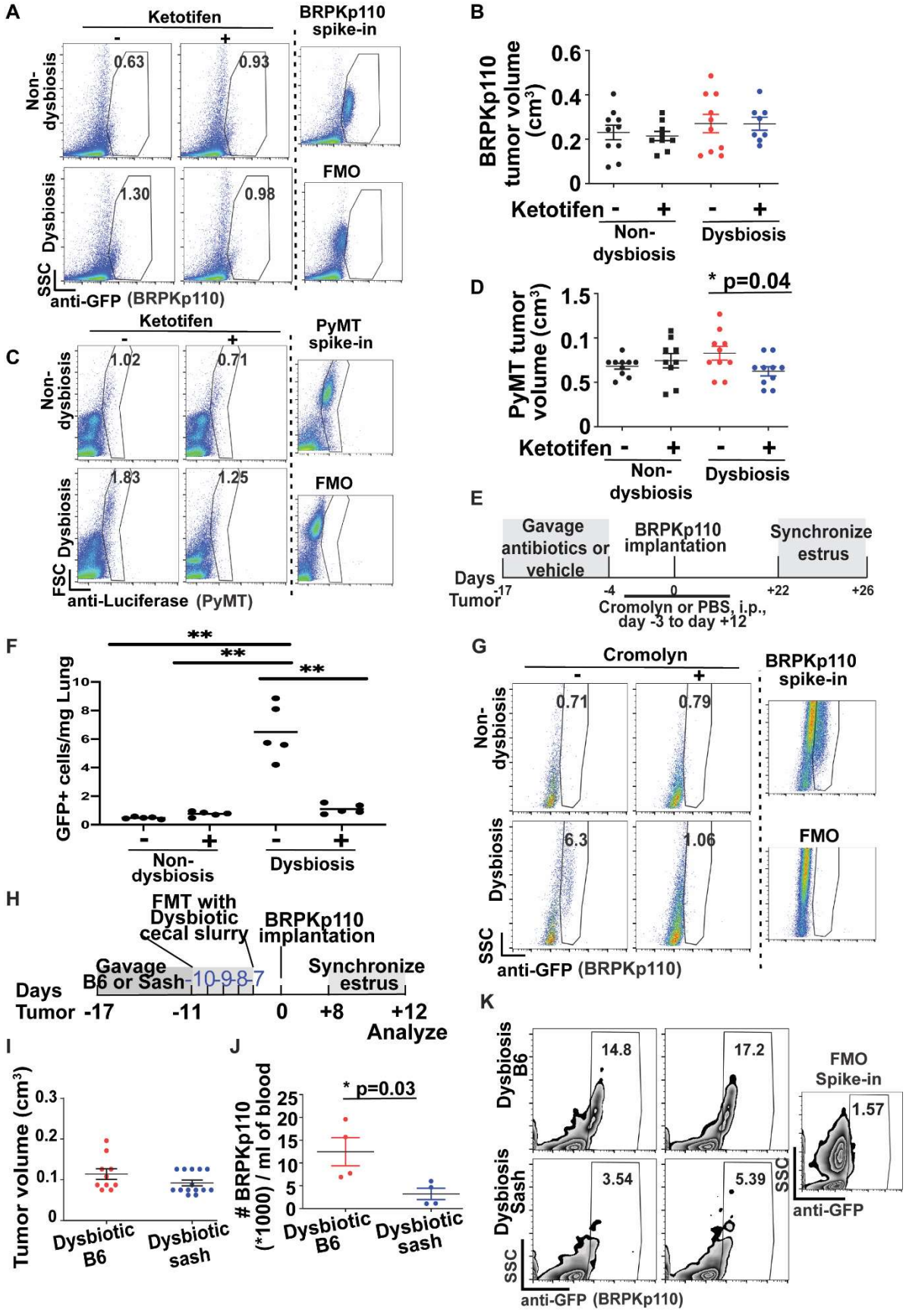
A
Ketotifen
BRPKp110 spike-in
Non-dysbiosis
Dysbiosis
0.63
0.93
1.30
0.98
FMO
SSC
anti-GFP (BRPKp110)
B
BRPKp110 tumor volume (cm3)
Ketotifen
Non-dysbiosis
Dysbiosis
C
PyMT spike-in
1.02
0.71
1.83
1.25
FSC
anti-Luciferase (PyMT)
D
PyMT tumor volume (cm3)
* p=0.04
E
Gavage antibiotics or vehicle
BRPKp110 implantation
Synchronize estrus
Days Tumor
-17
-4
0
+22
+26
Cromolyn or PBS, i.p., day -3 to day +12
F
GFP+ cells/mg Lung
**
G
Cromolyn
0.71
0.79
6.3
1.06
H
FMT with Dysbiotic cecal slurry
BRPKp110 implantation
Gavage B6 or Sash
-10-9-8-7
Synchronize estrus
Days Tumor
-17
-11
0
+8
+12
Analyze
I
Tumor volume (cm3)
Dysbiotic B6
Dysbiotic sash
J
BRPKp110 (*1000) / ml of blood
* p=0.03
K
Dysbiosis B6
Dysbiosis Sash
14.8
17.2
3.54
5.39
FMO Spike-in
1.57
anti-GFP

Figure 2.5

Mast cells enhance dissemination of HR$^+$ tumor cells in response to a dysbiotic microflora.

A, Representative plots demonstrating GFP$^+$ BRPKp110 cells in the lungs of mice 22 days post tumor initiation treated with or without Ketotifen. **B,** Final tumor volumes of BRPKp110 tumor-bearing mice treated with or without ketotifen 22 days post tumor-initiation (see experimental layout Figure 2.4A). **C,** Representative plots demonstrating luciferase$^+$ PyMT cells in the lungs of mice 22 days post tumor initiation treated with or without Ketotifen. **D,** Final tumor volumes of PyMT tumor-bearing mice treated with or without ketotifen 22 days post tumor-initiation (see experimental layout Figure 2.4A). **E,** Experimental scheme of F to G. Non-dysbiotic and dysbiotic mice were orthotopically implanted with BRPKp110 in the inguinal mammary fat pad at day 0. Mast cell stabilizer cromolyn (100 mg/kg) or PBS were intraperitoneally injected from 3 days prior to tumor initiation until 12 days post tumor initiation. Disseminated GFP$^+$ tumor cells in the lungs were quantified 26 days post tumor implantation. **F,** Numbers of disseminated tumor cells in the lungs were normalized to tissue weights. Each dot represents an individual mouse. **G,** Representative flow cytometry plots showing GFP$^+$ BRPKp110 cells in the lungs. For **A, C,** and **G** - the gating strategy was based upon a lung sample spiked with tumor cells and FMO controls. Numbers represent percent of gated tumor cells out of total live cells. **H,** Experimental design of **I-K**. Wild-type C57BL/6 (B6) mice and *Kit$^{w\text{-}sh/w\text{-}sh}$* (Sash) mice were gavaged with a cocktail of broad-spectrum antibiotics for 7 days followed by fecal transfer of dysbiotic cecal slurries (from wild-type C57BL/6 mice) for 4 consecutive days. The microbiome was allowed to establish for 7 days, followed by initiation of tumors using BRPKp110 tumor cells. **I,** Twelve-days post tumor implantation, tumor volumes were evaluated. Disseminated tumor cells in the peripheral blood were evaluated by flow cytometry **(J and K)**. **J,** Numbers of GFP$^+$ tumor cells in peripheral blood. **K,** Representative density flow cytometry plots showing GFP$^+$ BRPKp110 tumor cells in the peripheral blood. FMO spike-in represents a gating control of blood spiked with BRPKp110 tumor cells, minus an anti-GFP antibody. Numbers represent the percentage of gated GFP$^+$ tumor cells of CD45 negative cells. Each symbol represents an individual mouse, and statistical significance was determined by two-tailed Mann-Whitney *U* test.

CCL2-CCR2 signaling drives dysbiosis-induced mast cell accumulation in mammary tissue and subsequent early dissemination of HR$^+$ tumor cells.

Changes in mast cell numbers mirrored changes in chemokine levels of CCL2 and CXCL10[43], leading us to hypothesize that mast cells are accumulating in response to the elevation in CCL2 and/or CXCL10. To test this hypothesis, we first measured CCR2 and CXCR3 levels on mast cells in the mammary tissue of dysbiotic and non-dysbiotic mice, with the assumption that expression of CCR2 or CXCR3 corresponds with accumulation in response to each respective ligand, CCL2 or CXCL10. Analysis of mast cells from mammary tissues of non-tumor-bearing dysbiotic mice revealed that approximately 60% of mast cells expressed CCR2 compared with the 30% of mast cells expressing CCR2 from mammary tissues of non-dysbiotic mice. Importantly, no differences were observed for CXCR3-expressing mast cells between the two groups (Figure 2.6A). Notably, enrichment of a CCR2$^+$ mast cell population was also observed in Sash mice that received mast cells from dysbiotic mice (Figure 2.4E). These data suggest that mast cells are accumulating in response to CCL2, and that CCR2 expression is a signature of mammary tissue mast cells in dysbiotic mice.

To test whether mast cells accumulate in the mammary tissue in response to CCL2 signaling, CCL2 was neutralized using an antibody-based approach. Dysbiosis was established and on 8, 6, 4, and 2 days prior to tumor initiation, anti-CCL2 or an IgG isotype control were administered to mice (Figure 2.6B). Neutralization of CCL2 prior to tumor initiation significantly reduced the abundance of total (Figure 2.6C and 2.7A) and CCR2$^+$ (Figure 2.6D and 2.7B) mast cells infiltrating into adjacent mammary tissues of dysbiotic

mice. Reduced mast cell accumulation was not due to changes in tumor growth, as overall tumor burden was similar across groups (Figure 2.7C). Concomitant with the reduction of mast cells during CCL2 blockade, tumor dissemination into the peripheral blood (Figure 2.6E-F) and tumor-draining lymph nodes (Figure 2.6G-H) was significantly reduced in dysbiotic mice. Together, these results indicate that CCL2 is required for commensal dysbiosis-induced accumulation of mammary tissue mast cells and subsequent early dissemination of HR^+ tumor cells.

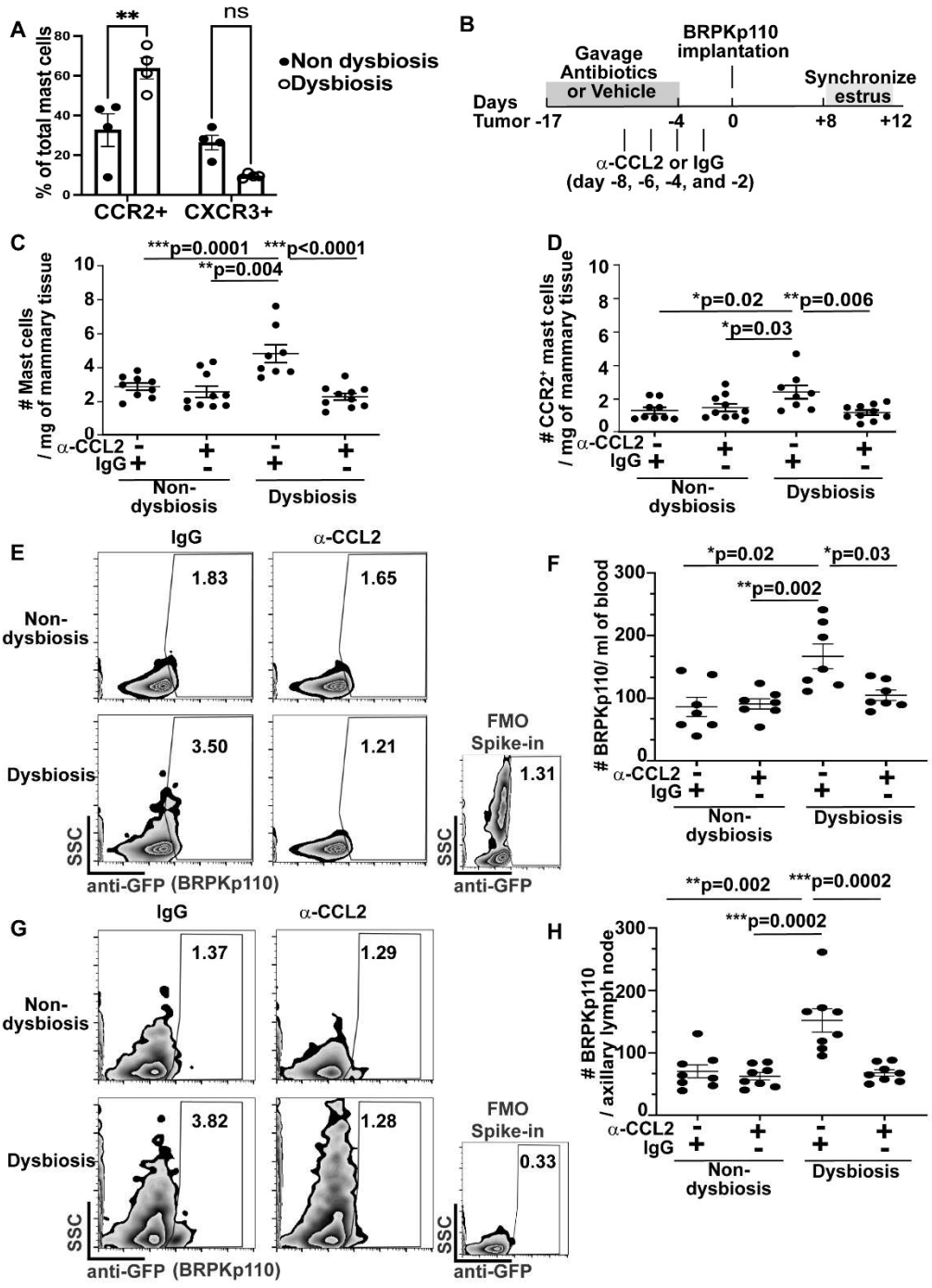
A
**
ns
% of total mast cells
Non dysbiosis
Dysbiosis
CCR2+
CXCR3+
B
BRPKp110 implantation
Gavage Antibiotics or Vehicle
Synchronize estrus
Days Tumor -17
-4
0
+8
+12
α-CCL2 or IgG (day -8, -6, -4, and -2)
C
***p=0.0001
***p<0.0001
**p=0.004
Mast cells / mg of mammary tissue
α-CCL2
IgG
Non-dysbiosis
Dysbiosis
D
*p=0.02
**p=0.006
*p=0.03
CCR2+ mast cells / mg of mammary tissue
E
IgG
α-CCL2
Non-dysbiosis
Dysbiosis
1.83
1.65
3.50
1.21
FMO Spike-in
1.31
SSC
anti-GFP (BRPKp110)
anti-GFP
F
*p=0.02
*p=0.03
**p=0.002
BRPKp110/ ml of blood
G
1.37
1.29
3.82
1.28
0.33
H
**p=0.002
***p=0.0002
BRPKp110 / axillary lymph node

Figure 2.6

CCL2-CCR2 signaling leads to dysbiosis-induced mast cell accumulation into mammary tissue and subsequent early dissemination of HR$^+$ tumor cells.

A, Mammary tissue mast cells were evaluated in dysbiotic and non-dysbiotic tumor-bearing mice at day 0, prior to tumor initiation. CCR2$^+$ and CXCR3$^+$ mammary tissue mast cells were quantitated using flow cytometry. The percentage of each mast cell population relative to total mast cells is represented. **B-H**, CCL2 blockade prior-to tumor initiation. **B,** Experimental design. Mice were intraperitoneally injected with 4 doses of anti-CCL2 or an isotype-matched control IgG 8, 6, 4 and 2 days prior-to tumor initiation. Tumors were then initiated on day 0. Mammary tissues **(C and D)** were evaluated and tumor dissemination **(E to H)** was quantified in blood and distal axillary lymph nodes 12 days-post tumor initiation. Mast cells **(C)** and CCR2$^+$ mast cells **(D)** from adjacent mammary tissues were quantitated using flow cytometry. GFP$^+$ BRPKp110 tumor cells were quantitated from the peripheral blood (representative flow plots in **E**, and tumor quantification in **F**) and distal tumor-draining axillary lymph nodes (representative flow plots in **G**, and tumor quantification in **H**). For flow plots, numbers represent the frequency of GFP$^+$ tumor cells from CD45 negative cells. Each symbol represents an individual mouse, and statistical significance was determined by two-tailed Mann-Whitney *U* test.

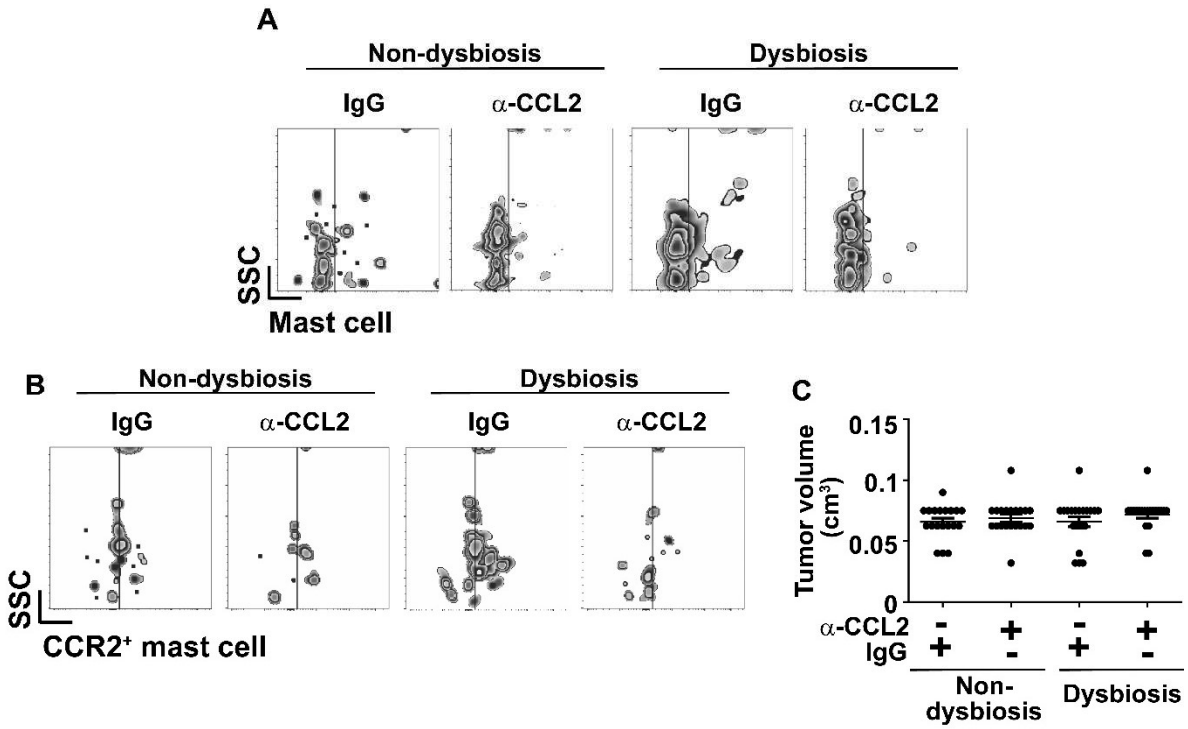

Figure 2.7

Commensal dysbiosis-induced CCL2 promotes mast cell accumulation into the mammary tissue.

A and B, Mice were intraperitoneally injected with 4 doses of anti-CCL2 or an isotype-matched control IgG prior to tumor initiation on 8, 6, 4 and 2 days prior to tumor initiation. Tumors were initiated on day 0. Mammary tissues were analyzed on day 12, similar to experimental schematic depicted in Figure 3B. Representative plots demonstrating total mast cells **(A)** and CCR2^{+} mast cells **(B)** in the mammary tissues of mice in Figure 2.6C and Figure 2.6D. **C,** Tumor volumes of anti-CCL2 antibody- or IgG-isotype treated mice 12 days post tumor implantation**.** Each symbol represents an individual tumor, and statistical significance was determined by two-tailed Mann-Whitney *U* test.

Mast cells are involved in commensal dysbiosis-mediated fibroblast activation in adjacent mammary tissues.

Mast cells contribute to fibroblast activation and tissue fibrosis in various organs in both humans and animals[111]. Activated fibroblasts, also called myofibroblasts, are involved in extracellular matrix (ECM) synthesis and remodeling, creating a conduit for tumor cells to egress out of the primary tissue and disseminate into peripheral organs[167]. To determine whether mast cells affected fibroblast activation and matrix remodeling, we first analyzed mammary tissue fibroblasts from mice prior to and during early tumor progression (Figure 2.8A). Collagen I^+ and smooth muscle actin $(SMA)^+$ were evaluated as markers of activation on fibroblasts using flow cytometry (Figure 2.9A). Commensal dysbiosis enhanced fibroblast expansion and activation in normal non-tumor-bearing mammary tissues, and this was evident prior to tumor initiation (Figure 2.8B). Although the numbers of activated fibroblasts diminished in the absence of a tumor (Figure 2.8C), tumor-bearing mice had a significant expansion of activated fibroblasts in adjacent mammary tissues of mice with pre-established commensal dysbiosis (Figure 2.8D). Collagen I protein levels in the adjacent mammary tissues of dysbiotic mice bearing BRPKp110 (Figures 2.8E, 2.9B) or PyMT (Figures 2.8F, 2.9C) tumors were similarly increased when compared with non-dysbiotic mice with equivalent tumor burden.

Using the FMT approach, transfer of a dysbiotic microflora, but not a non-dysbiotic microflora, significantly induced collagen I levels in adjacent mammary tissues of BRPKp110 tumor-bearing mice (Figures 2.8G, 2.9D). Despite not observing significant changes in tumor-associated mast cells (Figure 2.3G), tumors from dysbiotic mice had

significantly increased collagen I protein levels (Figure 2.9E), and collagen I levels in adjacent mammary tissue significantly correlated with tumor collagen I levels (Figure 2.9F). This association was not observed in tumors from non-dysbiotic mice (Figure 2.9G). Fibroblasts in mammary tumors are recruited from the adjacent mammary tissue environment[21], suggesting that dysbiosis-induced changes in tissue fibroblast activation resulted in a correspondingly increased collagen I density in mammary tumors. Altogether, our data indicate that commensal dysbiosis increases collagen levels in both mammary tissue and tumors.

We next evaluated whether mast cell accumulation into the tissue environment affects activation of tissue fibroblasts and deposition of collagen. Dysbiosis was initiated and mice were treated with the mast cell stabilizer ketotifen, as depicted in Figure 2.3A. Ketotifen significantly reduced the accumulation and activation of fibroblasts in the adjacent mammary tissue of tumor-bearing mice with commensal dysbiosis (Figure 2.9H). Importantly, ketotifen significantly reduced protein levels of collagen I in the adjacent mammary tissue of dysbiotic mice (Figure 2.8H-I). Next, we investigated whether fibroblasts become activated in response to commensal dysbiosis and HR^+ tumors in the absence of mast cells. To do this, dysbiosis was initiated in wild-type and mast cell-deficient *Kit*$^{w\text{-}sh/w\text{-}sh}$ Sash mice, similar to Figure 2.5H. Compared to C57BL/6 mice, dysbiotic Sash mice had reduced numbers of collagen I^+ SMA^+ fibroblasts in the adjacent mammary tissues (Figure 2.8J-K). Finally, reducing mammary tissue mast cell accumulation by neutralizing CCL2 also reduced the abundance and activation of fibroblasts in the adjacent mammary tissue of dysbiotic mice (Figure 2.8L-M). Together,

these results suggest that commensal dysbiosis-induced mammary tissue mast cells initiate fibroblast activation and shift the tissue millieu towards a pro-fibrogenic microenvironment.

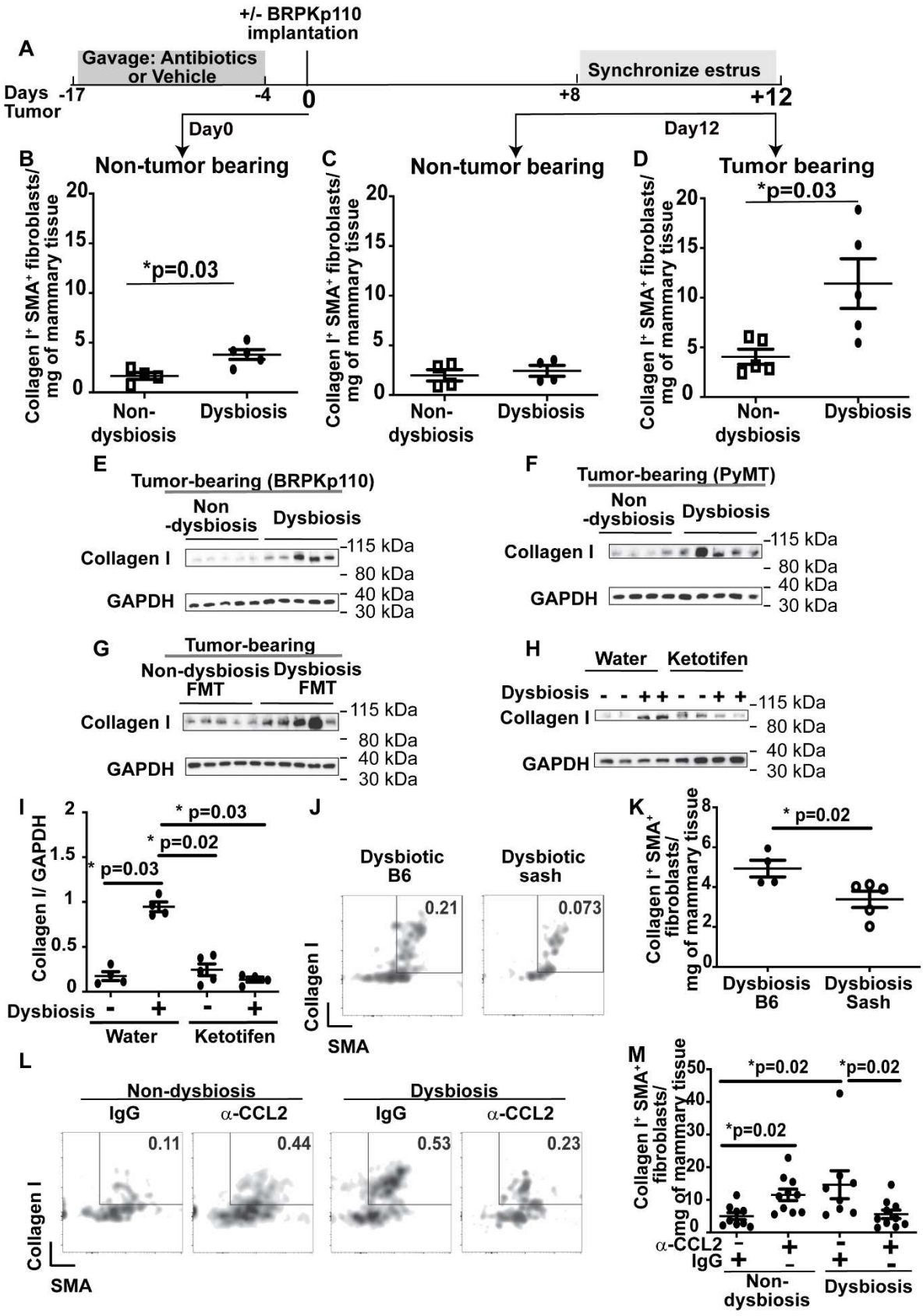
A
+/- BRPKp110 implantation
Gavage: Antibiotics or Vehicle
Synchronize estrus
Days Tumor
-17
-4
0
+8
+12
Day0
Day12
B
Non-tumor bearing
C
Non-tumor bearing
D
Tumor bearing
*p=0.03
Collagen I+ SMA+ fibroblasts/ mg of mammary tissue
Non-dysbiosis
Dysbiosis
E
Tumor-bearing (BRPKp110)
F
Tumor-bearing (PyMT)
Collagen I
GAPDH
115 kDa
80 kDa
40 kDa
30 kDa
G
Tumor-bearing
FMT
H
Water
Ketotifen
Dysbiosis
I
Collagen I/ GAPDH
* p=0.03
* p=0.02
J
Dysbiotic B6
Dysbiotic sash
0.21
0.073
Collagen I
SMA
K
* p=0.02
Dysbiosis B6
Dysbiosis Sash
L
Non-dysbiosis
IgG
α-CCL2
0.11
0.44
0.53
0.23
M
*p=0.02
α-CCL2
IgG

Figure 2.8

Commensal dysbiosis-induced mast cells activate tissue fibroblasts to produce collagen I.

A, Experimental scheme for **B-D**. Samples were collected at day 0 for **B** and +12 for **C** and **D**. **B,** Numbers of collagen I^+ SMA^+ fibroblasts in the mammary tissues of non-tumor-bearing dysbiotic or non-dysbiotic mice at day 0. **C and D,** Flow cytometric quantification of collagen I^+ SMA^+ fibroblasts in the mammary tissues from non-tumor-bearing **(C)** or adjacent mammary tissues of tumor-bearing **(D)** mice on day +12. Numbers are represented per milligram of mammary tissue. **E and F,** Protein levels of collagen I in the adjacent mammary tissues of mice bearing BRPKp110 **(E)** or PyMT **(F)** mammary tumors for 12 days. Collagen I was measured using immunoblot. GAPDH was included as a protein loading control. **G,** Mice received a fecal transplant of non-dysbiotic or dysbiotic cecal slurries prior to tumor initiation, as in Figure 2.1G. Levels of collagen I protein in the adjacent mammary tissue were evaluated 12 days post tumor implantation. **H and I,** Tumor-bearing non-dysbiotic or dysbiotic mice were treated with the mast cell stabilizer ketotifen or water as a control. Collagen I levels in the adjacent mammary tissues were evaluated by immunoblot 12 days post tumor implantation **(H)** and quantified based on GAPDH levels using ImageJ **(I)**. **J and K,** Dysbiosis was established in wild-type C57BL/6 mice (B6) or mast cell-deficient *Kit*$^{w\text{-}sh/w\text{-}sh}$ mice (Sash) as depicted in Figure 2.3I. Collagen I^+ SMA^+ fibroblasts in the mammary tissues was quantified using flow cytometry 12 days post tumor implantation. **(J)** Representative density plots depicting the percentage of collagen I^+ SMA^+ fibroblasts of total live cells. **(K)** Quantitation of total fibroblasts per milligram of mammary tissue using flow cytometry. **L and M,** anti-CCL2 antibody or control IgG were intraperitoneally injected into non-dysbiotic and dysbiotic mice prior to tumor implantation as depicted in Fig. 2.6B. At day +12, collagen I^+ SMA^+ fibroblasts in the mammary tissues were quantitated using flow cytometry. **(L)** Representative density plots depicting the percentage of collagen I^+ SMA^+ fibroblasts of total live cells. **(M)** Quantitation of total fibroblasts per milligram of mammary tissue using flow cytometry. For all flow cytometric analysis of fibroblasts, fibroblasts were identified as $CD45^+$ $CD31^-$ $gp38^+$ PDGFR-α^+ cells, as depicted in Figure 2.9A. Each symbol represents an individual mouse, and statistical significance was determined by two-tailed Mann-Whitney *U* test.

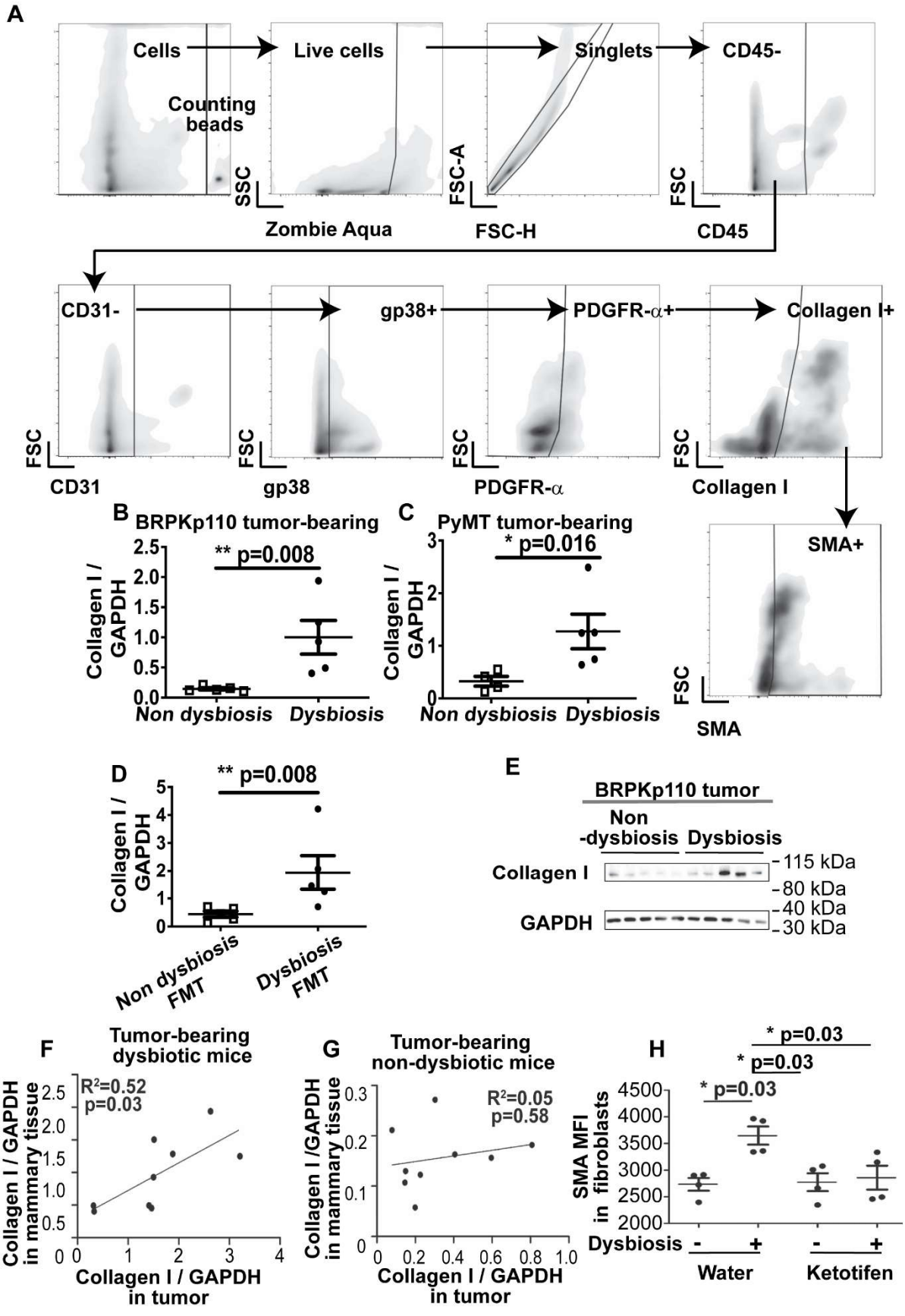
A
Cells
Live cells
Singlets
CD45-
Counting beads
SSC
Zombie Aqua
FSC-A
FSC-H
FSC
CD45
CD31-
gp38+
PDGFR-α+
Collagen I+
FSC
CD31
gp38
PDGFR-α
Collagen I
SMA+
SMA
B
BRPKp110 tumor-bearing
** p=0.008
Collagen I / GAPDH
Non dysbiosis
Dysbiosis
C
PyMT tumor-bearing
* p=0.016
Collagen I / GAPDH
Non dysbiosis
Dysbiosis
D
** p=0.008
Collagen I / GAPDH
Non dysbiosis FMT
Dysbiosis FMT
E
BRPKp110 tumor
Non -dysbiosis
Dysbiosis
Collagen I
GAPDH
115 kDa
80 kDa
40 kDa
30 kDa
F
Tumor-bearing dysbiotic mice
R²=0.52
p=0.03
Collagen I / GAPDH in mammary tissue
Collagen I / GAPDH in tumor
G
Tumor-bearing non-dysbiotic mice
R²=0.05
p=0.58
Collagen I /GAPDH in mammary tissue
Collagen I / GAPDH in tumor
H
* p=0.03
* p=0.03
* p=0.03
SMA MFI in fibroblasts
Dysbiosis
Water
Ketotifen

Figure 2.9

Protein levels of collagen I in the mammary tissue are positively correlated with collagen I protein levels in the tumors of mice with commensal dysbiosis, but not in mice without dysbiosis.

A, Gating strategy for identifying collagen I^+ SMA^+ fibroblasts. **B and C,** Collagen I levels in the mammary tissue were evaluated by immunoblot 12 days post BRPKp110 tumor implantation **(B)** or PyMT tumor implantation **(C)** and quantified based on GAPDH levels using ImageJ. **D,** Mice received a fecal transplant of non-dysbiotic or dysbiotic cecal slurries prior to tumor initiation, as in Figure 2.3I. Levels of collagen I protein in the mammary tissue were quantitated based on GAPDH protein levels using ImageJ 12 days post tumor implantation with BRPKp110. **E,** Immunoblotting of collagen I and GAPDH in tumors from non-dysbiotic and dysbiotic mice. **F and G,** Linear correlation of collagen I protein levels in the adjacent mammary tissues and tumors from dysbiotic mice **(F)** and non-dysbiotic mice **(G)**. **H,** Mean fluorescence intensity (MFI) of SMA in mammary tissue fibroblasts ($CD45^-$ $CD31^-$ $gp38^+$ PDGFR-α^+ cells) from tumor-bearing non-dysbiotic or dysbiotic mice after treatment with the mast cell stabilizer ketotifen or water, similar to Fig. 2.4H. Each symbol represents an individual mouse, and statistical significance was determined by linear correlation (C and D) or two-tailed Mann-Whitney *U* test (E).

Increased PDGF-B$^+$ mast cell numbers in dysbiotic mice correspond with increased PDGFR-α expression on fibroblasts.

Transfer of mast cells into Sash mice (Figures 2.4D-H) suggested that mast cells from dysbiotic mice were phenotypically distinct from those found in mammary tissues of non-dysbiotic mice. To address this hypothesis, we first evaluated expression levels of genes related to pro-fibrogenic pathways from mast cells sorted from adjacent mammary tissues and tumors of dysbiotic and non-dysbiotic mice after 12 days of tumor progression. The expression of *Pdgfb* was increased in mammary tissue mast cells from tumor-bearing dysbiotic mice, while other pro-fibrogenic mediators, including *Mcpt4*, *Mcpt5*, *Mcpt2*, *Pdgfa*, and *Tgfb1*, remained unchanged (Figure 2.10A). The mast cell marker *Cpa3* remained comparable between the two groups (Figure 2.10A). Interestingly, tumor-associated mast cells from dysbiotic mice also showed phenotypic differences, with increased *Mcpt2*, *Pdgfb*, and *Cpa3* expression compared to tumor-associated mast cells from non-dysbiotic mice (Figure 2.10B). These data suggest that the phenotype of mast cells is greatly influenced by dysbiosis-induced changes to the local tissue environment.

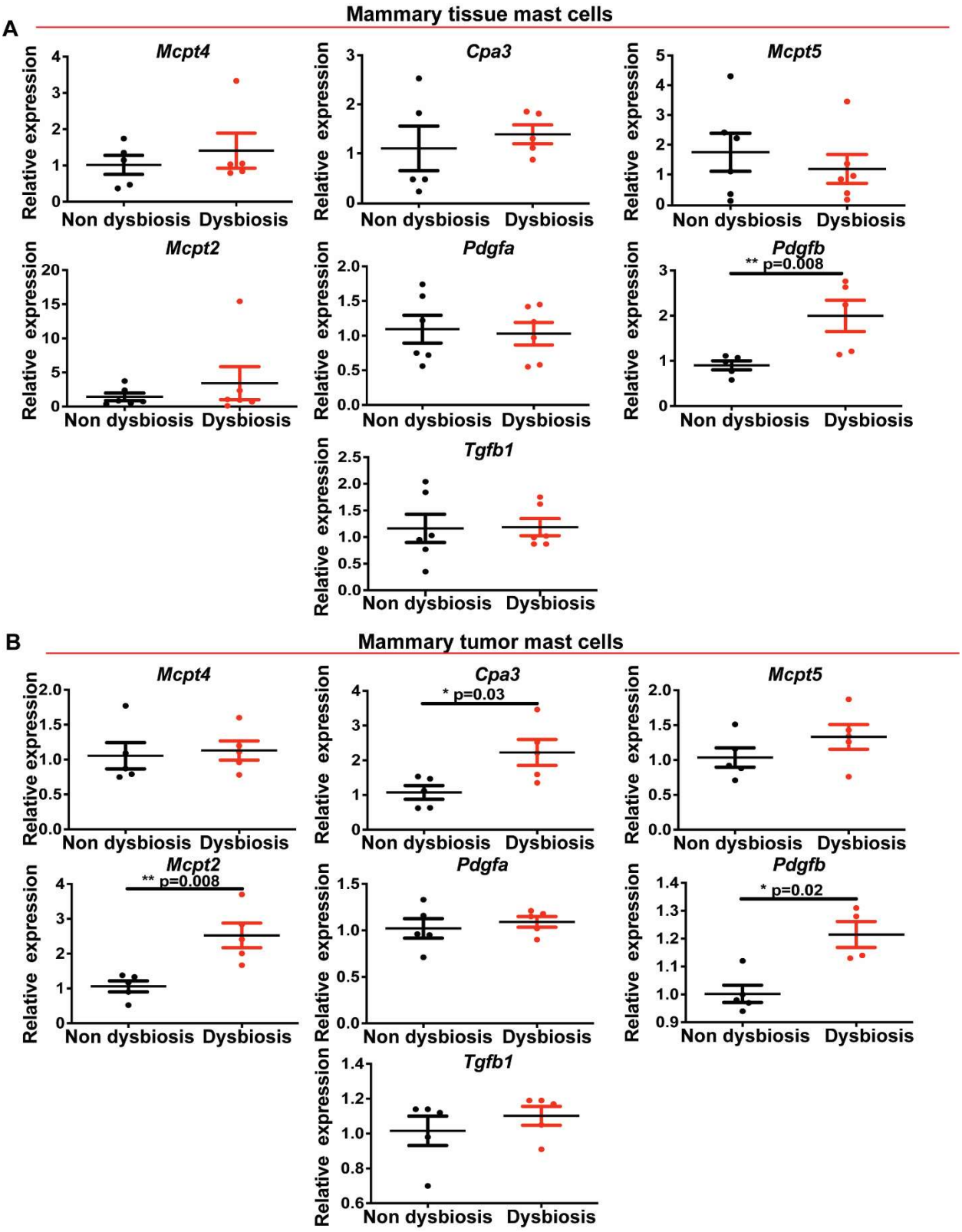
A
Mammary tissue mast cells
Mcpt4
Cpa3
Mcpt5
Mcpt2
Pdgfa
Pdgfb
** p=0.008
Tgfb1
Relative expression
Non dysbiosis
Dysbiosis
B
Mammary tumor mast cells
Mcpt4
Cpa3
* p=0.03
Mcpt5
Mcpt2
** p=0.008
Pdgfa
Pdgfb
* p=0.02
Tgfb1
Relative expression
Non dysbiosis
Dysbiosis

Figure 2.10

Mast cells from adjacent mammary tissues and tumors of dysbiotic tumor-bearing mice are phenotypically distinct from mast cells in non-dysbiotic mice.

Mast cells were sorted from adjacent mammary tissues **(A)** or tumors **(B)** of dysbiotic or non dysbiotic mice during early tumor progression. RNA was extracted from sorted cells and relative expression of each gene was measured using semi-quantitative PCR. Relative gene expression levels were calculated based upon CT value for each gene/sample and normalized to the averaged CT values of GAPDH and β-actin. Each symbol represents an experimental replicate, and statistical significance was determined by two-tailed Mann-Whitney *U* test.

Pro-fibrogenic mediator platelet-derived growth factor B (PDGF-B) is known to be involved in mast cell-mediated activation of fibroblasts[168]. Indeed, prior to tumor initiation, numbers of PDGF-B-expressing mast cells in mammary tissues of dysbiotic mice were significantly increased compared to mast cells in mammary tissues of non-dysbiotic mice (Figure 2.11A). Importantly, PDGF-B$^+$ mast cell numbers remained significantly elevated in adjacent mammary tissues during early tumor progression (Figure 2.11B), and changes in PDGF-B-expressing mast cell numbers corresponded with a significant increase in the expression of platelet-derived growth factor receptor alpha (PDGFR-α), the receptor for PDGF-B, on mammary tissue fibroblasts prior to (Figure 2.11C) and during tumor progression (Figure 2.11D). Global protein levels of PDGF-B in the mammary tissue were also measured using immunoblot. Similar to that observed in mast cells, dysbiotic tumor-bearing mice had enhanced PDGF-B protein levels in adjacent mammary tissues compared to non-dysbiotic mice (Figures 2.12A-B). A dysbiotic microflora was also found to be sufficient to induce PDGF-B protein levels in adjacent mammary tissues (Figure 2.12C-E). Importantly, tumor-bearing Sash mice had significantly lower levels of PDGF-B in response to FMT-induced dysbiosis, when compared to wild-type mice with dysbiosis (Figure 2.12F-G). As expected, a mast cell deficiency also reduced levels of tryptase in the mammary tissue (Figure 2.12F and 2.12H). Transforming growth factor beta-1 (TGF-β1) is another potent pro-fibrogenic and pro-metastatic mediator in multiple disease models, including breast cacer[169]. However, total protein levels of TGF-β1 in the adjacent mammary tissues and tumors of dysbiotic and non-dysbiotic mice were comparable (Figure 2.12I-J). These results suggest that TGF-β1 is not a major mediator of dysbiosis-mediated fibroblast activation and subsequent HR$^+$ tumor dissemination. All together,

these data implicate mast cell-mediated PDGF signaling in the activation of mammary tissue fibroblasts during commensal dysbiosis.

To test whether mammary tissue mast cells from dysbiotic mice promote fibrosis via PDGF signaling, mast cells sorted from mammary tissues of dysbiotic or non-dysbiotic mice were cocultured with NIH-3T3 fibroblasts for 24 hours (Figure 2.11E). The following day, activation of PDGFR-α-positive and PDGFR-α-negative fibroblasts was evaluated by measuring expression levels of SMA and collagen I using flow cytometry. Mast cells sorted from mammary tissues of dysbiotic mice induced significantly greater levels of SMA and increased levels of collagen I in the PDGFR-α^+ population of fibroblasts (Figure 2.11F and 2.11G). Although the collagen levels between PDGFR-α^+ fibroblasts cultured with dysbiotic versus non-dysbiotic mast cells were not significantly different, collagen I levels were significantly increased when comparing NIH-3T3 fibroblasts cultured alone versus those cultured with mast cells from dysbiotic mice (Figure 2.11F and 2.11I). On the other hand, mast cells from dysbiotic mice induced similar levels of SMA and collagen I in PDGFR-α^- fibroblasts (Figure 2.11F, 2.11H and 2.11J), suggesting that PDGF signaling may be involved in mast cell-mediated fibroblast activation. Indeed, when mast cells sorted from adjacent mammary tissues of dysbiotic mice 6 days after tumor initiation were incubated with the fibroblasts and the tyrosine kinase inhibitor imatinib, to inhibit PDGF signaling, there was a significant reduction in activation of all fibroblasts as measured by both SMA and collagen I levels (Figure 2.11K-M), further implicating that mast cell-derived PDGF signaling mediates fibroblast activation and collagen I production to establish a pro-metastatic tissue microenvironment.

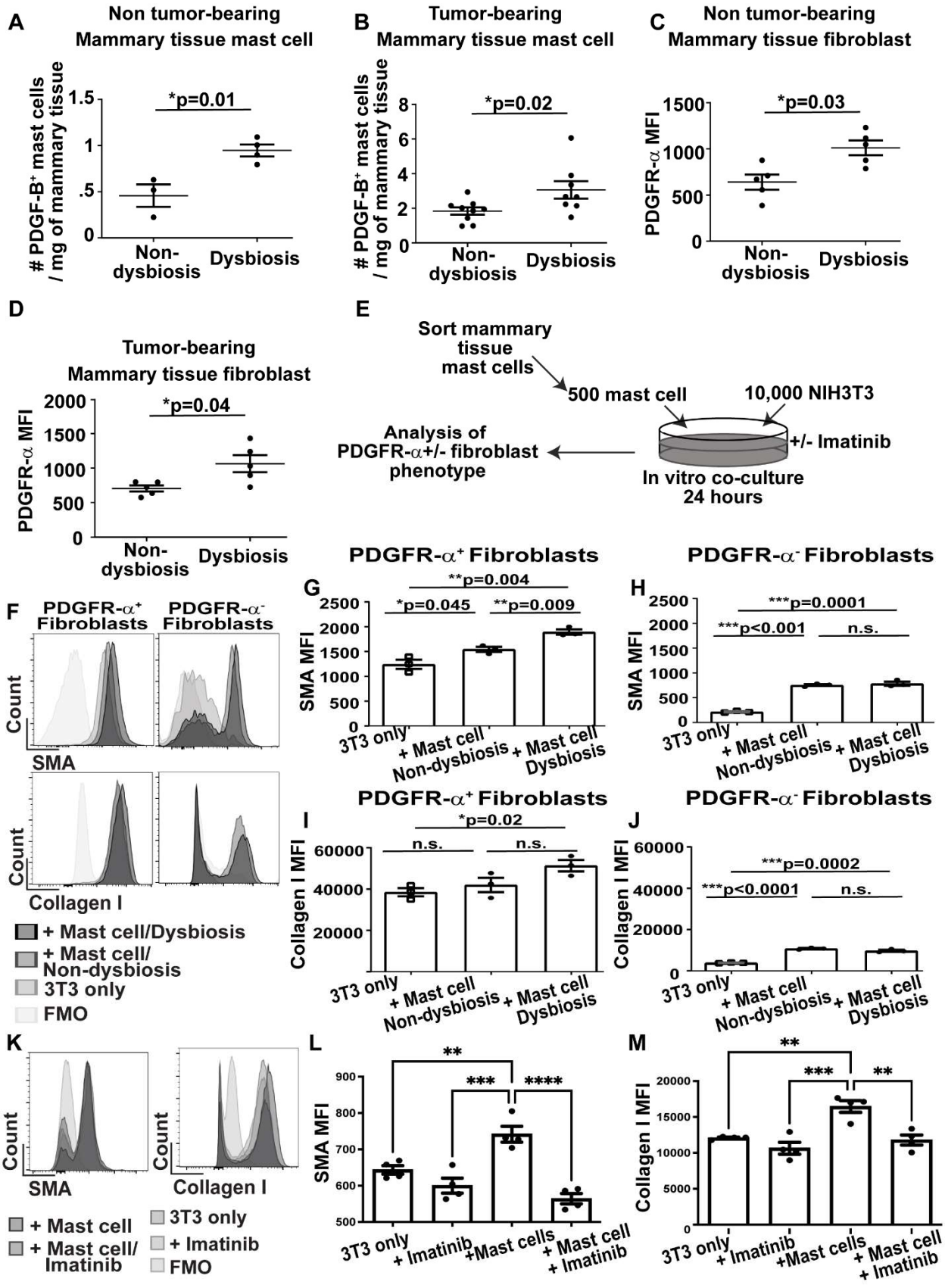
A
Non tumor-bearing
Mammary tissue mast cell
PDGF-B+ mast cells / mg of mammary tissue
*p=0.01
Non-dysbiosis
Dysbiosis
B
Tumor-bearing
Mammary tissue mast cell
*p=0.02
C
Non tumor-bearing
Mammary tissue fibroblast
PDGFR-α MFI
*p=0.03
D
Tumor-bearing
Mammary tissue fibroblast
*p=0.04
E
Sort mammary tissue mast cells
500 mast cell
10,000 NIH3T3
+/- Imatinib
Analysis of PDGFR-α+/- fibroblast phenotype
In vitro co-culture 24 hours
F
PDGFR-α+ Fibroblasts
PDGFR-α- Fibroblasts
Count
SMA
Collagen I
+ Mast cell/Dysbiosis
+ Mast cell/ Non-dysbiosis
3T3 only
FMO
PDGFR-α+ Fibroblasts
PDGFR-α- Fibroblasts
G
SMA MFI
**p=0.004
*p=0.045
**p=0.009
3T3 only
+ Mast cell Non-dysbiosis
+ Mast cell Dysbiosis
H
***p=0.0001
***p<0.001
n.s.
PDGFR-α+ Fibroblasts
PDGFR-α- Fibroblasts
I
Collagen I MFI
*p=0.02
n.s.
J
***p=0.0002
***p<0.0001
K
Count
SMA
Collagen I
+ Mast cell
+ Mast cell/ Imatinib
3T3 only
+ Imatinib
FMO
L
SMA MFI
**
***
****
3T3 only
+ Imatinib
+Mast cells
+ Mast cell + Imatinib
M
Collagen I MFI

Figure 2.11

During early tumor progression, commensal dysbiosis increases expression of PDGF-B$^+$ on mast cells with corresponding increases in PDGF receptor expression on fibroblasts.

A and B, Numbers of PDGF-B$^+$ mast cells in the mammary tissues from non-tumor-bearing **(A)** and tumor-bearing mice **(B).** Mast cells were quantitated using flow cytometry on mammary tissues disassociated into single cell suspensions on day +12, as depicted in Figure 2.3D. **C and D**, Evaluation of PDGFR-α staining intensity (mean fluorescent intensity - MFI) in mammary tissue fibroblasts from non-tumor-bearing **(C)** and tumor-bearing mice **(D)**. Each symbol represents an individual mouse, and statistical significance was determined by two-tailed Mann-Whitney *U* test. **E to M,** NIH-3T3 fibroblasts were co-cultured with mast cells that were sorted from mammary tissues of non-dysbiotic or dysbiotic mice at day 0 (**F-J**) or from adjacent mammary tissues of dysbiotic mice 6 days post-tumor-initiation (**K-M**). **E**, sorted mast cells were plated with NIH-3T3 fibroblasts at a ratio of 1:20. In some cultures, NIH-3T3 fibroblasts were plated without mast cells as negative controls or with imatinib, to inhibit PDGF signaling. After 24 hours co-culture with day 0 mast cells, the intensity of SMA and collagen I were measured using flow cytometry of either CD45$^-$ PDGFR-α^+ **(G and I)** or CD45$^-$ PDGFR-α^- **(H and J)** fibroblast populations in each well, using mean fluorescent intensity (MFI) as the readout. For **K-M**, total fibroblast populations co-cultured with mast cells sorted from adjacent tissues of dysbiotic mice 6-days-post tumor initiation in the presence or absence of imatinib using flow cytometry to measure MFI of SMA (**L**) or collagen I (**M**). **F** and **K**, Representative histogram overlays of SMA and collagen I expression in CD45$^-$ PDGFR-α^+ NIH-3T3 cultured with mammary tissue mast cells from non-dysbiotic or dysbiotic mice (**F**) or dysbiotic mice with or without imatinib (**K**). The fluorescence minus one (FMO) controls represent gating controls for stained NIH-3T3 cell, minus anti-SMA or anti-collagen I antibody. Each symbol represents an experimental replicate, and statistical significance was determined by two-tailed unpaired t-test.

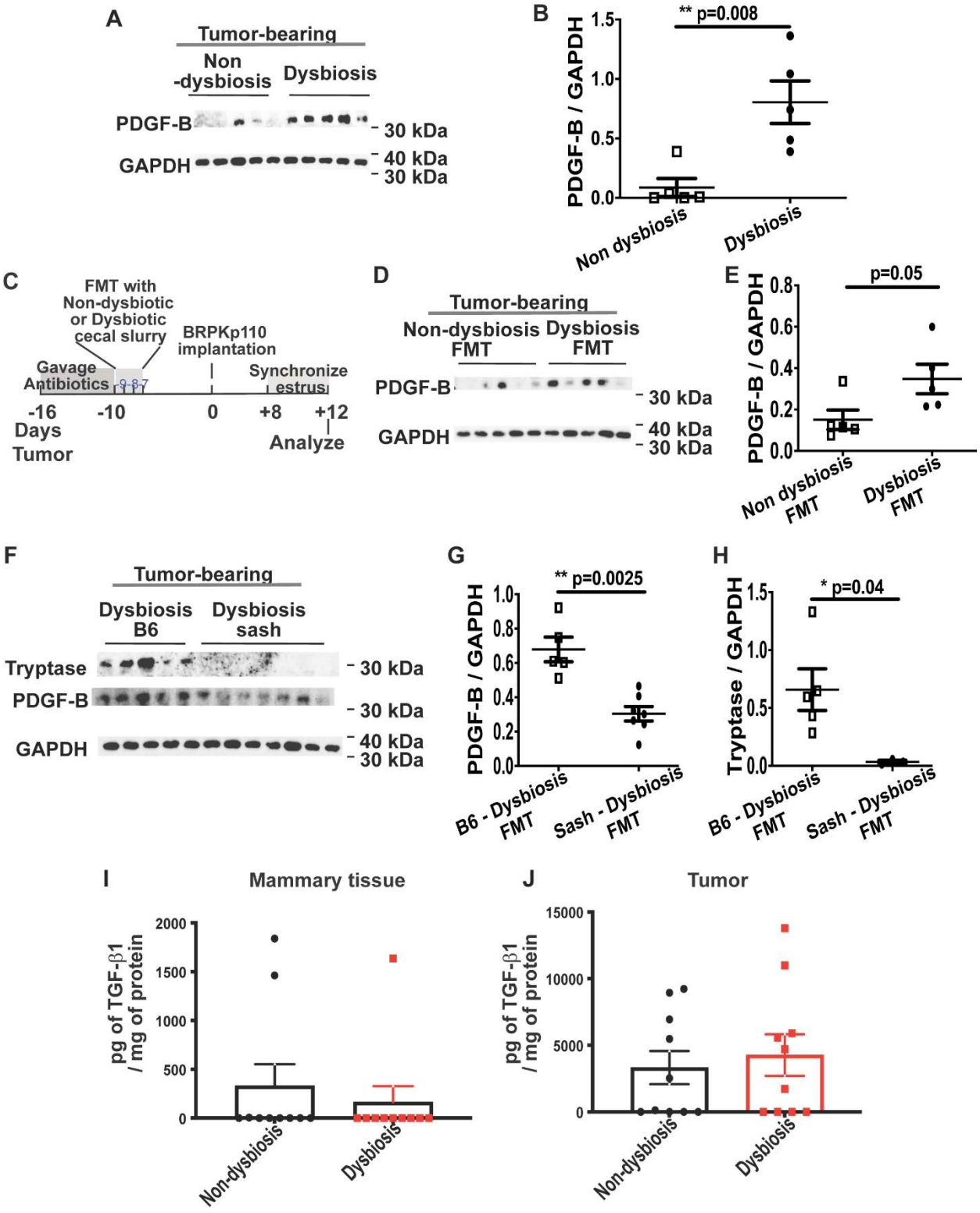
A
Tumor-bearing
Non -dysbiosis
Dysbiosis
PDGF-B
GAPDH
30 kDa
40 kDa
30 kDa
B
** p=0.008
PDGF-B / GAPDH
1.5
1.0
0.5
0.0
Non dysbiosis
Dysbiosis
C
FMT with Non-dysbiotic or Dysbiotic cecal slurry
BRPKp110 implantation
Gavage Antibiotics
Synchronize estrus
-16
-10
0
+8
+12
Days Tumor
Analyze
D
Tumor-bearing
Non-dysbiosis FMT
Dysbiosis FMT
PDGF-B
GAPDH
30 kDa
40 kDa
30 kDa
E
p=0.05
PDGF-B / GAPDH
0.8
0.6
0.4
0.2
0.0
Non dysbiosis FMT
Dysbiosis FMT
F
Tumor-bearing
Dysbiosis B6
Dysbiosis sash
Tryptase
PDGF-B
GAPDH
30 kDa
30 kDa
40 kDa
30 kDa
G
** p=0.0025
PDGF-B / GAPDH
1.0
0.8
0.6
0.4
0.2
0.0
B6 - Dysbiosis FMT
Sash - Dysbiosis FMT
H
* p=0.04
Tryptase / GAPDH
1.5
1.0
0.5
0.0
B6 - Dysbiosis FMT
Sash - Dysbiosis FMT
I
Mammary tissue
pg of TGF-β1 / mg of protein
2000
1500
1000
500
0
Non-dysbiosis
Dysbiosis
J
Tumor
pg of TGF-β1 / mg of protein
15000
10000
5000
0
Non-dysbiosis
Dysbiosis

Figure 2.12

Commensal dysbiosis increases protein levels of profibrogenic mediator PDGF-B in the mammary tissues and on mammary tissue-associated mast cells of tumor-bearing mice.

A, Immunoblot of PDGF-B from mammary tissue lysates of BRPKp110 tumor-bearing mice with or without commensal dysbiosis. **B,** PDGF-B levels in the mammary tissue were evaluated by immunoblot 12 days post BRPKp110 tumor implantation and quantified based on GAPDH levels using ImageJ. **C,** Experimental schematic for D and E. Mice received a fecal transplant of non-dysbiotic or dysbiotic cecal slurries prior to tumor initiation. **D,** Immunoblot of PDGF-B or GAPDH as a protein loading control in mice receiving a fecal transfer (FMT) with normal or dysbiotic fecal slurry. **E**, Quantitation of PDGF-B levels in the mammary tissue based on GAPDH levels using ImageJ. **F,** Tumor-bearing dysbiotic C57BL/6 mice (B6) and mast cell-deficient *Kit*$^{w\text{-}sh/w\text{-}sh}$ mice (Sash) were reconstituted with a dysbiotic cecal flora as demonstrated in B. Mammary tissues were analyzed 12 days post tumor initiation. Protein levels of tryptase and PDGF-B in the mammary tissues were determined by western blot. GAPDH served as a protein loading control. **G,** Quantitation of mammary tissue PDGF-B levels from the blot in F, based on GAPDH levels using ImageJ. **H,** Quantitation of mammary tissue Tryptase levels from the blot in F based on GAPDH levels using ImageJ. **I and J,** TGF-β1 protein levels from adjacent mammary glands **(I)** or paired tumors **(J)** from non-dysbiotic and dysbiotic mice 12 days post tumor initiation. Each symbol represents an individual mouse, and statistical significance was determined by two-tailed Mann-Whitney *U* test.

The abundance of mammary tissue-mast cells associates with increased collagen levels and metastatic recurrence in patients with HR$^+$ breast cancer.

To determine the clinical relevance of mast cell-mediated fibroblast activation with breast cancer, we first evaluated tissue sections from a small archival cohort (N = 14) of HR$^+$ breast cancer patients. Consecutive tissue sections were cut from pathologist-selected blocks of formalin fixed and paraffin embedded tissue specimens containing tumor-adjacent mammary tissue. Tissue sections were stained with picrosirius red to measure collagen levels and toluidine blue to enumerate mast cells. In line with our murine studies, collagen levels were positively and significantly correlated with mast cell numbers (Figure 2.13A-B), suggesting that mast cell abundance corresponds with collagen levels in HR$^+$ breast cancer patients.

We next wanted to ask whether a correlation between mast cell numbers and collagen I levels associated with increased risk of metastatic disease. To do this, we first analyzed collagen I and tryptase protein levels, a specific mast cell marker in both animal and human studies[115], from adjacent mammary tissues of tumor-bearing mice with or without commensal dysbiosis. There was a significant and positive association between collagen I and tryptase protein levels in adjacent mammary tissues from mice with dysbiosis, but not in mice without commensal dysbiosis (Figure 2.14A-B). To investigate whether this association exists in adjacent mammary tissues of patients that eventually develop metastatic disease, we evaluated a second cohort of archival tissues obtained from the Barts Cancer Institute Breast Cancer Now Tissue Bank. Within this cohort, we were able to analyze tissue samples from 18 patients diagnosed with HR$^+$ breast cancer who did

not experience metastatic recurrence in addition to 23 patients diagnosed with HR^+ breast cancer who developed metastatic disease (Table 2.1). There was a positive, although not significant, linear correlation between the numbers of mast cells and collagen levels in adjacent mammary tissues for patients that experienced a recurrence (Figure 2.14C and 2.14D). On the other hand, no association was observed in patients that did not experience a recurrence. The difference in the linear correlation between mast cells and collagen of each group was significant, indicating that depicting the data using two linear trajectories was an appropriate measure to visualize the differences between each group of patients (Figure 2.14D). Of note, the mast cell density was enriched in some patients without a recurrence, suggesting that qualitative, rather than quantitative, changes in the mammary tissue mast cell populations might be more representative for increased risk of metastatic disease.

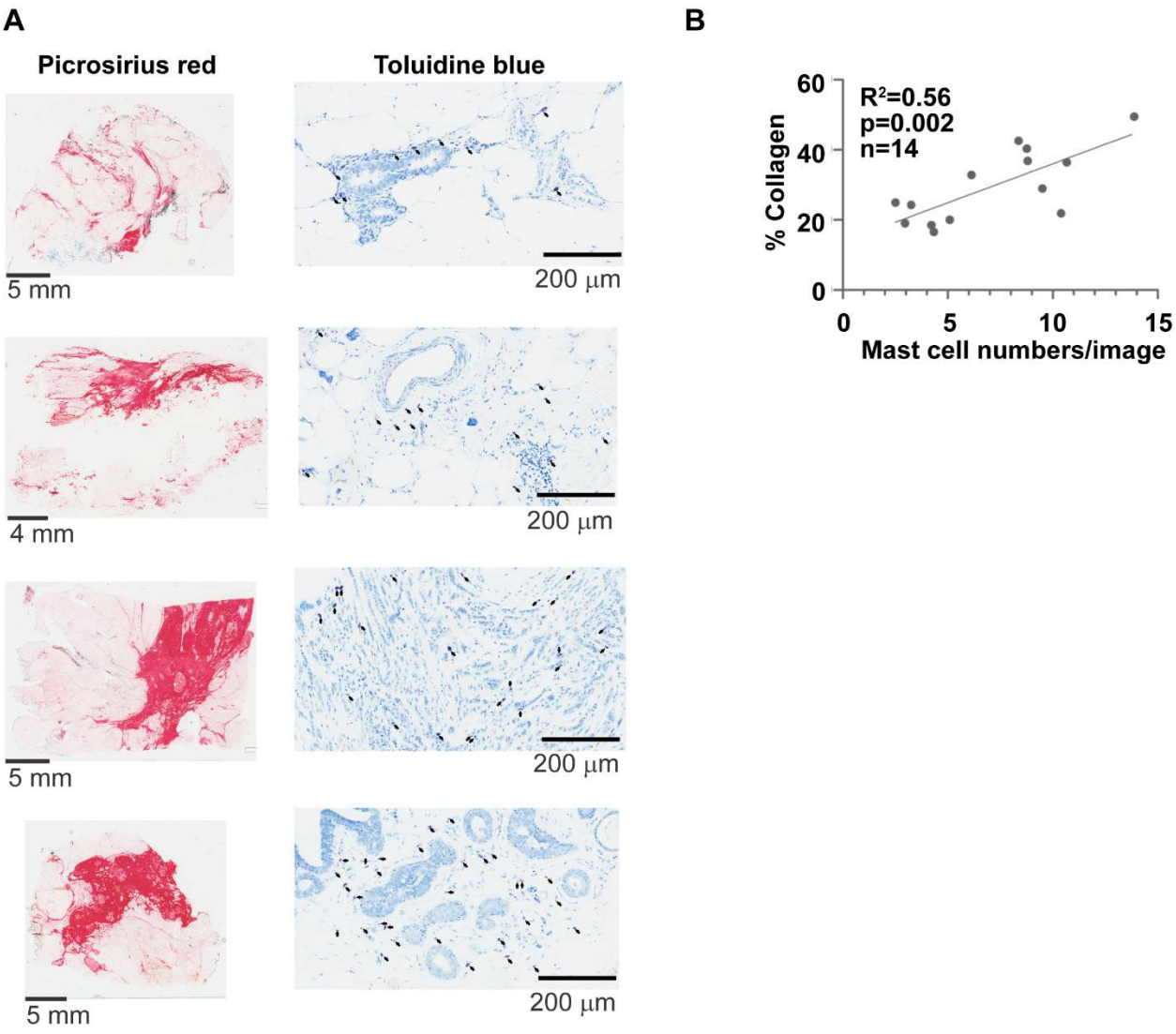
A
Picrosirius red
Toluidine blue
5 mm
200 μm
4 mm
200 μm
5 mm
200 μm
5 mm
200 μm
B
R²=0.56
p=0.002
n=14
% Collagen
Mast cell numbers/image
0
20
40
60
0
5
10
15

Figure 2.13

Mast cell abundance is positively correlated with collagen levels in breast tissues from HR^+ breast cancer patients.

A, Formalin-fixed paraffin-embedded (FFPE) breast tissues from 14 individuals previously diagnosed with HR^+ breast cancer were sectioned and stained with PicroSirus Red and toluidine blue to evaluate collagen levels and to enumerate mast cells, respectively. Representative images are shown. 1X and 20X for PicroSirus Red (scale bar = 4 mm or 5 mm as indicated in the figure) and toluidine blue (scale bar = 200 μm), respectively. **B,** Linear correlation of PicroSirus Red staining intensity versus mast cell number/image. PicroSirus Red intensity was calculated using ImageJ. Mast cells were quantitated by averaging the total mast cells counted for 15 - 20 randomly acquired 10X microscopic images, encompassing the entire tissue section. Consecutive tissue sections were evaluated for each respective stain in a blinded manner. Each symbol represents an individual human sample, and the correlation was determined by linear regression.

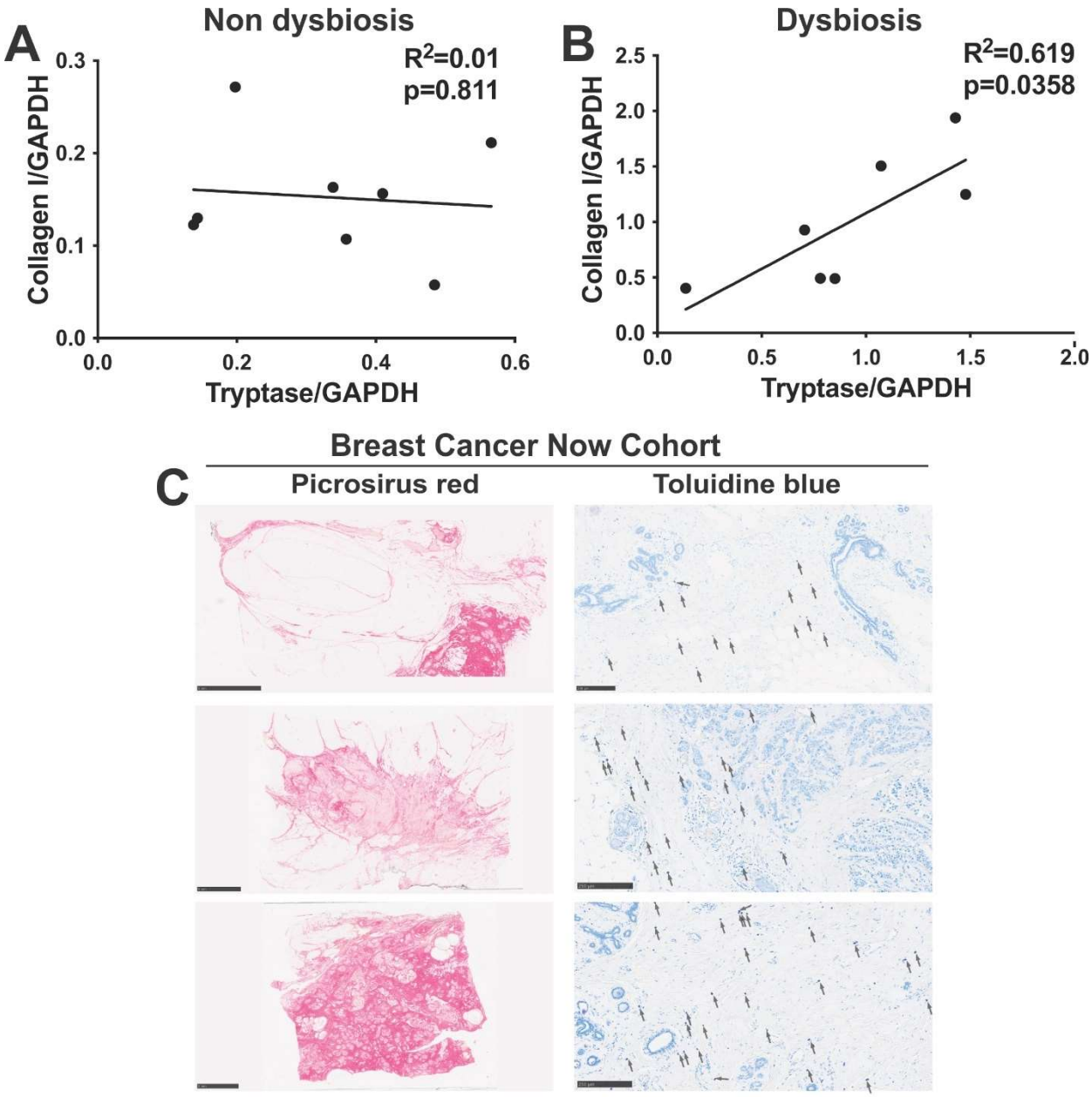
A
Non dysbiosis
R2=0.01
p=0.811
Collagen I/GAPDH
Tryptase/GAPDH
B
Dysbiosis
R2=0.619
p=0.0358
Collagen I/GAPDH
Tryptase/GAPDH
C
Breast Cancer Now Cohort
Picrosirus red
Toluidine blue
D
No Recurrence
Recurrence
*
% Collagen
Mast Cells /mm2

Figure 2.14

A positive association between mast cells and collagen I in adjacent mammary tissue of murine and patient samples that experience metastatic relapse.

A and B, Linear correlations of collagen I protein and tryptase protein in the adjacent mammary tissues from BRPKp110-bearing non-dysbiotic **(A)** and dysbiotic mice **(B)**. Protein levels of collagen I and tryptase were normalized to loading control GAPDH. **C and D,** Archival tissues specimens from patients diagnosed with HR^+ breast cancer were sectioned and stained with PicroSirus Red and toluidine blue to evaluate collagen levels and to enumerate mast cells, respectively. **C,** Representative images for PicroSirus Red (scale bar= 5 mm as indicated in the figure) and toluidine blue (scale bar= 250 μm) for patients that relapsed with metastatic disease. **D,** The percentage of PicroSirus Red-stained area in whole breast tissue sections were analyzed using ImageJ. For quantifying mast cells, average mast cell density (numbers of mast cell per mm^2) from 10-13 microscopic images from each section were measured using ImageJ. Image depicts the linear correlation of PicroSirus Red stained area versus mast cell density. Each symbol represents an individual subject. Statistical analysis was performed to determine whether the slopes for each patient cohort were statistically significant using a simple linear regression analysis and curve comparison.

Table 2.1

Breast Cancer Now cohort Meta Data		
	No Recurrence	Recurrence
Total Number of Cases	18	23
Age Range	30 - 78	34 - 77
Mean Age	57.39	55.3
Grade		
1	0	0
2	6	6
3	11	16
Unknown		1
DCIS	1	
Receptor Status		
ER+	18	23
ER-	0	0
PR+	15	18
PR-	1	1
Borderline	1	0
Not Done	1	4
Her2+	3	4
Her2-	13	13
Borderline Amplified	1	2
Borderline Non-Amplified	0	2
Not Done	1	2
Time to Recurrence Range	N/A	0 - 84
Time to Recurrence Mean	N/A	31.55
Survival Range (for 7 years in months)	6 - 84	0 - 84
Survival Mean (for 7 years in months)	79.67	64.77
Survival Number	16	7

Mast cell signatures and myofibroblastic genes are enriched in the mammary tissues of women susceptible to breast cancer.

Finally, we wanted to investigate whether the presence of mast cells and fibroblast activation may be detected in the mammary tissues of women prior to tumor diagnosis. To address this, we analyzed the transcriptomic sequencing data available from the Susan G. Komen Tissue Bank at Indiana University Simon Comprehensive Cancer Center. Normal breast tissues from either women prior to their breast cancer diagnosis (susceptible normal[15]) or age-matched healthy women were obtained. Patient characteristics are detailed in Table 5.1. Principal component analysis (PCA) uncovered a more uniform clustering of genes expressed in susceptible normal tissues while breast tissues from healthy donors had more heterogenous gene expression patterns (Figure 2.15A). Gene set enrichment analysis identified an increase in mast cell signatures[170] and PDGF-B (Table 5.2) in tissues from susceptible donors, while the breast cancer-associated myofibroblast genes[171] (Table 5.2) were significantly enriched (Figure 2.15B-C) in this subgroup, compared to those derived from healthy donors. These results raise the interesting possibility that mast cell-mediated fibroblast activation may be present prior to a tumor diagnosis. The caveats of this analysis are the limited number of samples and lack of confirmation using histological analysis of normal mammary tissues. Ideally, RNA sequencing needs to be repeated with a larger clinical cohort of susceptible versus healthy breast tissues and confirmed using immunohistochemistry to detect mast cells and fibroblasts.

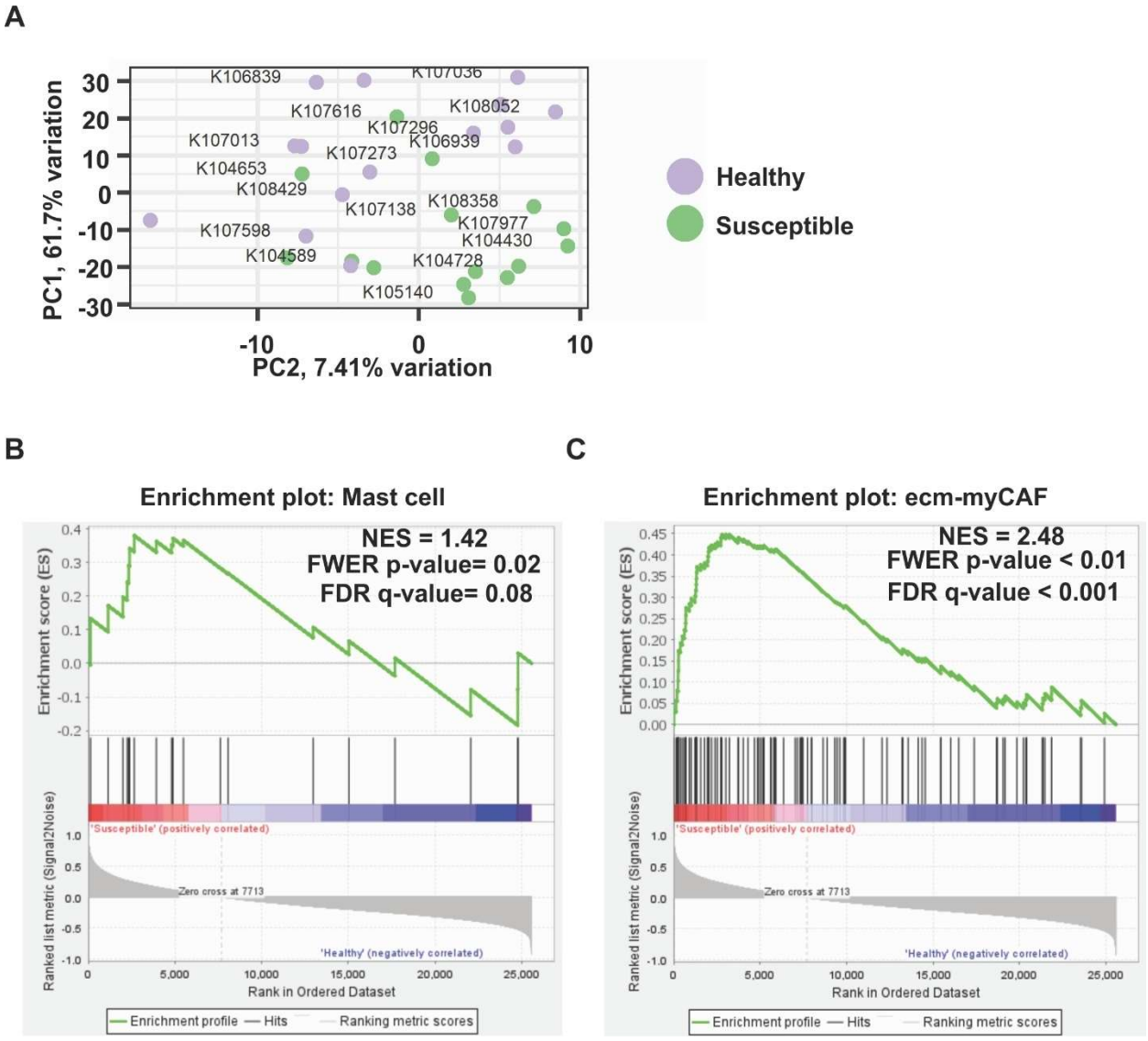

Figure 2.15

Normal breast tissues from women who later developed breast cancer have transcriptomic enrichment of mast cell and myofibroblastic gene signatures.

A, Principal component analysis (PCA) of the age-matched healthy donors and women who later went on to develop breast cancer (susceptible). **B and C,** Gene set enrichment analysis (GSEA) for mast cell **(B)** and myofibroblastic **(C)** genes was performed on the RNA-seq data. N=15 donated normal breast tissue samples per group. NES: Normalized enrichment score; FDR: False discovery rate; FWER: Familywise-error rate.

2.6 Discussion

Here, we demonstrate that mammary tissue mast cells in enhance metastatic dissemination of HR^+ tumors in response to gut commensal dysbiosis. The working model is shown in Figure 2.16. The role of mast cells in breast cancer has been controversial[172], likely due to the focus of associating quantitative changes in tumor- or lymph node-associated mast cells with outcomes instead of evaluating mast cells qualitatively. In doing so, some studies have identified a positive association with outcome[173-175] whereas others have associated mast cells with a poor prognosis[134, 176-178]. The work from Majorini *et al.* was one of the first studies to mechanistically define how mast cells influence the progression of breast tumors. In this seminal study, they demonstrated mast cells directly modulate estrogen receptor expression on breast tumor cells via activation of cMET, enhancing breast tumor growth[159]. Somasundaram *et al.* further went on to demonstrate that mast cells enhanced immune suppression and failure of immune therapy with PD-1 blockade[179].

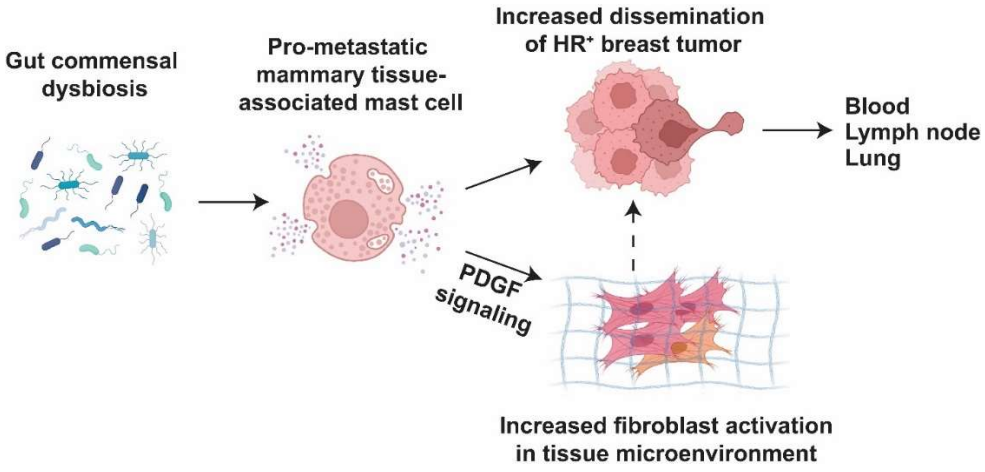

Figure 2.16 Graphical summary

In this study, we found that the mammary tissue-associated mast cells are skewed into pro-metastatic and pro-fibrogenic phenotype in response to gut commensal dysbiosis.

Mast cells are highly responsive to the microenvironment in which they reside[142], and in other non-cancer disease models induce endothelial cell tube formation[180], fibrosis[111] and inflammation[163]. Thus, it remains unknown how and when mast cell function is modulated to favor tumor growth, immune evasion, and metastasis. We observed that tumor-associated mast cells from dysbiotic mice expressed increased levels of both *Cpa3*, *Mcpt2,* and *Pdgfb* (Figure 2.10B), whereas mammary tissue-associated mast cells expressed more *Pdgfb* (Figure 2.10A). Our results demonstrate that mast cells residing in distinct tissue microenvironments are heterogenous and implicate the gut microbiome as a major contributor to mast cell functional heterogeneity. McKee and colleagues recently demonstrated that antibiotic-induced perturbations of the gut microbiome significantly increased the density of mast cells in stromal-dense regions of luminal A and B tumors, resulting in accelerated tumor growth[160]. Although we did not observe differences in tumor growth with our model of dysbiosis, this study supports the idea that changes to the gut microbiome can distally impact mast cells to favor poor breast cancer outcomes. Importantly, using our murine model, we demonstrate that microbiome-induced changes to mammary-tissue mast cells are established prior to tumor initiation.

Our findings also suggest that mast cells enhance the reservoir of tumor-associated fibroblasts through activation of tissue-associated fibroblasts[21] via PDGF signaling. Platelet-derived growth factor (PDGF)-B^+ expression in mast cells and expression of the PDGF receptor PDGFR-α in fibroblasts are increased during commensal dysbiosis. Mast cells are an important cellular source of PDGF, a well-known pro-fibrogenic signaling pathway. Indeed, mast cells sorted from mammary tissues of dysbiotic mice induced

significantly higher levels of SMA and collagen I in PDGFR-α^+ 3T3 fibroblasts after *in vitro* co-culture, compared to mast cells from non-dysbiotic mice, and activation of fibroblasts by mast cells sorted from mammary tissues of dysbiotic mice was inhibited *in vitro* with imatinib. Although PDGF signaling is associated with higher rates of breast cancer recurrence[181], treatment with the PDGF receptor inhibitor imatinib has limited efficacy in patients with metastatic HR^+ breast cancer[182-184]. Given the contribution of mast cells in the upregulation of PDGF signaling, imatinib therapy may benefit HR^+ patients with a high abundance of $PDGF^+$ mast cells in the adjacent mammary tissue or in patients with commensal dysbiosis. Alternatively, mast cell stabilizers could potentially enhance the efficacy of imatinib for these patients.

Clinically, high levels of fibrosis associate with increased invasiveness and poor outcomes for patients with breast cancer[185]. Indeed, for BRPKp110 and PyMT tumors, orthotopic models of luminal A[153, 186] and luminal B[187, 188] breast cancer, respectively, collagen levels in adjacent tissues and tumors were increased[153]. Chemical inhibition of mast cells was sufficient to reduce collagen levels, suggesting that for luminal A and B breast cancer, mast cells may be involved in increasing tissue stiffness and matrix reorganization, at least in the context of changes to the microbiome. Future studies will need to evaluate whether pre-existing dysbiosis affects the stroma and metastasis of triple negative or $HER2^+$ breast cancer subtypes.

Mechanistically, blockade of CCL2 prior to tumor initiation was sufficient to reduce mast cell accumulation and early dissemination of mammary tumor cells. These data uncover a potentially novel tumor-independent role for CCL2 in promoting metastatic spread. Although CCL2 is a well-known driver of breast tumor growth[189] and metastasis[161], tumor-independent triggers of CCL2 have not been investigated. Supporting the idea that CCL2 contributes to tissue fibrosis in the absence of tumors and negative breast cancer outcomes, Sun *et al.* demonstrated that overexpression of CCL2 in the pre-malignant mammary epithelium not only increased mammary tissue density, but also susceptibility to carcinogen-induced breast cancer[190]. Although the cell populations producing CCL2 in the mammary tissue in response to dysbiosis are undefined in our model, it is tempting to speculate that mast cells may be important for the fibrotic phenotype in the Sun *et al.* model. It would also be interesting to determine whether the CCL2-CCR2 axis is involved in programming of mast cells towards a more pro-fibrogenic phenotype.

Our analysis of transcriptomic data from normal breast tissues revealed gene enrichment of mast cell and cancer-associated fibroblast (CAF) subsets in patients who later developed breast cancer. These data suggest that, similar to CCL2[143], increased abundance of mast cells is a negative correlate of breast cancer outcomes. Because the CCL2-CCR2 axis regulates the recruitment of mast cell progenitors (Mcps) during pulmonary inflammation[90], future studies are aimed at defining whether the CCL2-CCR2 axis also regulates the recruitment of Mcps into mammary tissue, where they are matured into mast cells in response to early tumor growth. However, due to the limited sample size of this data set, making strong conclusions are not warranted until larger cohorts of

susceptible versus non-susceptible mammary tissue can be analyzed using a similar approach.

Breast cancer risk factors such as obesity, use of antibiotics, age, diet, and race, are all associated with altered composition of the commensal microbiome[66]. This highlights the necessity to define how an unbalanced commensal microbiome facilitates dissemination of breast tumor cells. There is a growing body of evidence indicating that the commensal microbiome affects multiple cancer outcomes and therapy responses[191, 192]. This study identifies a novel mechanism whereby an unbalanced and inflammatory microbiome enhances metastatic breast cancer through the promotion of cellular and molecular changes in normal mammary tissue. Considering the recent finding that specific gut microbiome differences in treatment-naïve breast cancer patients significantly associate with increased tumor aggressiveness, poor prognosis, and diminished therapy response[154], it is critical to address whether changes in the microbiome that favor metastatic breast cancer are present prior to diagnosis. Because it is not yet known how changes to the gut microbiome modulate mast cell phenotype and function, future studies will also be focused on more extensively characterizing mast cell phenotypic changes occurring in response to dysbiosis and defining how mast cells directly impact tumor cell stemness or cells in the immune environment. Importantly, to interrogate how changes in the tissue environment affect breast cancer outcomes, phenotypic evaluation of mast cells in the adjacent mammary tissues and possibly tumors of patient samples should also be performed. Based on this study, targeting mast cells in patients with early-stage

HR^+ breast cancer could serve as an adjuvant to existing therapies aimed at reducing recurrence with metastatic disease.

2.7 Author contributions and Acknowledgements

Author contributions

T. Feng: Conceptualization, formal analysis, validation, investigation, visualization, methodology, writing-original draft. **F.N. Azar**: Investigation and editing. **C.B. Rosean**: Investigation and editing. **M.T. McGinty**: Investigation and editing. **A.M. Putelo**: Investigation and editing. **S.H. Kolli**: Investigation. **S.A. Dreger**: Investigation, analysis and editing. **M.A. Carey**: Microbiome analysis. **W.J. Fowler**: Investigation, analysis and editing. **S. Greenfield**: Investigation. **S.D. Robinson**: Resources, analysis and editing. **M.R. Rutkowski**: Conceptualization, resources, analysis, visualization, supervision, funding acquisition, writing–original draft, writing–review and editing.

Acknowledgments

This study was supported by a CCR grant from Susan G Komen CCR17483602 and 1R01CA253285 from the NCI, with aid from Grant #IRG 81-001-26 from the American Cancer Society. TZF was supported by a trainee fellowship from the University of Virginia Comprehensive Cancer Center, CBR was supported by T32AI007496-21, MTM was supported by T32CA009109-46. SDR/SAD were supported by the BBSRC Institute Strategic Programme Gut Microbes and Health BB/R012490/1 and its constituent project

(BBS/E/F/000PR10355). SDR/WJF were also supported by Cancer Research UK (grant number C18281/A29019). The authors also wish to acknowledge the roles of the Breast Cancer Now Tissue Bank in collecting and making available the samples and/or data, and the patients who have generously donated their tissues and shared their data to be used in the generation of this publication. The authors are also grateful for the extrordinary support from the University of Virginia Comprehensive Cancer Center, the Center for Research Histology, Biorepository and Tissue Research Facility, Flow Cytometry Core Facility, Center for Comparative Medicine, Trans University Microbiome Initiative and the Carter Immunology Center. Additionally, we would like to thank Dr. Jose R. Conejo-Garcia for the BRPKp110 HR^+ breast tumor cell line, Dr. Paula D. Bos for the PyMT cell line, Dr. Kimberly D. Kelly for the NIH-3T3 fibroblast cell line, and Dr. Sanja Arandjelovic for critical reading of the manuscript.

Chapter 3: Future directions

In the previous chapter, I demonstrated the importance of mammary tissue mast cells during commensal dysbiosis-induced HR^+ tumor dissemination. However, how commensal dysbiosis phenotypically changes the mammary tissue mast cells remains unclear. Beyond our present research, aging is also associated with dysbiotic changes to the commensal microbiome[193] and a skewed stromal tissue environment[44], raising the possibility that mast cells could be involved in the formation of an unhealthy stromal microenvironment in aged animals and humans. Below, I will outline plans for future studies.

3.1 Investigate the cellular source(s) of dysbiosis-induced CCL2 in the mammary tissues.

We demonstrated that blockade of CCL2 prior to tumor initiation reduces mast cell accumulation in the mammary tissue, resulting in a subsequent reduction of tumor dissemination in mice with commensal dysbiosis. Although CCL2 is a well-known driver of breast tumor growth[189] and metastasis[161], tumor-independent triggers of CCL2 have not been investigated. Supporting the idea that CCL2 contributes to tissue fibrosis in the absence of tumors, Sun *et al.* demonstrated that overexpression of CCL2 in the pre-malignant mammary epithelium not only increased mammary tissue density, but also susceptibility to carcinogen-induced breast cancer[190]. However, the systemic trigger for mammary tissue CCL2 and the cell populations producing CCL2 in the mammary tissue in response to dysbiosis remain undefined. Here, I will outline experiments to identify the cells producing CCL2. The B6.Cg-*Ccl2*$^{tm1.1Pame}$/J mouse (also known as Ccl2-RFP^{flox}

mouse) has RFP expression in all CCL2-expressing cells, enabling the use of RFP expression to distinguish the cellular sources of CCL2 in the mammary tissues. As depicted in figure 3.1, commensal dysbiosis will be induced in Ccl2-RFP^{flox} mice using fecal microbiota transplantation (FMT). Antibiotics-treated Ccl2-RFP^{flox} mice will be gavaged with cecal slurries from wild-type non-dysbiotic or dysbiotic mice for 3 consecutive days. We will collect mammary tissues at day 13, 15, and 17 after the cessation of gavage. As indicated in our established model, estrus cycles will be synchronized in all experimental mice using a modified Whitten effect[43] four days prior to each endpoint. At each time point, CCL2-expressing cells will be detected using flow cytometry. The markers of immune cells, adipocytes, fibroblasts, endothelial cells, and epithelial cells are listed below: mast cells ($CD45^+Lin^-cKit^+Fc\varepsilon RI\alpha^+$), eosinophils ($CD45^+CD11b^+F4/80^+Siglec\text{-}F^+$), neutrophils ($CD45^+CD11b^+Ly6G^+F4/80^-$) , dendritic cells ($CD45^+CD11c^+MHC^+Ly6C^-Ly6G^-B220^-F4/80^-$), macrophages (M0: $CD45^+CD11b^+F4/80^+CD86^-CD206^-$; M1: $CD45^+CD11b^+F4/80^+CD86^+CD206^-$; M2: $CD45^+CD11b^+F4/80^+CD86^-CD206^+$), T cells (helper T cell: $CD45^+CD3^+CD4^+CD8^-$; cytotoxic T cell: $CD45^+CD3^+CD4^-CD8^+$), B cells ($CD45^+CD19^+B220^+$), NK cells ($CD45^+NKP46^+$), $\gamma\delta$T cells ($CD45^+CD3^+TCR\gamma\delta^+$), adipocytes ($CD45^-Adiponectin^+$), fibroblasts ($CD45^-CD31^-gp38^+PDGFR\text{-}\alpha^+$), endothelial cells ($CD45^-CD31^+$), and epithelial cells ($CD45^-EpCAM^+$). The spatial distributions and cellular interactions occurring in mammary tissues between CCL2-expressing cells and other cell types will be investigated using multiplex fluorescence imaging at the similar temporal timepoints depicted in Figure 3.1. Wild-type C57BL/6 mice with or without commensal dysbiosis will be utilized for imaging. Fluorochrome-conjugated antibodies will be used to detect the

CCL2 and CCR2 expression on the following immune or non-immune cells: mast cells (CD45, cKit, FcεRIα, Tryptase); myeloid cells (CD11b, CD206, F4/80); fibroblasts (smooth muscle actin, podoplanin); epithelial cells (pan cytokeratin); endothelial cells (CD31); adipocytes (adiponectin); and a nuclear stain. Mammary tissues will be stained by serial multiplexing, followed by imaging and analysis using the Canopy ZellScanner ChipCytometry instrument. This instrument provides quantitative single-cell resolution of cell surface and intracellular protein expression. Overall, these proposed experiments will allow us to understand the cellular source(s) of CCL2 in the mammary tissue in response to commensal dysbiosis, and the cellular interactions occurring between CCL2-expressing cells and other cell types in the mammary tissues. Indeed, we cannot rule out that other chemokines or pro-inflammatory mediators, for instance CXCL10, in mammary tissues are also increased in response to commensal dysbiosis and involved in metastatic dissemination when a tumor is present. However, our data demonstrating that increased $CCR2^+$ mast cells accumulate in mammary tissues in response to commensal dysbiosis whereas $CXCR3^+$ mast cells remain unchanged, in addition to CCL2 neutralization reducing mast cell accumulation implicate CCL2/CCR2 signaling as a major mediator of dysbiosis-induced mast cell accumulation. To determine whether additional chemokine/cytokine pathways downstream or upstream of CCL2 signaling are involved in mast cell accumulation, we will measure various chemokine/cytokines in mammary tissues from each group of mice using Luminex. This approach will allow us to more deeply understand how commensal dysbiosis shapes the mammary tissue microenvironment. Based on our data, dysbiosis-induced CCL2 also critically regulates early metastatic dissemination of HR^+ breast tumor cells. To define how dysbiosis-

induced CCL2 signaling evolves in the presence of a tumor, experiments will be repeated in mice bearing HR+ tumors BRPKp110 or PyMT for 12 days. We hypothesize that defining the cellular source of CCL2 in the mammary tissue will pave the way towards understanding how the gut microbiome influences the mammary tissue immune microenvironment, and the relevance of this pathway to metastatic breast cancer.

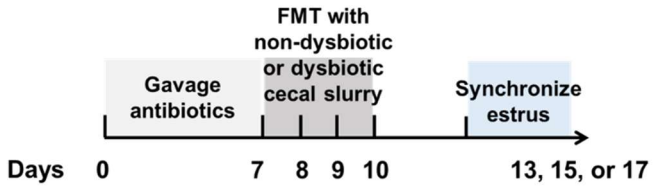

Figure 3.1 Experimental layouts of investigating the cellular source(s) of CCL2 in mammary tissue in response to dysbiotic microbiome.

We will use the above model to define the CCL2-expressing cell population(s) in mammary tissues using FMT. Specifically, Ccl2-RFP^{flox} mice will receive broad-spectrum antibiotics for 7 days, to reduce the endogenous microbiome. Antibiotic-treated mice will then be orally gavaged with cecal slurries from non-dysbiotic or dysbiotic wild type mice for 3 consecutive days. CCL2-expressing cell population(s) in the mammary tissues at day 13, 15, or 17. A modified Whitten effect will be used to synchronize estrus prior to the sample collection.

3.2 Investigate the effects of COX-1/PGE_2 signaling in the activation of mast cells in dysbiotic mice.

PGE_2 is associated with metastasis in breast cancer[194]. In our animal model, dysbiotic BRPKp110-bearing mice had significantly increased PGE_2 levels in the adjacent mammary tissues when compared to non-dysbiotic controls with comparable tumor burden (Figure 3.2A), suggesting that the elevation of PGE_2 is induced independently of primary tumor burden. Although PGE_2 is considered as a downstream product of COX2-dependent signaling in breast cancer[195], we found the protein levels of COX-1, but not COX-2, were increased in the adjacent mammary tissues in response to commensal dysbiosis (Figure 3.2B), suggesting PGE_2 is being synthesized via a COX-1-dependent axis. Importantly, treatment of dysbiotic mice with the COX-1-specific inhibitor SC-560 significantly reduced activation of fibroblasts (detected by vimentin and SMA positivity) in adjacent mammary tissues. Importantly, SC-560 treatment significantly reduced dissemination of tumor cells in the circulation (Figure 3.2C) and to distal axillary lymph nodes (Figure 3.2D) in dysbiotic mice. These data indicate that this signaling pathway is also involved in the activation of fibroblasts and facilitating early tumor dissemination.

PGE_2 can induce bone marrow-derived mast cells to degranulate through signaling via the PGE receptor EP3[124]. I would therefore want to test the hypothesis that PGE_2 regulates the release of pro-fibrogenic mediator(s) and induces early metastatic dissemination by activating mast cells through the EP3 receptor. PGE_2 can also inhibit the degranulation of mast cells by signaling through other EP receptors, such as EP2[196] and EP4[197]. Intriguingly this signaling pathway is complex, with studies demonstrating the

ability of EP receptors counteracting one another's cellular effects when co-expressed[198]. To identify EP receptor expression on the mammary tissue mast cells in response to commensal dysbiosis, we will measure the expression of EP receptors 1-4 in mammary tissue mast cells of non-dysbiotic and dysbiotic mice using real-time PCR, flow cytometry or immunoblot. We will next inhibit PGE_2 signaling via relevant EP receptors by intraperitoneally injecting EP1 inhibitor SC51089 (2 mg/kg/day[199]), EP1 and EP2 inhibitor AH6809 (0.5 mg/kg/day[200]), EP3 inhibitor L-798,106 (5 mg/kg/day[201]), or orally gavaging mice with EP4 inhibitor E7046 (150 mg/kg/day[202]), from day +6 to day +11 post BRPKp110 implantation. Mammary tissues and tumors will be collected on day +12 with the following readouts being performed: 1) Measuring protein levels of degranulation markers CD63 and CD107a on mammary tissue mast cells. Lysotracker and Annexin V will be included to measure granule content and identify degranulating mast cells, respectively. 2) Quantify $CD45^-CD31^-gp38^+PDGFR\text{-}\alpha^+SMA^+Collagen\ I^+$ myofibroblasts and protein levels of collagen I in adjacent mammary tissues. 3) Measure tumor dissemination by quantification of GFP^+ BRPKp110 cells in the blood and axillary lymph nodes. 4) Measure primary tumor volume. These proposed experiments will illustrate whether commensal dysbiosis affects the expression of the EP receptors on mammary tissue mast cells, and which EP receptor(s) might be involved in dysbiosis-mediated tumor dissemination.

Ultimately, these experiments will allow us to understand how PGE_2 signaling affects metastatic dissemination, the effects of PGE_2 on mast cell and fibroblast activation. We expect that EP3 is either upregulated in mast cells isolated from dysbiotic mammary

tissues, or that mast cells from both dysbiotic and non-dysbiotic mice express similar levels of the receptor, whereas the ligand PGE_2 is only expressed at high levels in dysbiotic mammary tissues. We would also predict EP2/4 receptors are not expressed at high levels for mast cells from dysbiotic mammary tissues. Because of the role that EP3 has during mast cell regulation, and our data demonstrating that COX-1-PGE_2 synthesis similarly affects HR^+ tumor dissemination to levels of that observed during mast cell inhibition, we would hypothesize that these two pathways are linked, and that PGE_2 induces mast cell degranulation and early metastatic dissemination through binding of EP3 on mast cells. We would hypothesize that inhibiting mast cell degranulation by blockade of EP3 would subsequently correspond to reduced fibroblast activation and macrophage polarization. Systemic inhibition of EP3 will still not exclusively define whether changes in tumor dissemination arise due to inhibition of EP3 on mast cells, unless EP3 is only expressed on mammary tissue mast cells. Measuring mast cell degranulation in the presence or absence of EP3 inhibition will help to provide evidence for the effects of EP3 on mast cells. If we identify multiple cell subsets expressing EP3 at high levels, we will consider restricting an EP3-deficiency to mast cells. However, the mice are not available on a full B6 background. A more likely approach would be to test the effects of EP3 on other cell subsets using Sash mice.

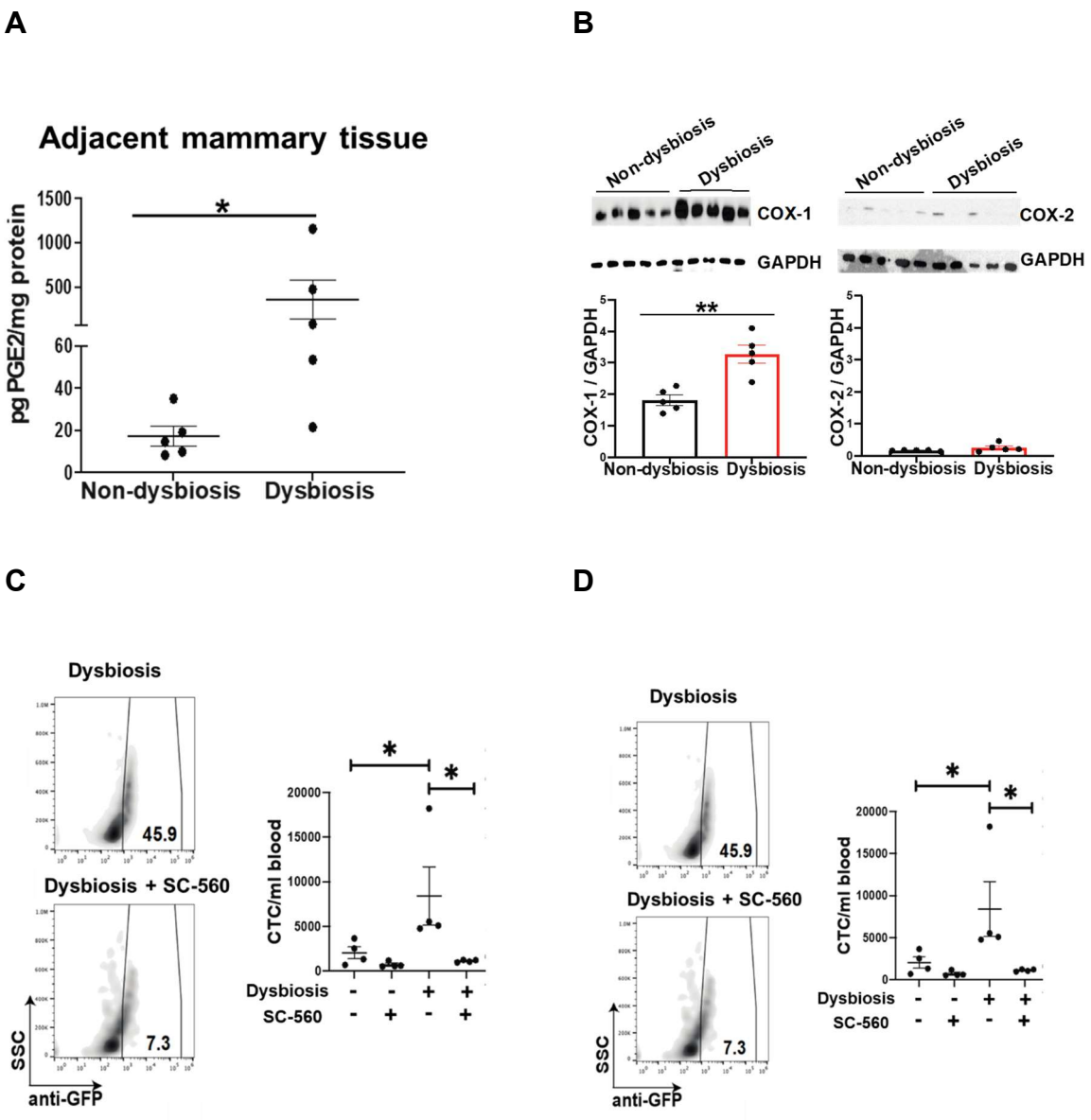
A
Adjacent mammary tissue
pg PGE2/mg protein
1500
1000
500
60
40
20
0
*
Non-dysbiosis
Dysbiosis
B
Non-dysbiosis
Dysbiosis
COX-1
GAPDH
COX-2
GAPDH
COX-1 / GAPDH
**
COX-2 / GAPDH
Non-dysbiosis
Dysbiosis
C
Dysbiosis
45.9
Dysbiosis + SC-560
7.3
SSC
anti-GFP
CTC/ml blood
20000
15000
10000
5000
0
*
*
Dysbiosis - - + +
SC-560 - + - +
D
Dysbiosis
45.9
Dysbiosis + SC-560
7.3
SSC
anti-GFP
CTC/ml blood
20000
15000
10000
5000
0
*
*
Dysbiosis - - + +
SC-560 - + - +

Figure 3.2 COX-1/PGE_2 signaling is involved in the dysbiosis-induced HR^+ tumor dissemination.

A, Measured concentration of PGE_2 in adjacent mammary tissues from day 12 BRPKp110-bearing non-dysbiotic and dysbiotic animals. PGE_2 was quantitated using a PGE_2 ELISA kit and normalized to total mammary tissue protein. **B,** Protein levels of COX-1 and COX-2 in the adjacent mammary tissues were measured using immunoblot of mammary tissue protein lysates. GAPDH was included as protein loading control. **C and D,** BRPKp110-bearing non-dysbiotic and dysbiotic mice were treated with the COX-1 specific inhibitor SC-560 (i.p. 3.34 mg/kg/day) or with an equal volume of vehicle solution from day 3 to day 11 post tumor implantation. Using flow cytometry, the numbers of GFP^+ tumor cells in the blood (**C**) and tumor-draining lymph nodes (**D**) were measured at day 12 post tumor injection. Each symbol represents a biological replicate (4-5 mice/group). Statistical significance was determined by two-tailed Mann-Whitney *U* test.

3.3 Determine whether mast cell-derived IL-13 influences the accumulation or polarization of tumor-associated macrophages in the mammary tissue microenvironment of tumor-bearing dysbiotic mice.

In our animal model (Figure 3.3A), commensal dysbiosis enhances infiltration of $CD11b^+$ myeloid cells into adjacent mammary tissues (Figure 3.3D) and tumors (Figure 3.3F) during tumor progression (12 days after tumor implantation) but not in non-tumor bearing mice (Figure 3.3B). Interestingly, M2-like macrophages, which in the context of cancer provide an immunosuppressive microenvironment, represent the major population of $CD11b^+$ myeloid cell infiltrates. A number of *in vitro* and *in vivo* studies have identified a role for tumor associated M2-like macrophages in breast cancer in the promotion of tumor cell proliferation, immunosuppression, and induction of angiogenesis[203]. Using CD163 as a marker to identify M2 macrophages, multiple studies have demonstrated that increased $CD163^+$ macrophages in the tumor stroma positively correlate with metastasis in patients diagnosed with breast cancer[204, 205]. These results suggest that the increased abundance of M2 macrophages in the mammary tissue microenvironment could facilitate dysbiosis-induced tumor dissemination.

As discussed, mast cells can shape the immune microenvironment through the release of various cytokines, chemokines, growth factors, and proteases. Recently, Finlay *et al.* found that that mast cell-derived IL-13 polarized macrophages into tolerogenic M2 phenotypes *in vitro*[140]*.* Interestingly, we also found increased levels of *Il13* transcript in mast cells isolated from the adjacent mammary tissues of tumor-bearing dysbiotic mice (Figure 3.3C). Notably, dysbiosis did not alter expression of IL-13 in tumor-associated

mast cells (Figure 3.3E), suggesting the tissue microenvironment regulates the function of mast cells. IL-4 is also able to polarize M2 macrophages. Using our antibiotics-induced dysbiosis model, we found that commensal dysbiosis did not result in a change of protein levels of IL-4 in the mammary tissues as compared with non-dysbiotic controls (Figure 3.3G-I), suggesting IL-4 may not be involved macrophage recruitment or polarization within mammary tissues. Based upon these results, I would test the hypothesis that commensal dysbiosis-induced IL-13 expression in mast cells facilitates the polarization of M2-like macrophages in the adjacent mammary tissues and that this pathway leads to early dissemination of tumors. This hypothesis will be tested by performing the following experiments outlined below.

Firstly, we will test whether *in vivo* inhibition of IL-13 signaling influences myeloid cell populations in adjacent mammary tissues. This will be done by intraperitoneal injection of tumor-bearing non-dysbiotic and dysbiotic mice with 200 μg of isotype-matched control IgG or anti-IL-13 antibody (eBio 1316H) on days 2, 4, 6, 8 and 10 post-tumor implantation. In addition to testing this hypothesis in the luminal-A-like BRPKp110 model, we will also use the luminal-B-like PyMT tumor model to identify putative tumor subtype-specific phenotypes. A modified Whitten effect will be used to synchronize estrus prior to each temporal point. On days 12 or 26 post-tumor, we will perform the following readouts: 1) Investigate the abundance of the following immune cells and fibroblasts in the adjacent mammary tissues and tumors using flow cytometry: total mast cells ($CD45^+Lin^-cKit^+Fc\varepsilon RI\alpha^+$), IL-$13^+$ and IL-4^+ mast cells, M0 ($CD45^+CD11b^+F4/80^+CD86^-CD206^-$), M1 ($CD45^+CD11b^+F4/80^+CD86^+CD206^-$), M2 ($CD45^+CD11b^+F4/80^+CD86^-CD206^+$), and

myofibroblasts ($CD45^-CD31^-gp38^+PDGFR\text{-}\alpha^+$Collagen I^+SMA^+), dendritic cells (CD45, CD11c, MHCII), NK cells (CD45, NKP46), $\gamma\delta$T cells (CD45, CD3, panTCR$\gamma\delta$), CD4 and CD8 T cells (CD45, CD3, CD4, CD8) in addition to quantitation of PD-1, TIM3, CTLA4 and TGIT to measure T cell immune suppression, CD44 and CD62L to measure T cell subsets, and IFNγ and TNFα to assess T cell function. 2) Quantify the disseminated GFP^+ BRPKp110 or $luciferase^+$ PyMT in the blood and axillary lymph nodes at the day 12 timepoint. Disseminated tumors in the lungs will be quantified 26 days post-tumor 3) Measure the protein levels of collagen I in the adjacent mammary tissues and tumors using immunoblot at all timepoints.

Secondly, we will test whether mast cells from mammary tissues of dysbiotic mice are able to polarize bone marrow-derived macrophages (BMDMs) in an IL-13-depedent manner. BMDMs will be co-cultured with mast cells at a 2:1 ratio for 3-6 days. Inhibition of IL-13-signaling will be performed by using 10 μg/ml of anti-IL-13 (eBio 1316H) antibody or by using blockade of IL-4Rα. Isotype-matched IgG1 will be included in parallel in the co-culture experiments. The expression of CD206, IL-6, and arginase-1 on or in the BMDM will be investigated using flow cytometry. Both IL-6 and arginase-1 are significantly elevated in $CD206^+$ M2-like macrophages from adjacent mammary tissues of dysbiotic mice[43]. The immune suppressive activity of mast cell-polarized BMDM will be tested using CD3/CD28-stimulated T cells. The direct effects of mast cell polarized BMDM on tumor invasion will be investigated by co-culturing with tumor spheroids or co-injection with BRPKp110 or PyMT tumor cells, at a 10:1 tumor:macrophage ratio.

Here, we will test whether mast cell-derived IL-13 induces the polarization of macrophages, thereby affecting tumor dissemination and immune suppression in HR^+ breast tumor-bearing dysbiotic mice. If the hypothesis is true, we expect that neutralization of IL-13 will reduce the abundance of M2 macrophages in the adjacent mammary tissue, and that this would lead to reduced tumor dissemination in dysbiotic mice. Because we have observed that treatment of mice with the mast cell stabilizer ketotifen results in significant reduction of $CD11b^+$ myeloid cells in dysbiotic mice (Figure 3.3J), it is possible that additional mast cell-derived factors are involved in the polarization of M2 macrophages. To identify the additional mast cell mediators, we will sort out mast cells from normal or adjacent mammary tissues of non-dysbiotic or dysbiotic mice. The adjacent mammary tissues will be collected at day +6 and +12 post tumor implantation. Mass spectrometry will be utilized to identify and quantify proteases, cytokines, chemokines, growth factors, and other protein effectors in mast cells. We will establish the co-culture of mast cells and BMDMs to define additional factors involved in macrophage proliferation and polarization by inhibiting mast cell mediators identified to be significantly different between dysbiotic versus non-dysbiotic mast cells. Together, these experiments will allow us to interrogate whether and which mast cell-derived mediators are involved in the polarization of M2 macrophage leading to increased tumor dissemination. Additionally, they will provide insight into the role of IL-13 in promoting metastatic dissemination of HR^+ breast cancer.

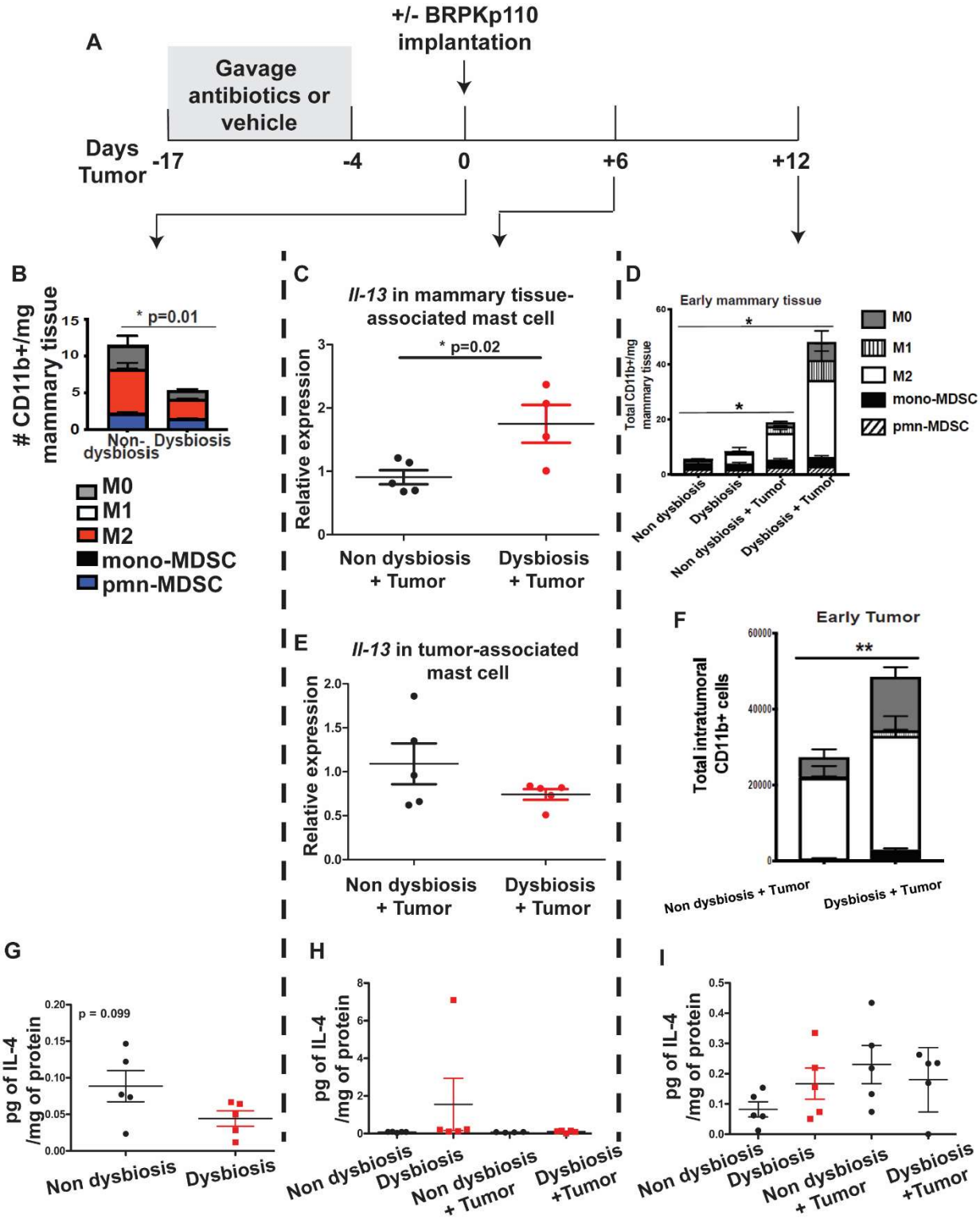
A
+/- BRPKp110 implantation
Gavage antibiotics or vehicle
Days Tumor
-17
-4
0
+6
+12
B
CD11b+/mg mammary tissue
* p=0.01
Non-dysbiosis
Dysbiosis
M0
M1
M2
mono-MDSC
pmn-MDSC
C
Il-13 in mammary tissue-associated mast cell
* p=0.02
Relative expression
Non dysbiosis + Tumor
Dysbiosis + Tumor
D
Early mammary tissue
Total CD11b+/mg mammary tissue
M0
M1
M2
mono-MDSC
pmn-MDSC
Non dysbiosis
Dysbiosis
Non dysbiosis + Tumor
Dysbiosis + Tumor
E
Il-13 in tumor-associated mast cell
Relative expression
Non dysbiosis + Tumor
Dysbiosis + Tumor
F
Early Tumor
Total intratumoral CD11b+ cells
Non dysbiosis + Tumor
Dysbiosis + Tumor
G
pg of IL-4 /mg of protein
p = 0.099
Non dysbiosis
Dysbiosis
H
pg of IL-4 /mg of protein
Non dysbiosis
Dysbiosis
Non dysbiosis + Tumor
Dysbiosis +Tumor
I
pg of IL-4 /mg of protein
Non dysbiosis
Dysbiosis
Non dysbiosis + Tumor
Dysbiosis +Tumor

J

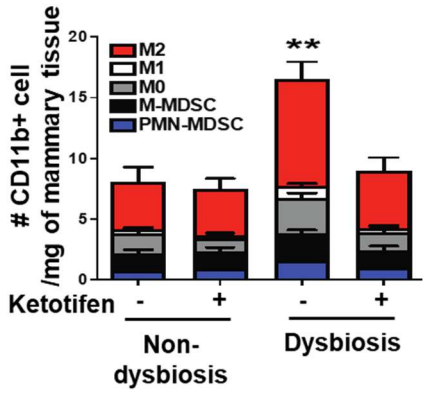

Figure 3.3 Commensal dysbiosis-induced IL-13 in mammary tissue-associated mast cells may cause M2 macrophages accumulation in tissue microenvironment.

A Experimental scheme. Mammary tissues or tumors from non-dysbiotic and dysbiotic mice were collected at day 0, 6, or 12 days post BRPKp110 implantation. At day 0 (**B**) and +12 (**D and F**), $CD45^+CD11b^+$ myeloid cells in the mammary tissues (**B and D**) or tumors (**F**) were quantified using flow cytometry. (M0: $F4/80^+CD86^-CD206^-$; M1: $F4/80^+CD86^+CD206^-$; M2: $F4/80^+CD86^-CD206^+$; Polymorphonuclear MDSC: $F4/80^-Ly6C^{mid}Ly6G^+$; Monocytic MDSC: $F4/80^-Ly6C^{hi}Ly6G^-$). Real-time PCR was utilized to evaluate the gene expression of IL-13 in the $CD45^+cKit^+FC\varepsilon RI\alpha^+$ mast cells from the adjacent mammary tissues (**C**) or tumors (**E**) at day +6 post tumor implantation. The following primers were used: *Il13* forward primer: 5'- TGGGTGACTGCAGTCCTGGCT-3' and reverse primer 5'- GTTGCTTTGTGTAGCTGAGCA-3'. Each symbol represents an experimental replicate. Statistical significance was determined by two-tailed Mann-Whitney *U* test. **G - I** The protein levels of IL-4 were evaluated in the lysates of mammary tissues at day 0 (**G**), +6 (**H**), and +12 (**I**) using a custom multiplex U-PLEX assay from Meso Scale Diagnostics. **J** Quantification of $CD11b^+$ myeloid cells in adjacent mammary tissues from BRPKp110-tumor mice after treatment with ketotifen using the same markers in A. Each symbol represents a biological replicate. Statistical significance was determined by two-tailed Mann-Whitney *U* test. Quantifications of myeloid cells (**B,D, and F**) and IL-4 (**G to I**) were provided by Dr. Claire Buchta Rosean.

3.4 Investigate whether extracellular vesicles in tumor-bearing dysbiotic mice induce epithelial-mesenchymal transition (EMT) in HR^+ breast cancer cells.

Extracellular vesicles (EVs) are heterogeneous, cell-derived membranous particles that function as signal transporters. Initially, EVs were thought to function solely as a cellular waste disposal mechanism[206]. However, it is now apparent that EVs are important messengers contributing to intercellular, interorganismal, and interspecies communication[206]. EVs are classified into two groups based on their mechanism of biogenesis: exosomes (40-100 nm in diameter) are generated by the endosomal system, and microvesicles (up to ~1000 nm in diameter) are generated by blebs of plasma membrane. Regardless of their origin, all EVs contain heterogeneous DNA, RNA, lipids, and proteins that enable extracellular communication. EVs have a phospholipid bilayer that protects the cargo and facilitates long-distance communication. In the context of breast cancer, tumor-derived EVs can promote invasiveness of human cancer cells. Singh *et al.* demonstrated that the highly metastatic human breast cancer cell line MDA-MB-231 secreted higher levels of miR-10b microRNA when compared to non-metastatic breast cancer cells; the MDA-MB-231-derived EVs induced invasiveness of non-malignant human mammary epithelial (HMLE) cells through regulating HOXD10 and KLF4[207]. Similarly, EVs from the plasma of young breast cancer patients induced the invasion of non-invasive MCF10DCIS.com cell line as compared to the EVs from age-matched healthy donors[208]. In addition to directly acting on cancer cells, breast tumor-derived EVs can regulate tumor progression by functionally modulating stromal cells and immune cells. For instance, Fong *et al.* showed that the miR-122 in MDA-MB-231-derived EVs reduced glucose uptake in lung fibroblasts and supporting the establishment of pre-

metastatic niches in the lungs[209]. EVs from breast cancer cells increased TGF-β-mediated immunosuppression[210] and the expression of CD206, a marker of pro-tumor M2 macrophages, in tumor-draining lymph nodes[211]. Recently, Keklikoglou *et al.*, elegantly demonstrated that the chemotherapy drug paclitaxel elicits annexin-A6 (ANXA6)-enriched EVs in the 4T1 breast tumor model and that this induces $Ly6C^{+}CCR2^{+}$ monocyte expansion in the pulmonary pre-metastatic niche[212]. The work of Keklikoglou *et al.* suggests that non-tumor-intrinsic factors, such as cytotoxic agents, induce different cargoes in tumor-derived EVs, and that these changes can systemically influence pro- or anti-tumor immunity.

We have preliminary data suggesting that circulatory EVs (around 100 nm in diameter, Figure 3.4A) from BRPKp110-bearing dysbiotic animals promote invasion, measured as the numbers of spikes formation per μm^2 of organoid area, in mammary organoids compared to equal numbers of EVs from tumor-bearing non-dysbiotic or non-tumor bearing mice (Figure 3.4B and 3.4C). This EV-driven invasion is reduced by the addition of heparin, an inhibitor of EV uptake by mammary organoids (Figure 3.4B and 3.4C). In addition to non-malignant organoids, we confirmed that the circulatory EVs from tumor-bearing dysbiotic animals were also able to induce significantly greater invasion in tumor spheroids as compared to non-dysbiotic tumor-bearing animals (Figure 3.4D and 3.4E). Indeed, dysbiotic mice have increased HR^{+} breast tumor dissemination in the blood, tumor-draining lymph nodes, and lungs, suggesting HR^{+} breast tumor cells acquire increased invasive capabilities in dysbiotic hosts. These data suggest that commensal dysbiosis induces pro-invasive cargoes in the circulatory EVs. Epithelial-mesenchymal

transition (EMT) has a crucial role in the initiation of metastatic dissemination due to promoting the loss of cell-cell adhesion, acquisition of invasive mesenchymal traits, and increased cell motility[213]. We hypothesize that circulatory EVs from tumor-bearing dysbiotic mice induce EMT signatures in tumor cells, thereby increasing metastatic dissemination. The hypothesis will be tested with the following experiments outlined below.

Circulatory EVs will be isolated with ExoQuick and characterized based on the requirements provided by the International Society for Extracellular Vesicles (ISEV)[214]. Specifically, we will classify EVs by protein expression of CD81, CD63, and TSG101, but not Golgi-matrix protein GM130, using immunoblot. We will use Nanoparticle tracking analysis (NTA) instrument ZetaView to quantify EVs and cryo-electron microscopy to identify their morphology. EVs will be isolated from tumor-bearing non-dysbiotic or dysbiotic mice 12 days post HR^+ tumor implantation. EVs will be normalized to particle concentration and added to tumor spheroid cultures. After 4 days of incubation, we will evaluate the EMT markers[214], including measuring whether E-cadherin is downregulated and N-cadherin, vimentin, Slug and Snail are upregulated in tumor spheroids treated with dysbiosis-associated EVs. In addition to the *in vitro* assay, we will co-inject the circulatory EVs with HR^+ tumor cells into the mammary fat pad of non-manipulated wild-type mice to test whether EVs from tumor-bearing dysbiotic mice enhance dissemination of tumors into the blood, to tumor-draining lymph nodes, and lungs. Both the luminal A-like BRPKp110 and luminal B-like PyMT breast tumor models will be included in the above experiments. If our hypothesis is true, we expect that circulatory EVs from tumor-bearing

dysbiotic animals will induce higher levels of EMT markers in the tumor spheroids and in vivo, in addition to increasing tumor dissemination in co-injection experiments as compared to tumors co-injected with EVs from non-dysbiotic controls. Follow-up studies will use untargeted transcriptomic and proteomic analysis to identify molecular mechanisms associated with enhanced EMT and tumor cell dissemination.

If the EVs do not directly induce tumor cell invasion after co-injection, we will test whether circulatory EVs facilitate the formation of pro-metastatic niches through activation of pro-invasive fibroblasts within tumor microenvironment. However, based upon our *in vitro* assays, we expect EVs from dysbiotic mice will have a direct effect *in vivo*. Interestingly, we have observed slightly increased protein levels of alpha-smooth muscle actin (SMA) in tumor lysates from dysbiotic mice as compared to that in tumors from non-dysbiotic mice. SMA is extensively expressed in cancer associated fibroblasts (CAFs) of multiple tumor types, including breast cancer. Importantly, SMA^{hi} CAFs are positively associated with metastasis in breast cancer patients[215]. Because dysbiotic mice show increased protein levels of collagen and enhanced abundance of disseminated tumor cells in lungs, it raises the possibility that circulatory EVs in tumor-bearing dysbiotic mice could also induce fibroblast activation in lungs to facilitate the formation of a pro-metastatic environment. We will test the hypothesis that the circulatory EVs from dysbiotic mice induce pro-invasive fibroblasts using the following experiments. $CD45^{-}CD31^{-}gp38^{+}$ fibroblasts sorted from the mammary tissues of wild-type female mice will be primed with circulatory EVs from tumor-bearing non-dysbiotic or dysbiotic mice. After 24 hours incubation, we will evaluate the expression of SMA, collagen I, and PDGFR-α (markers

that are observed to be increased in dysbiotic mice) in the EV-primed fibroblasts using flow cytometry. The invasive area in BRPKp110 spheroids cocultured with the EV-primed fibroblasts will also be measured to quantify the pro-invasive ability of the EV-primed fibroblasts. If circulatory EVs from dysbiotic mice induce higher pro-invasive activity in fibroblasts than circulatory EVs from non-dysbiotic mice in the *in vitro* assay, we will further test the pro-invasive activity *in vivo* by co-injecting BRPKp110 tumor cells and EV-primed fibroblasts into the mammary fat pad and measuring tumor size and tumor dissemination as described above. We will intravenously inject the circulatory EVs isolated from tumor-bearing dysbiotic and non-dysbiotic mice into BRPKp110-bearing mice to investigate the protein levels of collagen I and the expression levels of SMA, collagen I, and PDGFR-α in $CD45^{-}CD31^{-}gp38^{+}$ fibroblasts from tumors, mammary tissues, lungs, and livers at 12- and 26-days post tumor implantation. The abundance of disseminated BRPKp110 in those organs will be quantified at the same time points. The luminal B-like breast tumor PyMT will be utilized to understand whether EV-driven fibroblast activation is a BRPKp110-specific phenomenon. Untargeted proteomics and transcriptomic assays will be used to define potential molecular mechanism(s) of the EV-induced fibroblast activation at systemic sites and the subsequent tumor dissemination. One additional possibility, given the body of my thesis work, is that EVs can act on mast cells directly, which can be tested using in vitro co-culture with bone marrow-derived mast cells or normal mast cells with or without heparin. The goal would be to determine whether mast cells acquire phenotypic characteristics similar to those isolated from dysbiotic mice in the absence of heparin. This would implicate EVs isolated from dysbiotic mice have the potential to phenotypically program mast cells towards a pro-fibrogenic phenotype.

Together, the proposed experiments will allow us to investigate the following hypotheses: 1) circulatory EVs in tumor-bearing dysbiotic mice directly induce tumor invasiveness through the initiation of EMT; 2) circulatory EVs in tumor-bearing dysbiotic mice stimulate pro-invasive fibroblasts at systemic sites to promote the egress of tumor cells from primary sites and recruitment of or survival of disseminated tumor cells at distal organs. Currently, identifying dysbiotic microbiome in patients is still challenging due to the lack of characterization of “normal-healthy microbiome”. Targeting pro-invasive EVs in blood biopsy from patients may be a more practical strategy for predicting and/or preventing metastasis.

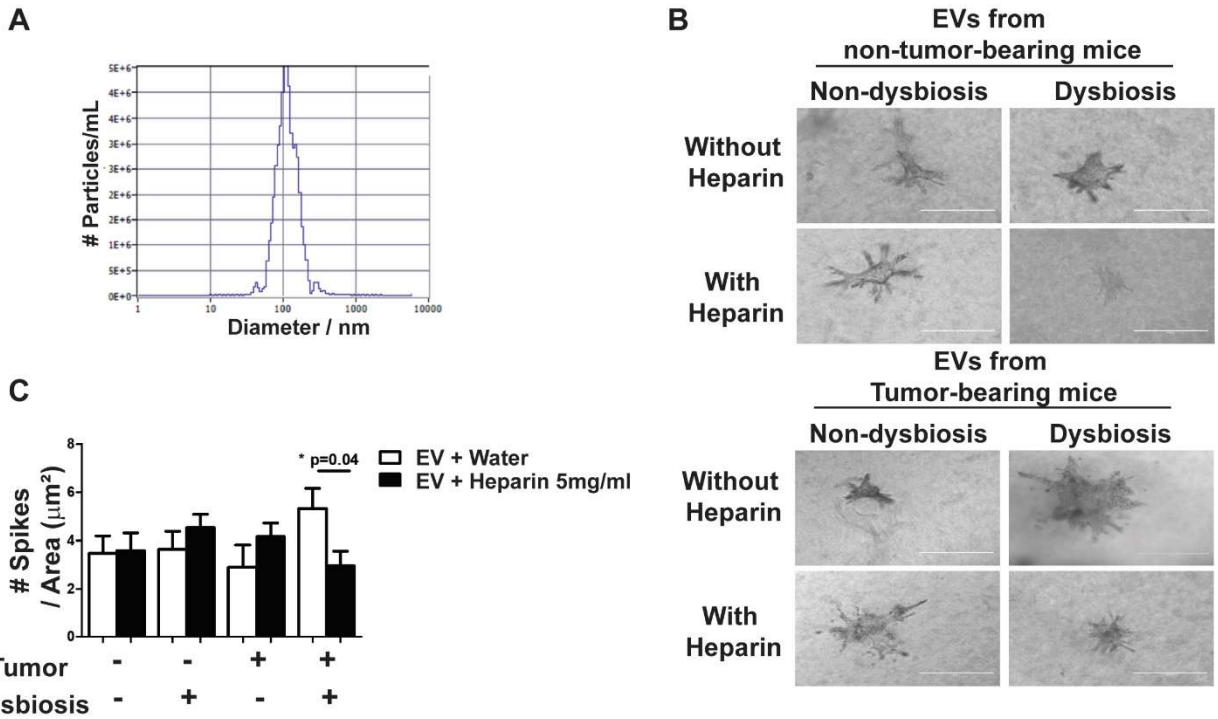
A
Particles/mL
Diameter / nm
B
EVs from non-tumor-bearing mice
Non-dysbiosis
Dysbiosis
Without Heparin
With Heparin
EVs from Tumor-bearing mice
C
Spikes / Area (µm²)
* p=0.04
EV + Water
EV + Heparin 5mg/ml
Tumor
Dysbiosis

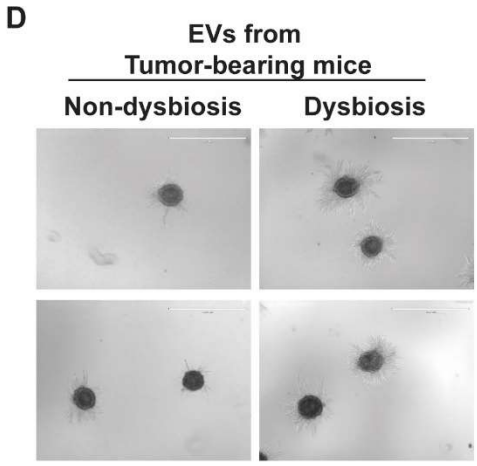
D
EVs from Tumor-bearing mice
Non-dysbiosis
Dysbiosis

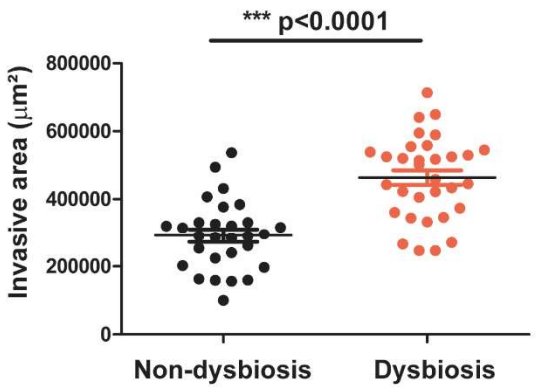
E
*** p<0.0001
Invasive area (µm²)
Non-dysbiosis
Dysbiosis

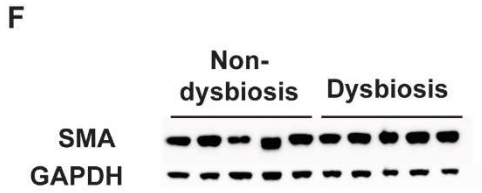
F
Non-dysbiosis
Dysbiosis
SMA
GAPDH

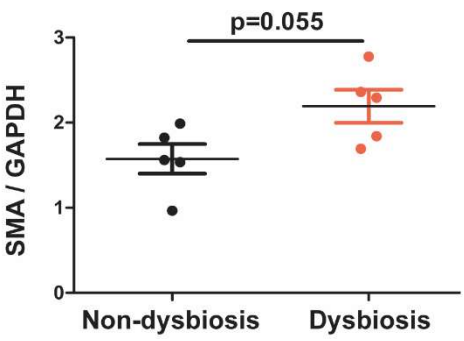
G
p=0.055
SMA / GAPDH
Non-dysbiosis
Dysbiosis

Figure 3.4 Circulatory EVs from dysbiotic tumor-bearing mice induce invasion in mammary organoids and tumor spheroids.

A Representative plot of the size and particle concentration of circulatory EVs isolated from blood of tumor-bearing non-dysbiotic and dysbiotic mice. The samples were analyzed using ZetaView. **B and C** Mammary organoids were established from mammary duct fragments of wild-type female C57BL/6 mice. Mammary organoids were incubated with circulatory EVs from the following donors: 1) non-tumor-bearing dysbiotic mice; 2) non-tumor-bearing dysbiotic mice; 3) BRPKp110-bearing non-dysbiotic mice; 4) BRPKp110-bearing dysbiotic mice. 5 μg/ml of heparin or equal volume of water was added in the cultures to inhibit the uptake of EVs. Organoids (**B**) were imaged after 4-days of incubation. Invasion (**C**) was determined by quantitating the numbers of spikes per μm^2 of organoid area. N=3 wells per condition. Scale bar = 400 μm. **D and E** BRPkp110 spheroids were cultured with EVs from tumor-bearing non-dysbiotic or dysbiotic mice for 48 hrs. Representative images of tumor spheroids are in (**D**). Invasion of tumor spheroids were determined by measuring invasive area, which is total spheroid area minus sphere area. Scale bar = 1 mm. **F and G** Protein levels of SMA in tumor lysates from non-dysbiotic and dysbiotic mice were evaluated by immunoblot (**F**). ImageJ was utilized to quantify the blots. The expression levels of SMA were normalized to the levels of each loading-control GAPDH (**G**). N=5 mice per group. Each symbol represents an experimental replicate. Statistical significance was determined by two-tailed Mann-Whitney *U* test.

3.5 Determine the role of mammary tissue mast cells in changing the stromal environment of aged mice.

HR^+ breast cancer is considered a disease related to aging. The median age for the diagnosis of HR^+ breast cancer is 61 years, and approximately 10% of the patients are older than 80 years[1, 216]. These statistics highlight the importance of understanding the tissue microenvironment in aged subjects. Compared to young animals, aged mice have elevated inflammation in the mammary tissue microenvironment that may facilitate the proliferation and metastatic behavior of tumor cells[217-219]. Recently, single-cell sequencing results of mammary tissues from aged mice and young mice revealed that aged mice have an altered stromal and immunological environment in the mammary tissue. Utilizing flow cytometry, Li *et al.* further found reduced numbers of fibroblasts, increased numbers of endothelial cells, and enhanced numbers of CXCL2- and PD-L1-expressing macrophages[44]. Notably, it is well known that pro-inflammatory microbes are enriched in the gut of aged animals and humans. However, little remains known about how the aged commensal microbiome affects cancer outcomes or influences the mammary tissue microenvironment.

In aged animals, an increased abundance of mast cells has been observed in the mesenteric lymphatic vessels[220] and skin[221]. Interestingly, aged human skin has an increased proximity of mast cells adjacent to macrophages[221], suggesting that the interaction between mast cells and macrophages enhances inflammation in the aged tissue microenvironment. With our antibiotics-induced dysbiotic animal model, we found that the mammary tissue mast cells from dysbiotic mice express PDGF-B and IL-13,

raising the possibility that these mast cells can influence both stromal and immunological compartments. This was further validated in experiments where mast cell degranulation was inhibited resulting in a subsequent reduction in tumor-associated macrophages only in tissues of dysbiotic mice. Thus, we hypothesize that mammary tissue mast cells could also orchestrate stromal and immune changes in the mammary tissue microenvironment in response to ageing and an aged microbiome. We will test this hypothesis with the following experiments.

We will use untargeted proteomics approach to identify the changes in mast cells ($CD45^+cKit^+Fc\varepsilon RI\alpha^+$), fibroblasts ($CD45^-CD31^-gp38^+$), endothelial cells ($CD45^-CD31^+$), and macrophages ($CD45^+CD11b^+F4/80^+$) sorted out from mammary tissues of young (3-4 months-old) or aged (13-14 months-old) female mice. Particularly, we will focus on the signatures of fibroblasts, endothelial cells, and macrophages that are identified by Li *et al.*.[44] (Table 3.1).

Fibroblast		Endothelial cell		Macrophage	
Stress	Extracellular matrix	Cytokine	Cell-cell junction	Cytokine	Immune suppression
Hspa1a (↑)	Col5a3 (↓)	Csf3 (↑)	Ctnnb1 (↓)	Ccl5 (↑)	Pdl1 (↑)
Sqstm1 (↑)	Col6a3 (↓)	Cxcl1 (↑)	Jup (↓)	Cxcl2 (↑)	Ilt3 (↑)
Ubc (↑)	Fn1 (↓)	Cxcl16 (↑)	Pvrl2 (↓)	Gdf15 (↑)	
Cebpb (↑)	Mmp23 (↓)	Il6 (↑)	Cldn5 (↓)		

Table 3.1. The gene signatures of fibroblast, endothelial cell, and macrophage in aged mammary tissues. (↑): increased in aged mammary tissues; (↓): reduced in aged mammary tissues.

To test whether an aged commensal microbiome affects the mammary tissue microenvironment, we will use fecal microbiota transplantation (FMT) to test the sufficiency of an aged microbiome to attenuate the phenotype and function of mast cells, fibroblasts, endothelial cells, and macrophages in the mammary tissue environment of young wild-type or mast cell-deficient mice (Wild-type mice: C57BL/6 mice, mast cell-deficient mice: *Kit*$^{w\text{-}sh/w\text{-}sh}$ mice). The experimental scheme is depicted in the following figure 3.5.1. Briefly, the microbiome of C57BL/6 mice and *Kit*$^{w\text{-}sh/w\text{-}sh}$ mice will be eliminated by gavaging recipient mice with a cocktail of broad-spectrum antibiotics for 7 days. Immediately after the cessation of antibiotics, mice will be orally gavaged with cecal slurries isolated from young (3-4 months-old) or aged (13-14 months-old) female C57BL/6 mice for 3 consecutive days. Mice will then rest for 7 days to allow the engraftment of the transferred commensal microbes. Because female mice do not go through a significant decline in basal estrogen levels that resembles human menopause[222], the estrus cycle will be synchronized by a modified Whitten effect prior to the samples collection to eliminate the hormone-mediated variations. As an alternative approach, mice will be ovariectomized prior to implantation of the microbiome. The phenotype and functional changes to mast cells, fibroblasts, endothelial cells, and macrophages in the mammary tissues will be evaluated using immunoblot on sorted subpopulations and/or flow cytometry as described in previous sections. If the aged commensal microbiome influences the stromal and immunological environment in the mammary tissue, we expect that the aging-related signatures will be increased in the C57BL/6 mice with aged commensal microbiome when compared to the C57BL/6 mice receiving a young commensal microbiome. Using *Kit*$^{w\text{-}sh/w\text{-}sh}$ mice, we will be able to determine whether the

microbiome associated effects observed in WT mice are facilitated via mast cells or directly on macrophages, fibroblasts, etc.

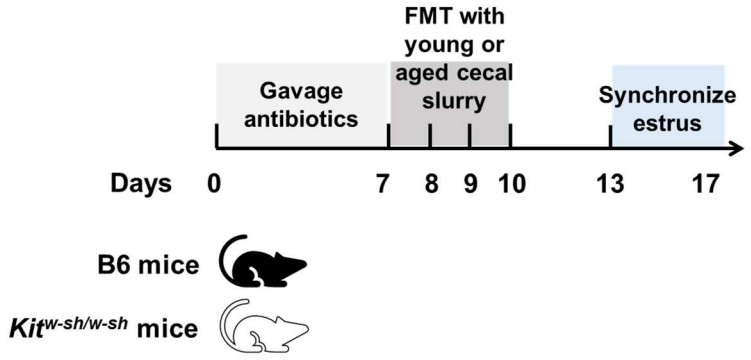

Figure 3.5.1 Experimental scheme of investigating the role of mast cell in aged microbiome-induced changes in mammary tissue-associated macrophages and fibroblasts.

We will reconstitute young or aged microbiome in WT or mast cell-deficient Sash mice using FMT. The phenotypes of stromal cells and immune cells in the mammary tissue will be investigated 7 days post microbiome transplantation.

If we observe significant changes to stromal cells in wild type mice but not mast cell deficient mice, we will hypothesize that an aged microbiome is acting directly on mast cells that then subsequently activate fibroblasts, macrophages or endothelial cells within the tissue environment. To test this, we will orthotopically transfer equal numbers of mammary tissue mast cell sorted from wild type mice receiving a young (3-4 months-old) or aged (13-14 months-old) microbiome into young mast cell deficient *Kit*$^{w\text{-}sh/w\text{-}sh}$ mice (Figure 3.5.2). A modified Whitten effect will be applied to synchronize the estrus cycle before the sample collection. The expression of aging-related signatures in mast cells, fibroblasts, endothelial cells, and macrophages from the mammary tissue that were identified in the aforementioned experiments will be measured from each subset 7 days after mast cell transfer. If mammary tissue mast cells from mice receiving an aged microbiome are sufficient to induce the aging-related signatures, a follow-up study would investigate which mast cell-derived mediators may skew the tissue microenvironment and we would also perform metagenomic sequencing and metabolomics on the microbiome to define which attributes of an aged microbiome contribute to changes in mast cell phenotype.

Finally, we will repeat these experiments in tumor-bearing animals, to determine how an aged microbiome affects breast tumor growth or metastasis. Because these experiments are proposed based solely on my interest in aging, fibrosis, and the microbiome, and that we do not have sufficient preliminary data to make meaningful conclusions or predictions on the experimental outcomes, our expectations are not as clearly defined. However, based upon what is known in the literature, I would predict that if an aging microbiome

significantly affects mast cells, having this knowledge in hand could pave the way towards engineering therapies to reverse the aging-related phenotypic changes in tissue-associated mast cells. This could be done through modulation of the gut microbiome or through targeting of mast cells using the functional readouts gained from these experiments.

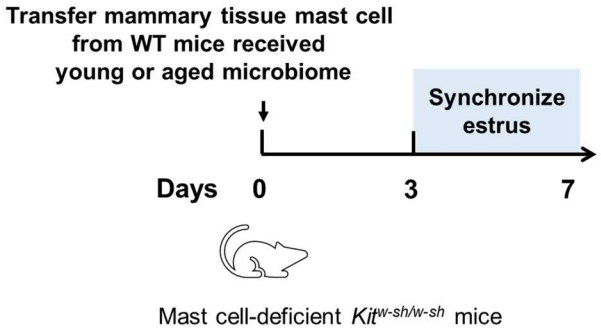

Figure 3.5.2 Experimental scheme of investigating the influence of young or aged microbiome-induced mast cells on the mammary tissue microenvironment.

We will sort the mammary tissue mast cells from WT mice reconstituted with young or aged microbiome. These sorted mast cells will be orthotopically transferred into the mammary fat pad of Sash mice. We will investigate the phenotypes of stromal cells and immune cells in the mammary tissues of the Sash mice 7 days post mast cell transfer.

Chapter 4: Concluding Remarks

The gut microbiome has recently become a focus in breast cancer research following the discovery of commensal microorganisms capable of metabolizing estrogens[39, 42, 223-226] and subsequent epidemiologic studies associating frequent antibiotic use with increased breast cancer incidence[227, 228]. Gut microbiome sequencing from patients diagnosed with HR^+ breast cancer revealed that patient microbiomes were unbalanced and dysbiotic compared to those of healthy individuals[229]. However, these studies did not demonstrate causation between having an unbalanced microbiome and breast cancer risk. One of the first studies to establish that an inflammatory gut microbiome directly influenced breast cancer incidence utilized APCMin/+ mice infected with *H. hepaticus* to induce dysbiosis. Compared to uninfected controls, *H. hepaticus* infection increased mammary tumor formation[230]. Subsequent investigation into the association between the commensal microbiome and breast cancer identified associations with antibiotics usage and breast tumor growth[160], and the effects of enterotoxigenic *Bacteroides fragilis* on growth and metastasis of triple negative breast tumors[231].

Using a novel murine model of HR^+ breast cancer[150-153, 186], we showed that establishing commensal dysbiosis (an inflammatory gut microbiome with low biodiversity) *prior to tumor initiation* elevated mammary tissue levels of CCL2, PGE2, macrophages, and fibrosis, all of which have been shown to correlate with poor disease outcome in patients. *Importantly,* while primary tumor growth remained unchanged following the establishment of commensal dysbiosis, *metastatic dissemination of HR^+ tumors was significantly enhanced* under these conditions[153]. Ours was the first to identify gut dysbiosis as a host-

intrinsic mediator of breast tumor metastasis. In patients, increased age, poor diet, and certain genetic polymorphisms, all of which induce commensal dysbiosis, associate with increased risk of metastatic breast cancer[232-238]. Additionally, recent sequencing of the gut microbiome from treatment-naïve patients diagnosed with early HR^+ breast cancer demonstrated that an inflammatory gut microbiome associated with tumor aggressiveness, poor prognosis, and diminished therapy response[154]. These studies provide a clinical basis in support of our findings that gut commensal dysbiosis enhances HR^+ breast tumor metastasis.

Previous studies have primarily focused upon associating a diseased (tumor-affected[239]) microbiome with breast cancer outcomes, evaluating non-HR^+ breast tumor subtypes, and interrogating how differences in the gut microbiome affect primary tumor growth. It is not currently known if and how a ***non-cancer-affected*** gut microbiome can impact long-term risk of metastatic HR^+ breast cancer. By using our tractable model of antibiotics-induced dysbiosis[153], we have accumulated multiple pieces of data indicating that commensal dysbiosis culminates in CCL2-induced inflammation in normal mammary tissues, leading to accumulation of pro-fibrogenic mast cells, activation of tissue fibroblasts, and enhanced metastatic dissemination.

The role of mast cells in breast cancer has remained controversial[172], partially due to the fact that the majority of prior studies investigated tumor-associated mast cells. In some cases, a positive association between mast cells and outcome was seen[173, 175] whereas other studies associated mast cells with poor prognosis[134, 176-178]. However, the role of

mammary tissue-resident mast cells in promoting breast cancer metastasis is completely unknown. To our knowledge, ours is the first study to define how the gut microbiome distally programs mast cells within the normal and benign-adjacent mammary tissue to promote breast tumor dissemination. We tested the novel hypothesis that mammary tissue mast cells act upstream of tumor-associated macrophages and fibroblasts to enhance collagen remodeling of the mammary tissue, leading to increased metastasis. Mast cells are evolutionarily conserved innate immune cells, highly attuned to the environment of the organs they reside in. Our data indicates that mast cells are one of the only mammary tissue leukocytes changed in response to dysbiosis, further supporting a model whereby mast cells are reprogrammed by the gut microbiome, possibly CCL2, and orchestrate metastatic dissemination of HR^+ tumor cells via PDGF signaling and subsequent activation of tissue fibroblasts.

Emerging evidence demonstrated that fibroblasts in human breast cancer are highly heterogenous[240]. Using single-cell analysis, Kieffer *et al.* further identified one subtype of cancer-associated fibroblast links to the induction of Treg and immunotherapy resistance[171]. Interestingly, mast cells are also involved in the failure of PD-1 therapy[179]. Our preliminary data also suggest the increased IL-13 in mast cells may induce pro-tumor M2 macrophage polarization. Collectively, our findings provide novel insights into how the gut microbiome shapes the mammary tissue microenvironment to favor metastatic breast cancer. Based on these discoveries, I suspect that in depth understanding of the interplays between gut microbiome and mast cells in the mammary tissues will pave a

way toward developing novel the therapeutic strategies with ultimate goal of reducing metastasis in HR^+ breast cancer.

Mechanistically, we demonstrate that blockade of CCL2 prior to tumor initiation is sufficient to reduce mast cell accumulation in the mammary tissue and to diminish dysbiosis-induced dissemination of HR^+ tumor cells[241]. Although CCL2 is a well-known driver of breast tumor growth[189] and metastasis[161], tumor-independent triggers of CCL2 have not been investigated. Supporting the idea that CCL2 contributes to tissue fibrosis in the absence of tumors, Sun *et al.* demonstrated that overexpression of CCL2 in the pre-malignant mammary epithelium not only increased mammary tissue density, but also susceptibility to carcinogen-induced breast cancer[190]. However, the systemic trigger for mammary tissue CCL2 and the cell populations producing CCL2 in the mammary tissue remain undefined. Future studies will address these gaps in knowledge in an effort to clarify the novel tumor-independent role for CCL2 in the promotion of metastatic breast cancer.

In summary, this project established that gut commensal dysbiosis is a distal trigger that changes the cellular and molecular composition of normal non-tumor-bearing mammary tissue, increasing the long-term risk of metastatic HR^+ breast cancer. These studies have paved the groundwork for repurposing *clinically available drugs or drug combinations* to target tissue CCL2, mast cell degranulation, and/or PDGF as interventions capable of preventing metastatic HR^+ breast cancer through restoration of tissue homeostasis. In the long-term, defining the mast cell-associated or gut microbial and/or diffusible metabolic

triggers of mammary tissue CCL2 could unveil a novel gut-associated molecular pathway that promotes HR^+ tumor dissemination and metastatic growth.

Chapter 5: Materials and Methods

5.1 Mice

5-8-week-old female C57BL/6 mice were purchased from Charles River Laboratories. B6.Cg-*Kit*$^{W\text{-}sh}$/HNihrJaeBsmJ (*Kit*$^{w\text{-}sh/w\text{-}sh}$; Sash)[242-244] mice were purchased from The Jackson Laboratory and maintained in-house at the University of Virginia. All animals were maintained in specific-pathogen-free barrier conditions. All experiments in this study were approved by the University of Virginia Institutional Animal Care and Use Committee.

5.2 Tumor implantation

The poorly metastatic HR$^+$ mouse mammary cancer cell line BRPKp110 has been described previously[150]. 5E5 BRPKp110 cells were injected orthotopically into the abdominal mammary fat pad. The highly metastatic mouse luciferase-expressing mammary cancer cell line PyMT was cloned from a metastatic tumor derived from the HR$^+$ MMTV-PyMT model as previously described[164]. In experiments using this cell line, 1E5 PyMT cells were injected orthotopically into the abdominal mammary fat pad. Cell lines were authenticated by maintaining at less than four passages, monitoring of morphology, and testing for mycoplasma.

5.3 Antibiotics administration

Commensal dysbiosis was initiated in mice by orally gavaging mice daily for 14 days with 100 μl of an antibiotic cocktail containing vancomycin (0.5 mg/ml, Gold Biotechnology),

ampicillin (1 mg/ml) metronidazole (1 mg/ml), neomycin (1 mg/ml), and gentamicin (1 mg/ml) – all from Sigma Aldrich, as previously reported[153]. Vehicle-treated mice received 100 μl of water. Mice were then left untreated for 4 days to allow the establishment of commensal dysbiosis before tumor implantation.

Fecal microbiota transplantation (FMT) experiments were performed as previously described[153]. Briefly, dysbiosis was induced in donor mice as described above. Cecal contents from dysbiotic and non-dysbiotic vehicle-treated (water) animals were collected, homogenized, and frozen at -80°C in sterile 1:1 glycerol/PBS. Recipient mice were then orally gavaged with the antibiotic cocktail used for inducing dysbiosis for 7 days, followed by 3 or 4 consecutive days of oral gavage with 200 μl of either dysbiotic or non-dysbiotic cecal contents. After the final day of gavage, recipient mice were rested for 7 days before tumor initiation to allow for microbial engraftment.

5.4 Treatment with mast cell stabilizers and anti-CCL2 antibody

Mast cell stabilizers ketotifen (Sigma-Aldrich) and cromolyn (Alfa Aesar) solution were freshly prepared prior to each treatment by diluting in sterile water followed by passage through a 0.22 μM syringe filter. Mice were orally gavaged with 100 μl of ketotifen (10 mg/kg) or 100 μl of water daily beginning 1-day post tumor implantation, and continuing until day 5 post tumor. In the experiments using cromolyn, mice were intraperitoneally injected with 100 μl of cromolyn (10mg/kg) or 100 μl of PBS once per day from 3-days prior to until 12-days post tumor initiation.

To the role of CCL2/CCR2 axis in the accumulation of mammary tissue mast cells in the dysbiotic mice, mice were intraperitoneally injected with four doses of 200 µg of anti-mouse CCL2 (Bio X Cell) monoclonal antibody or 200 µg of the isotype matched control IgG (Bio X Cell) in 100 µl of PBS once per day at 8-day, 6-day, 4-day, and 2-day prior to the implantation of breast tumor cells.

5.5 Flow cytometry

Mammary tissues, tumors, and tumor draining lymph nodes were collected, weighed, homogenized, and digested with collagenase type I (Gibco) for 30 minutes at 37C prior to filtration using a 70 μm strainer. All the samples were stained with Zombie Aqua (BioLegend) and Fc receptor blocker anti-CD16/32 for differentiating live cells and inhibiting non-specific binding, respectively. Fibroblasts were identified by surface staining with anti-mouse CD45-PE-Cy7 (30-F11), CD31-PerCP-Cy5.5 (390), gp38-APC-Cy7 (8.1.1), and PDGFR-α-BV605 (APA5) and intracellular staining with anti-mouse smooth muscle actin (SMA)-AF647 (SPM32) and type I collagen-AF488 (1310-30). Mast cells and basophils were identified by surface staining with anti-mouse CD45-APC-Fire (30-F11), Lineage cocktail-Biotin (145-2C11; RB6-8C5; RA3-6B2; Ter-119; M1/70), CD49b-FITC (HMa2), cKit-BV650 (ACK2), FcεRIα -Biotin (MAR_1), CCR2-AF647 (SA203G11), CXCR4-PE/Dazzle (L276F12), CXCR3-PerCP-Cy5.5 (S18001A), Streptavidin-PerCP-Cy5.5, Streptavidin-PE-Cy7, and intracellular staining with anti-mouse PDGFB-AF488 (F-3). Myeloid cell infiltration was identified by surface staining with anti-mouse CD45-APC (30-F11), CD11b-PE-Cy7 (M1/70), Ly6C-APC-Cy7 (HK1.4),

Ly6G-FITC (1A8), F4/80-PerCP-Cy5.5 (BM8), CD206-PE/Dazzle (C068C2), CD86-BV650 (GL-1). T cells, NK cells, and NKT cells were detected by surface staining with anti-mouse CD45-PE (30-F11), CD3-FITC (17A2), CD4-PE-Cy7 (GK1.5), CD8-APC-Cy7 (53-6.7), and NK1.1 (PK136).

Tumor cell dissemination was quantitated using single-cell suspensions from lungs and tumor-draining lymph nodes through surface staining with anti-mouse CD45 (30-F11, APC) and intracellular staining with anti-GFP (B-2, PE) or anti-luciferase (C-12, PE). Circulating tumor cells from the blood were isolated and quantitated as previously described[153, 245]. Briefly, equal volumes of EDTA-treated blood underwent red blood cell lysis, were plated into 6-well culture dishes, and incubated for 7 days. Cells were detached and stained as described for quantitation of disseminated tumor cells.

All antibodies were purchased from BioLegend with the exception of anti-SMA (Novus Biologicals), anti-type I collagen (SouthernBiotech), anti-GFP (Santa Cruz) and anti-luciferase (Santa Cruz). Counting beads (AccuCount, Spherotech) were added into samples prior to acquisition on the flow cytometer. All antibodies and counting beads were added into samples at the manufacturer's recommended concentration. Samples were run on an Attune NxT flow cytometer (Thermo Fisher Scientific) and analyzed with FlowJo software. Absolute numbers were quantitated per the manufacturer's instructions.

5.6 *In vitro* co-culture with mammary tissue mast cells and fibroblasts

$CD45^+$ $cKit^+$ $Fc\varepsilon RI\alpha^+$ mast cells were sorted from mammary tissues from non-dysbiotic or dysbiotic C57BL/6 mice using a BD FACSAria Fusion flow sorter (Flow Cytometry Core Facility, University of Virginia). The sorted mast cells were then co-cultured with NIH-3T3 fibroblasts (Mast cell: NIH-3T3 fibroblast = 1:20) for 24 hours in serum-free DMEM at 37C, 5% CO_2. To test the role of PDGF signaling, the tyrosine kinase inhibitor imatinib was added to the fibroblast-mast cell co-cultures. Specifically, fibroblasts were pretreated with 0.1 μg/ml of imatinib for 20 minutes, followed by incubation with mast cells (Mast cell: NIH-3T3 fibroblast = 1:20) and 0.1 μg/ml of imatinib in serum-free DMEM at 37C, 5% CO_2 for 24 hours. At the end of incubations, the phenotype of NIH-3T3 fibroblasts was analyzed by surface staining of anti-mouse CD45-PE, PDGFR-α-BV605, and intracellular staining with SMA-AF647, and collagen I-AF488.

5.7 Mast cell transfer

Mast cells ($CD45^+$ $cKit^+$ $Fc\varepsilon RI\alpha^+$ cells) were sorted from mammary tissues of non-dysbiotic or dysbiotic C57BL/6 mice as described above. Equal numbers of mammary tissue mast cells were reconstituted in 100 μl of PBS and orthotopically transferred to the mammary tissues (approximately ~300 mast cells/mammary tissue were injected for each experiment) of $Kit^{w\text{-}sh/w\text{-}sh}$ (Sash) mice. Eighteen hours after the transfer of sorted mast cells, 5E5 BRPKp110 tumor cells were injected into the same mammary fat pad of $Kit^{w\text{-}sh/w\text{-}sh}$ (Sash) recipient mice.

5.8 Immunoblot

Mammary tissues and tumors were snap-frozen in liquid nitrogen and homogenized and sonicated in ice cold RIPA buffer (Thermo Fisher Scientific) supplemented with proteinase inhibitors (Thermo Fisher Scientific), per manufacturer instructions. Equal amounts of protein (5-10 μg/lane) were loaded into precast gels (Thermo Fisher Scientific) and transferred onto PVDF membranes. Membranes were blocked with 1X PBS- 0.1% Tween (PBST) containing 5% non-fat dry milk, and probed with primary antibodies overnight at 4°C followed by incubation with horseradish peroxidase (HRP)-linked secondary antibodies. Membranes were imaged using ChemiDoc Imaging System (Bio-Rad). Antibodies used were: anti-mast cell tryptase antibody (EPR9522, Abcam), anti-collagen I antibody (ab34710, Abcam), goat-anti rabbit IgG H&L (HRP) (Abcam), anti-PDGF-B (F-3, Santa Cruz), anti-GAPDH antibody (6C5, Santa Cruz), and mouse-IgGκ-HRP (Santa Cruz). The immunoblots were quantified using ImageJ software.

5.9 Histology and microscopy

Tissues were fixed in neutral-buffered formalin, paraffin-embedded, and cut in 5 μm sections (Research Histology Core, University of Virginia. A second cohort of tissue samples were obtained from the Barts Cancer Institute Breast Cancer Now Tissue Bank (Tissue Request TR241). Samples were stratified into two groups: No recurrence (n=18) and Recurrence (to distant sites - bone, lung, liver) (n=23). For detecting mast cells, slides were stained using 0.1% toluidine blue solution (pH 2.0-2.5). To investigate collagen deposition, slides were stained using PicroSirius Red (0.1% Direct Red 80 in saturated

aqueous picric acid, Sigma-Aldrich). Collagen deposition was quantified using ImageJ software by calculating the stained area per section. The total numbers of mammary tissue mast cells were normalized to the area of mammary tissues. The slides were imaged with a Slide Scanner (Leica) or a NanoZoomer S210 slide scanner (Hamamatsu).

5.10 Transcriptome analysis of human samples

Normal breast tissues from women either prior to their BC diagnosis (susceptible normal, [15]) or age-matched healthy women were obtained from the Susan G. Komen Tissue Bank at Indiana University Simon Comprehensive Cancer Center (Table 5.1). Subjects were recruited under a protocol approved by the Indiana University Institutional Review Board (IRB protocol number 1011003097 and 1607623663). Total RNA was extracted from fresh frozen breast tissues using 3 mm zirconium beads (Benchmark Scientific, cat.# D1032-30) and the AllPrep DNA/RNA/miRNA kit (Qiagen) as previously described[246]. Then, a cDNA library was prepared using the TruSeq Stranded Total RNA Kit (Illumina, San Diego, CA) and sequenced using Illumina HiSeq4000. Reads were adapter trimmed and quality filtered using Trimmomatic ver. 0.38[247] setting the cutoff threshold for average base quality score at 20 over a window of 3 bases. Reads shorter than 20 bases post-trimming were excluded (parameters: LEADING:20 TRAILING:20 SLIDINGWINDOW:3:20 MINLEN:20). Cleaned reads mapped to Human genome reference sequence GRCh38.p12 with gencode v.28 annotation, using STAR version STAR_2.5.2b[248]. (parameters: --outFilterMultimapNmax 20 --seedSearchStartLmax 16 --twopassMode Basic). Gene expression was quantified by counting the number of reads

mapped to the exonic regions of the genes using featureCounts tool ver. 2.0.0 of subread package (parameters: -s 2 -p -B -C). Differential Expression Analysis was performed using DESeq2 ver. 1.12.3. The *p*values for genes indicating the probabilities of no differential expression across the sample groups were corrected for multiple testing using Benjamini-Hochberg method.

5.11 Availability of data and materials

The dataset including transcriptome profiling of susceptible breast samples and age-matched healthy controls is available in GEO (accession number GSE166044, https://www.ncbi.nlm.nih.gov/geo/query/acc.cgi?acc=GSE166044).

Table 5.1: Demographics of the women who donated either healthy or susceptible breast. Samples were analyzed through transcriptome profiling.

Group	Barcode	Age	BMI	Tyrer-Cuzick Lifetime score	Racial Background	Hispanic	Age at menarche	Menopausal Status	Genetic mutation on either BRCA1 or BRCA2	Ever Pregnant	Breast Feed
HC	K107036	35	34.4	13.8	AFRNAMER	No	12	Pre-menopausal	No	Yes	Yes
HC	K107548	43	25.1	11.3	WHITE	No	12	Pre-menopausal	No	Yes	Yes
HC	K107280	52	30.5	7.3	WHITE	No	11	Uterine Ablation	No	Yes	Yes
HC	K107296	60	31.5	7.2	WHITE	No	12	Post-menopausal	No	Yes	Yes
HC	K107598	30	23.3	20.6	WHITE	No	13	Pre-menopausal	No	Yes	Yes
HC	K107913	55	29.9	N/A	WHITE	No	13	Post-menopausal	No	Yes	Yes
HC	K108003	39	24.3	N/A	WHITE	No	12	Pre-menopausal	No	Yes	Yes
HC	K108052	47	24.9	N/A	WHITE	No	16	Pre-menopausal	No	Yes	Yes
HC	K108157	61	39.7	N/A	WHITE	No	13	Post-menopausal	No	Yes	Yes
HC	K108429	55	25	N/A	WHITE	No	11	Post-menopausal	No	Yes	Yes
HC	K106839	59	26.1	N/A	WHITE	No	13	Post-menopausal	No	Yes	Yes
HC	K107013	42	30.1	8.4	WHITE	No	12	Post-menopausal	No	Yes	Yes
HC	K107069	44	27.8	24.5	WHITE	No	13	Pre-menopausal	No	Yes	Yes
HC	K106939	46	30.7	N/A	WHITE,NATHAWPI	No	13	Pre-menopausal	No	Yes	Yes
HC	K107235	44	22.8	13	~~OTHRACE	No	13	Pre-menopausal	No	Yes	Yes

Susceptible	K107912	60	20.7	5.9	WHITE	No	13	Post-menopausal	No	No	None
Susceptible	K107237	64	24.4	13	WHITE	No	11	Post-menopausal	No	Yes	No
Susceptible	K107273	66	25.7	11.5	WHITE	No	11	Post-menopausal	No	Yes	Yes
Susceptible	K107138	46	32.3	18.4	WHITE	No	16	Pre-menopausal	No	Yes	Yes
Susceptible	K107616	57	20.1	32.9	WHITE	No	11	Post-menopausal	No	Yes	Yes
Susceptible	K107977	68	28.3	3	WHITE	No	15	Post-menopausal	No	Yes	No
Susceptible	K108358	64	33.4	8.6	WHITE	No	14	Post-menopausal	No	Yes	Yes
Susceptible	K105316	60	44.8	4.2	WHITE	No	15	Post-menopausal	N/A	Yes	N/A
Susceptible	K104430	62	29.8	7.2	WHITE	No	16	Post-menopausal	No	Yes	Yes
Susceptible	K104589	32	20.5	N/A	WHITE	No	14	Pre-menopausal	No	No	N/A
Susceptible	K104653	51	31.9	N/A	WHITE	No	14	Post-menopausal	No	Yes	Yes
Susceptible	K104728	68	26.1	N/A	WHITE	No	13	Post-menopausal	No	Yes	Yes
Susceptible	K105140	53	37.6	10.4	WHITE	No	13	Post-menopausal	N/A	Yes	Yes
Susceptible	K106357	58	45.7	7.7	WHITE	No	12	Post-menopausal	N/A	Yes	Yes
Susceptible	K106859	47	31.6	10.3	WHITE	No	13	Pre-menopausal	No	Yes	No

5.12 16S microbiome sequencing

Sequencing was performed by the University of Maryland Institute for Genome Science.

Sequences were demultiplexed using the mapping file split_libraries_fastq.py, a QIIME-dependent script. Fastq files were split by using seqtk (https://github.com/lh3/seqtk), primer sequences removed using TagCleaner (0.16), followed by downstream processing using DADA2 Workflow for Big Data and dada2 (v. 1.5.2) (https://benjjneb.github.io/dada2/bigdata.html). Forward and reverse reads were trimmed using lengths of 255 and 225 bp, respectively, to contain no ambiguous bases, have a minimum quality score of 2, and contain less than two expected errors based on quality score. Reads were assembled and chimeras removed per dada2 protocol.

Taxonomic assignments

Taxonomy was assigned to each amplicon sequence variant (ASV) generated by dada2 using a combination of the SILVA v128 database and the RDP naïve Bayesian classifier as implemented in the dada2 R package species level assignments. Read counts for ASVs assigned to the same taxonomy were summed for each sample.

Diversity Analysis

Alpha diversity of microbiome samples was measured using Shannon alpha diversity measure. Beta diversity of microbiome sequences was assessed using Bray-Curtis dissimilarity measures based upon relative abundance data.

5.13 Real-time PCR analysis of sorted mast cells

Total RNA was extracted from mast cells sorted from adjacent mammary tissues or day 6 tumors using an RNeasy Micro Kit (Qiagen) followed by reverse transcription using

High-Capacity cDNA Reverse Transcription Kits (Thermo Fisher). For amplicon detection, the Power SYBR® Green PCR Master Mix (Thermo Fisher) was used as described by the manufacturer. RT-PCR was performed in a QuantStudio 6 Real-Time PCR Systems (Thermo Fisher) as follows: initial denaturation at 95°C for 10 mins; amplification for 35 cycles of denaturation (95°C for 1 mins), annealing (55°C for 2 mins), and extension (72°C for 3 mins). Specificity of the amplicon was determined by melting curve. The relative levels of mRNA were determined by comparative CT method and normalized by housekeeping genes GAPDH and β-actin RNA.

The following primers were used:

Pdgfa: Forward primer 5'- GTGCGACCTCCAACCTGA-3' and reverse primer 5'-GGCTCATCTCACCTCACATCT

Pdgfb: Forward primer 5'- CGGCCTGTGACTAGAAGTCC-3' and reverse primer 5'-GAGCTTGAGGCGTCTTGG-3'

Tgf-β1 forward primer 5'- TGGAGCAACATGTGGAACTC-3' and reverse primer 5'-CAGCAGCCAATTACCAAG-3'

Cpa3 forward primer 5'- ATCGCAGGCACGCACAGTTAT-3' and reverse primer 5'-AACCCAGTCTAAGGAAGAGCC-3'

Mcpt4 forward primer 5'- ACCACTGAGAGAGGGTTCACAGC-3' and reverse primer 5'-GAAGACTCTGATGCACGCAGG-3'

Mcpt5 forward primer 5'- CTGAGAACTACCTGTCGGCCTGC-3' and reverse primer 5'-TCCAGTTCCAGATTTCCTCACGG-3'

Mcpt2 forward primer 5'- CCACTAAGAACGGTTCGAAGGAG-3' and revere primer 5'-GCTGGGATGAACTCAGAGGTACC-3'

β-actin forward primer 5'- GTGGGCCGCTCTAGGCACCAA-3' and reverse primer 5'-CTCTTTGATGTCACGCACGATTTC-3'

Gapdh forward primer 5'- CATCACTGCCACCCAGAAGACTG-3' and reverse primer 5'-ATGCCAGTGAGCTTCCCGTTCAG-3'

5.14 In vitro culture of circulatory extracellular vesicles (EVs) with mammary organoid and BRPKp110 tumor spheroids

Circulatory EVs in peripheral blood from experimental mice were isolated with ExoQuick (SBI) as per manufacturer's instructions. The size and the concentration of circulatory EVs are analyzed with a Nanoparticle tracking analysis (NTA) instrument ZetaView. Mammary organoids were established from 6–8-week-old female mice with the method established by Dr. Andrew Ewald (Ewald Cold Spring Harbor Protocol. https://pubmed.ncbi.nlm.nih.gov/23378653/). BRPKp110 tumor spheroids were established using hanging-drop method (Lin Biotech J 2008 https://pubmed.ncbi.nlm.nih.gov/18566957/). Mammary organoids or tumor spheroids were mixed with Matrigel before platting followed by culturing in complete RPMI at 37°C, 5% CO_2. EVs were normalized to particle concentration before adding into the cultures.

5.15 Statistical analysis

Statistical analysis was performed using Prism software (GraphPad). Statistical difference between data sets was evaluated using two-tailed Mann-Whitney *U* test or unpaired t-test as indicated in the figure legends. Correlation analysis was performed using linear regression.

Gene Set Enrichment Analysis (GSEA) software version 4.1.0 (Broad Institute)[249] was applied for the RNA-seq data from healthy and susceptible human donors. The gene

signatures of mast cells[170] and cancer-associated fibroblasts[171] subsets are listed in Table M2. PDGF-B was also included in the analysis of mast cell signatures. The following options were selected in the software: numbers of permutations: 1000; chip platform: Human_ENSEMBL_Gene_ID_MSigDB.V7.4.chip; permutation type: gene_set. The results from GSEA are evaluated based on the enrichment scores (ES), which represents the gene set is overrepresented at the top or bottom of a ranked list of genes of interested. The normalized enrichment score (NES) represents the enrichment score that has been normalized to the size of gene sets. The false discovery rate (FDR q-value) represents the estimated probability of a false positive finding. The familywise-error rate (FWER p-value) stands for a probability that the NES represents a false positive finding.

P-values <0.05 were considered significant.

Table 5.2 Gene signatures of mast cells and ecm-MyCAF

Mast cell (Adjusted from Motakis et al., Blood 2014)	ecm-MyCAF (Kieffer et al., Cancer Discovery 2020)			
KIT	AEBP1	FN1	SDC1	FNDC1
IL1RL1	ANXA2	CCN1	ACTN1	CTHRC1
FCER1G	BGN	ITGB1	CTSB	COL2A1
MS4A2	BMP1	ITGB5	PPIB	COL11A2
ENPP3	SERPINH1	LOX	ASPN	MDK
HDC	COL1A1	LOXL1	P3H1	ACTB
CMA1	COL1A2	LOXL2	P4HA3	MYLK
CPA3	COL3A1	LUM	ACTG1	MYL9
ERVFRD-1	COL5A1	MATN3	ACTN4	MYL12A
SVOPL	COL5A2	MFAP2	CAPZB	NRP2
FCER1A	COL6A1	MMP2	CFL1	GJA1
TPSAB1	COL6A2	MMP11	FLNA	GJB2
TPSAB2	COL6A3	MMP14	MARCKS	PTK7
TPSD1	COL8A1	HTRA1	PFN1	PKM
CTSG	COL10A1	SFRP2	S100A10	RAB31
HPGDS	COL11A1	SPARC	TPM1	RUNX2
LTC4S	COL12A1	COL14A1	TPM2	CDH11
MRGPRX2	COL16A1	ADAM12	TPM4	LRRC17
RGS13	COMP	MMP23B	ARPC2	ACTA2
SIGLEC6	VCAN	P3H4	PDLIM3	TNFRSF12A
VWA5A	CCN2	POSTN	ENAH	ARF4
C1orf150	CTSK	SULF1	THBS2	INHBA
C20orf118	FAP	SULF2	CILP	LGALS1
PDGFB	FBN1	CREB3L1	APON1	MYH9
		P4HB	MXRA5	NREP
				CD99

Abbreviations

Abbreviation	Definition
BMDM	Bone marrow-derived macrophages
CAF	Cancer-associated fibroblast
CCL2	C-C Motif Chemokine Ligand 2
CCL3	C-C Motif Chemokine Ligand 3
CCL4	C-C Motif Chemokine Ligand 4
CCL5	C-C Motif Chemokine Ligand 5
CCR2	C-C Motif Chemokine Receptor 2
CDCA	Chenodexoycholic acid
C/EBPα	CCAAT/enhancer binding protein α
CMP	Common myeloid progenitors
COX-1	Cyclooxygenase-1
COX-2	Cyclooxygenase-2
CPA3	Carboxypeptidase A3
CTMC	Connective-tissue mast cell
CXCL2	C-X-C motif chemokine ligand 2
CXCL10	C-X-C motif chemokine ligand 10
CXCL16	C-X-C motif chemokine ligand 16
CXCR3	C-X-C Motif Chemokine Receptor 3
CXCR4	C-X-C Motif Chemokine Receptor 4
CXCR6	C-X-C Motif Chemokine Receptor 6
DC	Dendritic cell
ECM	Extracellular matrix
EMT	Epithelial-mesenchymal transition
EP1	E type prostaglandin receptor 1
EP2	E type prostaglandin receptor 2
EP3	E type prostaglandin receptor 3
EP4	E type prostaglandin receptor 4
ER	Estrogen receptor
EV	Extracellular vesicles
FFAR2	Free Fatty Acid Receptor 2
FFAR3	Free Fatty Acid Receptor 3
FFPE	Formalin-fixed paraffin-embedded
FGF	Fibroblast growth factor
FMT	Fecal microbiota transplantation
FXR	Farnesoid X receptor
GAPDH	Glyceraldehyde-3-Phosphate Dehydrogenase
GATA-2	GATA-binding factor 2
GATA-3	GATA-binding factor 3
GCDC	Glycochenodeoxycholic acid

GF	Germ-free
GMP	Granulocyte-monocyte progenitors
HDAC	Histone deacetylase
HER2	Human epidermal growth factor receptor 2
HMLE	Human mammary epithelial
HOXD10	Homeobox D10
HR	Hormone receptor
IFN-γ	Interferon gamma
IL1RL1	Interleukin 1 receptor-like 1
ILC	Innate lymphoid cells
MAMP	Microbe-associated molecular patterns
MBC	Metastatic breast cancer
MCT	Mast cells containing mainly tryptase
MCTC	Mast cells containing both tryptase and chymase
MDSC	Myeloid-derived suppressor cells
MMC	Mucosal mast cell
NK	Natural killer cell
NKT	Natural killer T cell
NOD-1	Nucleotide-binding oligomerization domain-containing protein 1
PAR-2	Proteinase activated receptor-2
PD-1	Programmed cell death protein-1
PD-L1	Programmed Cell Death Ligand 1
PDGF-B	Platelet-derived growth factor B
PDGFR-α	Platelet-derived growth factor receptor alpha
PGE2	Prostaglandin E2
RORγt	Retinoid orphan receptor gamma t
SCF	Stem cell factor
SCFA	Short-chain fatty acids
SMA	Alpha-smooth muscle actin
SPF	Specific pathogen-free
STAT3	Signal Transducer And Activator Of Transcription 3
TGF-β1	Transforming growth factor-beta 1
Th1	Type 1 T helper cells
Th17	Type 17 T helper cells
TGIT	T cell immunoglobulin and ITIM domain
TIM3	T-cell immunoglobulin mucin-3
TLR2	Toll-like receptor 2
TNBC	Triple-negative breast cancer
TNF-α	Tumor necrosis factor alpha
TSG101	Tumor Susceptibility 101

References

1. National Cancer Institute. Surveillance E, and End Results program website., http://www.seer.cancer.gov. 2022
2. Gerratana L, Fanotto V, Bonotto M, Bolzonello S, Minisini AM, Fasola G, et al. Pattern of metastasis and outcome in patients with breast cancer. *Clinical & experimental metastasis*. 2015;32:125-133
3. Neophytou C, Boutsikos P, Papageorgis P. Molecular mechanisms and emerging therapeutic targets of triple-negative breast cancer metastasis. *Frontiers in oncology*. 2018;8:31
4. Yersal O, Barutca S. Biological subtypes of breast cancer: Prognostic and therapeutic implications. *World journal of clinical oncology*. 2014;5:412-424
5. Howlader N, Cronin KA, Kurian AW, Andridge R. Differences in breast cancer survival by molecular subtypes in the united states. *Cancer epidemiology, biomarkers & prevention : a publication of the American Association for Cancer Research, cosponsored by the American Society of Preventive Oncology*. 2018;27:619-626
6. Howlader N, Altekruse SF, Li CI, Chen VW, Clarke CA, Ries LA, et al. Us incidence of breast cancer subtypes defined by joint hormone receptor and her2 status. *Journal of the National Cancer Institute*. 2014;106
7. Hosseini H, Obradović MMS, Hoffmann M, Harper KL, Sosa MS, Werner-Klein M, et al. Early dissemination seeds metastasis in breast cancer. *Nature*. 2016;540:552-558
8. Hüsemann Y, Geigl JB, Schubert F, Musiani P, Meyer M, Burghart E, et al. Systemic spread is an early step in breast cancer. *Cancer cell*. 2008;13:58-68
9. Colleoni M, Sun Z, Price KN, Karlsson P, Forbes JF, Thürlimann B, et al. Annual hazard rates of recurrence for breast cancer during 24 years of follow-up: Results from the international breast cancer study group trials i to v. *Journal of clinical oncology : official journal of the American Society of Clinical Oncology*. 2016;34:927-935
10. Peeters DJ, van Dam PJ, Van den Eynden GG, Rutten A, Wuyts H, Pouillon L, et al. Detection and prognostic significance of circulating tumour cells in patients with metastatic breast cancer according to immunohistochemical subtypes. *British journal of cancer*. 2014;110:375-383
11. Panagopoulou M, Esteller M, Chatzaki E. Circulating cell-free DNA in breast cancer: Searching for hidden information towards precision medicine. *Cancers*. 2021;13
12. Tabor S, Szostakowska-Rodzos M, Fabisiewicz A, Grzybowska EA. How to predict metastasis in luminal breast cancer? Current solutions and future prospects. *International journal of molecular sciences*. 2020;21
13. Albain KS, Gray RJ, Makower DF, Faghih A, Hayes DF, Geyer CE, et al. Race, ethnicity, and clinical outcomes in hormone receptor-positive, her2-negative, node-negative breast cancer in the randomized tailorx trial. *Journal of the National Cancer Institute*. 2021;113:390-399
14. Troester MA, Hoadley KA, D'Arcy M, Cherniack AD, Stewart C, Koboldt DC, et al. DNA defects, epigenetics, and gene expression in cancer-adjacent breast: A study from the cancer genome atlas. *NPJ breast cancer*. 2016;2:16007
15. Marino N, German R, Rao X, Simpson E, Liu S, Wan J, et al. Upregulation of lipid metabolism genes in the breast prior to cancer diagnosis. *NPJ breast cancer*. 2020;6:50
16. Nussbaum K, Burkhard SH, Ohs I, Mair F, Klose CSN, Arnold SJ, et al. Tissue microenvironment dictates the fate and tumor-suppressive function of type 3 ilcs. *The Journal of experimental medicine*. 2017;214:2331-2347

17. Wang Z, Aguilar EG, Luna JI, Dunai C, Khuat LT, Le CT, et al. Paradoxical effects of obesity on t cell function during tumor progression and pd-1 checkpoint blockade. *Nature medicine*. 2019;25:141-151
18. Zhang C, Yue C, Herrmann A, Song J, Egelston C, Wang T, et al. Stat3 activation-induced fatty acid oxidation in cd8(+) t effector cells is critical for obesity-promoted breast tumor growth. *Cell metabolism*. 2020;31:148-161.e145
19. Xu H, Cao D, He A, Ge W. The prognostic role of obesity is independent of sex in cancer patients treated with immune checkpoint inhibitors: A pooled analysis of 4090 cancer patients. *International immunopharmacology*. 2019;74:105745
20. McQuade JL, Daniel CR, Hess KR, Mak C, Wang DY, Rai RR, et al. Association of body-mass index and outcomes in patients with metastatic melanoma treated with targeted therapy, immunotherapy, or chemotherapy: A retrospective, multicohort analysis. *The Lancet. Oncology*. 2018;19:310-322
21. Arina A, Idel C, Hyjek EM, Alegre ML, Wang Y, Bindokas VP, et al. Tumor-associated fibroblasts predominantly come from local and not circulating precursors. *Proceedings of the National Academy of Sciences of the United States of America*. 2016;113:7551-7556
22. Sender R, Fuchs S, Milo R. Revised estimates for the number of human and bacteria cells in the body. *PLoS biology*. 2016;14:e1002533
23. Stinson LF, Boyce MC, Payne MS, Keelan JA. The not-so-sterile womb: Evidence that the human fetus is exposed to bacteria prior to birth. *Frontiers in microbiology*. 2019;10:1124
24. Reyman M, van Houten MA, van Baarle D, Bosch A, Man WH, Chu M, et al. Impact of delivery mode-associated gut microbiota dynamics on health in the first year of life. *Nature communications*. 2019;10:4997
25. Bonder MJ, Kurilshikov A, Tigchelaar EF, Mujagic Z, Imhann F, Vila AV, et al. The effect of host genetics on the gut microbiome. *Nature genetics*. 2016;48:1407-1412
26. Lopera-Maya EA, Kurilshikov A, van der Graaf A, Hu S, Andreu-Sánchez S, Chen L, et al. Effect of host genetics on the gut microbiome in 7,738 participants of the dutch microbiome project. *Nature genetics*. 2022;54:143-151
27. Strachan DP. Hay fever, hygiene, and household size. *BMJ (Clinical research ed.)*. 1989;299:1259-1260
28. Scudellari M. News feature: Cleaning up the hygiene hypothesis. *Proceedings of the National Academy of Sciences of the United States of America*. 2017;114:1433-1436
29. Stiemsma LT, Reynolds LA, Turvey SE, Finlay BB. The hygiene hypothesis: Current perspectives and future therapies. *ImmunoTargets and therapy*. 2015;4:143-157
30. David LA, Maurice CF, Carmody RN, Gootenberg DB, Button JE, Wolfe BE, et al. Diet rapidly and reproducibly alters the human gut microbiome. *Nature*. 2014;505:559-563
31. De Filippo C, Cavalieri D, Di Paola M, Ramazzotti M, Poullet JB, Massart S, et al. Impact of diet in shaping gut microbiota revealed by a comparative study in children from europe and rural africa. *Proceedings of the National Academy of Sciences of the United States of America*. 2010;107:14691-14696
32. Chen L, Wilson JE, Koenigsknecht MJ, Chou WC, Montgomery SA, Truax AD, et al. Nlrp12 attenuates colon inflammation by maintaining colonic microbial diversity and promoting protective commensal bacterial growth. *Nature immunology*. 2017;18:541-551
33. Modi SR, Collins JJ, Relman DA. Antibiotics and the gut microbiota. *The Journal of clinical investigation*. 2014;124:4212-4218
34. Maier L, Pruteanu M, Kuhn M, Zeller G, Telzerow A, Anderson EE, et al. Extensive impact of non-antibiotic drugs on human gut bacteria. *Nature*. 2018;555:623-628

35. Zheng D, Liwinski T, Elinav E. Interaction between microbiota and immunity in health and disease. *Cell research*. 2020;30:492-506
36. Fan Y, Pedersen O. Gut microbiota in human metabolic health and disease. *Nature reviews. Microbiology*. 2021;19:55-71
37. Warner BB. The contribution of the gut microbiome to neurodevelopment and neuropsychiatric disorders. *Pediatric research*. 2019;85:216-224
38. Morais LH, Schreiber HLt, Mazmanian SK. The gut microbiota-brain axis in behaviour and brain disorders. *Nature reviews. Microbiology*. 2021;19:241-255
39. Kwa M, Plottel CS, Blaser MJ, Adams S. The intestinal microbiome and estrogen receptor-positive female breast cancer. *J Natl Cancer Inst*. 2016;108
40. Adlercreutz H, Martin F, Pulkkinen M, Dencker H, Rimér U, Sjöberg NO, et al. Intestinal metabolism of estrogens. *The Journal of clinical endocrinology and metabolism*. 1976;43:497-505
41. Adlercreutz H, Martin F, Tikkanen MJ, Pulkkinen M. Effect of ampicillin administration on the excretion of twelve oestrogens in pregnancy urine. *Acta endocrinologica*. 1975;80:551-557
42. Martin F, Peltonen J, Laatikainen T, Pulkkinen M, Adlercreutz H. Excretion of progesterone metabolites and estriol in faeces from pregnant women during ampicillin administration. *J Steroid Biochem*. 1975;6:1339-1346
43. Buchta Rosean C, Bostic RR, Ferey JCM, Feng TY, Azar FN, Tung KS, et al. Preexisting commensal dysbiosis is a host-intrinsic regulator of tissue inflammation and tumor cell dissemination in hormone receptor-positive breast cancer. *Cancer research*. 2019;79:3662-3675
44. Li CM, Shapiro H, Tsiobikas C, Selfors LM, Chen H, Rosenbluth J, et al. Aging-associated alterations in mammary epithelia and stroma revealed by single-cell rna sequencing. *Cell reports*. 2020;33:108566
45. Shively CA, Register TC, Appt SE, Clarkson TB, Uberseder B, Clear KYJ, et al. Consumption of mediterranean versus western diet leads to distinct mammary gland microbiome populations. *Cell reports*. 2018;25:47-56.e43
46. Cole SW. Chronic inflammation and breast cancer recurrence. *Journal of clinical oncology : official journal of the American Society of Clinical Oncology*. 2009;27:3418-3419
47. Feng T-Y, Azar FN, Rosean CB, McGinty MT, Putelo AM, Koli S, et al. Reciprocal interactions between the gut microbiome and mammary tissue mast cells promote metastatic dissemination of hr⁺ breast tumors. *bioRxiv*. 2021:2021.2012.2023.474065
48. Round JL, Mazmanian SK. The gut microbiota shapes intestinal immune responses during health and disease. *Nature reviews. Immunology*. 2009;9:313-323
49. Talham GL, Jiang HQ, Bos NA, Cebra JJ. Segmented filamentous bacteria are potent stimuli of a physiologically normal state of the murine gut mucosal immune system. *Infection and immunity*. 1999;67:1992-2000
50. Umesaki Y, Setoyama H, Matsumoto S, Imaoka A, Itoh K. Differential roles of segmented filamentous bacteria and clostridia in development of the intestinal immune system. *Infection and immunity*. 1999;67:3504-3511
51. Cahenzli J, Köller Y, Wyss M, Geuking MB, McCoy KD. Intestinal microbial diversity during early-life colonization shapes long-term ige levels. *Cell host & microbe*. 2013;14:559-570
52. Ahern PP, Maloy KJ. Understanding immune-microbiota interactions in the intestine. *Immunology*. 2020;159:4-14
53. Cummings JH, Pomare EW, Branch WJ, Naylor CP, Macfarlane GT. Short chain fatty acids in human large intestine, portal, hepatic and venous blood. *Gut*. 1987;28:1221-1227

54. Furusawa Y, Obata Y, Fukuda S, Endo TA, Nakato G, Takahashi D, et al. Commensal microbe-derived butyrate induces the differentiation of colonic regulatory t cells. *Nature*. 2013;504:446-450
55. Park J, Kim M, Kang SG, Jannasch AH, Cooper B, Patterson J, et al. Short-chain fatty acids induce both effector and regulatory t cells by suppression of histone deacetylases and regulation of the mtor-s6k pathway. *Mucosal immunology*. 2015;8:80-93
56. Singh N, Gurav A, Sivaprakasam S, Brady E, Padia R, Shi H, et al. Activation of gpr109a, receptor for niacin and the commensal metabolite butyrate, suppresses colonic inflammation and carcinogenesis. *Immunity*. 2014;40:128-139
57. Round JL, Lee SM, Li J, Tran G, Jabri B, Chatila TA, et al. The toll-like receptor 2 pathway establishes colonization by a commensal of the human microbiota. *Science*. 2011;332:974-977
58. Dasgupta S, Erturk-Hasdemir D, Ochoa-Reparaz J, Reinecker HC, Kasper DL. Plasmacytoid dendritic cells mediate anti-inflammatory responses to a gut commensal molecule via both innate and adaptive mechanisms. *Cell host & microbe*. 2014;15:413-423
59. Iwamura C, Bouladoux N, Belkaid Y, Sher A, Jankovic D. Sensing of the microbiota by nod1 in mesenchymal stromal cells regulates murine hematopoiesis. *Blood*. 2017;129:171-176
60. Khosravi A, Yanez A, Price JG, Chow A, Merad M, Goodridge HS, et al. Gut microbiota promote hematopoiesis to control bacterial infection. *Cell Host Microbe*. 2014;15:374-381
61. Balmer ML, Schürch CM, Saito Y, Geuking MB, Li H, Cuenca M, et al. Microbiota-derived compounds drive steady-state granulopoiesis via myd88/ticam signaling. *Journal of immunology (Baltimore, Md. : 1950)*. 2014;193:5273-5283
62. Urbaniak C, Cummins J, Brackstone M, Macklaim JM, Gloor GB, Baban CK, et al. Microbiota of human breast tissue. *Appl Environ Microbiol*. 2014;80:3007-3014
63. Nejman D, Livyatan I, Fuks G, Gavert N, Zwang Y, Geller LT, et al. The human tumor microbiome is composed of tumor type-specific intracellular bacteria. *Science*. 2020;368:973-980
64. Dickson RP, Huffnagle GB. The lung microbiome: New principles for respiratory bacteriology in health and disease. *PLoS pathogens*. 2015;11:e1004923
65. Sedman PC, Macfie J, Sagar P, Mitchell CJ, May J, Mancey-Jones B, et al. The prevalence of gut translocation in humans. *Gastroenterology*. 1994;107:643-649
66. Buchta Rosean C, Feng TY, Azar FN, Rutkowski MR. Impact of the microbiome on cancer progression and response to anti-cancer therapies. *Advances in cancer research*. 2019;143:255-294
67. Hand T, Belkaid Y. Microbial control of regulatory and effector t cell responses in the gut. *Current opinion in immunology*. 2010;22:63-72
68. Nomura M, Nagatomo R, Doi K, Shimizu J, Baba K, Saito T, et al. Association of short-chain fatty acids in the gut microbiome with clinical response to treatment with nivolumab or pembrolizumab in patients with solid cancer tumors. *JAMA network open*. 2020;3:e202895
69. Woods DM, Sodré AL, Villagra A, Sarnaik A, Sotomayor EM, Weber J. Hdac inhibition upregulates pd-1 ligands in melanoma and augments immunotherapy with pd-1 blockade. *Cancer immunology research*. 2015;3:1375-1385
70. Coutzac C, Jouniaux JM, Paci A, Schmidt J, Mallardo D, Seck A, et al. Systemic short chain fatty acids limit antitumor effect of ctla-4 blockade in hosts with cancer. *Nature communications*. 2020;11:2168
71. Sharma M, Arora I, Stoll ML, Li Y, Morrow CD, Barnes S, et al. Nutritional combinatorial impact on the gut microbiota and plasma short-chain fatty acids levels in the prevention of mammary cancer in her2/neu estrogen receptor-negative transgenic mice. *PloS one*. 2020;15:e0234893
72. Thirunavukkarasan M, Wang C, Rao A, Hind T, Teo YR, Siddiquee AA, et al. Short-chain fatty acid receptors inhibit invasive phenotypes in breast cancer cells. *PloS one*. 2017;12:e0186334

73. Farvid MS, Spence ND, Holmes MD, Barnett JB. Fiber consumption and breast cancer incidence: A systematic review and meta-analysis of prospective studies. *Cancer*. 2020;126:3061-3075
74. Hofmann AF. The continuing importance of bile acids in liver and intestinal disease. *Archives of internal medicine*. 1999;159:2647-2658
75. Wani B, Aziz SA, Ganaie MA, Mir MH. Metabolic syndrome and breast cancer risk. *Indian journal of medical and paediatric oncology : official journal of Indian Society of Medical & Paediatric Oncology*. 2017;38:434-439
76. McGlone ER, Bloom SR. Bile acids and the metabolic syndrome. *Annals of clinical biochemistry*. 2019;56:326-337
77. Tang W, Putluri V, Ambati CR, Dorsey TH, Putluri N, Ambs S. Liver- and microbiome-derived bile acids accumulate in human breast tumors and inhibit growth and improve patient survival. *Clin Cancer Res*. 2019;25:5972-5983
78. Baker PR, Wilton JC, Jones CE, Stenzel DJ, Watson N, Smith GJ. Bile acids influence the growth, oestrogen receptor and oestrogen-regulated proteins of mcf-7 human breast cancer cells. *British journal of cancer*. 1992;65:566-572
79. Alasmael N, Mohan R, Meira LB, Swales KE, Plant NJ. Activation of the farnesoid x-receptor in breast cancer cell lines results in cytotoxicity but not increased migration potential. *Cancer letters*. 2016;370:250-259
80. Journe F, Durbecq V, Chaboteaux C, Rouas G, Laurent G, Nonclercq D, et al. Association between farnesoid x receptor expression and cell proliferation in estrogen receptor-positive luminal-like breast cancer from postmenopausal patients. *Breast cancer research and treatment*. 2009;115:523-535
81. Ma C, Han M, Heinrich B, Fu Q, Zhang Q, Sandhu M, et al. Gut microbiome-mediated bile acid metabolism regulates liver cancer via nkt cells. *Science*. 2018;360
82. Cheng S, Zhu L, Faden HS. Interactions of bile acids and the gut microbiota: Learning from the differences in clostridium difficile infection between children and adults. *Physiological genomics*. 2019;51:218-223
83. Sipe LM, Chaib M, Pingili AK, Pierre JF, Makowski L. Microbiome, bile acids, and obesity: How microbially modified metabolites shape anti-tumor immunity. *Immunological reviews*. 2020;295:220-239
84. Coussens LM, Pollard JW. Leukocytes in mammary development and cancer. *Cold Spring Harbor perspectives in biology*. 2011;3
85. Cha YJ, Koo JS. Role of tumor-associated myeloid cells in breast cancer. *Cells*. 2020;9
86. Mager LF, Burkhard R, Pett N, Cooke NCA, Brown K, Ramay H, et al. Microbiome-derived inosine modulates response to checkpoint inhibitor immunotherapy. *Science (New York, N.Y.)*. 2020;369:1481-1489
87. Wang T, Gnanaprakasam JNR, Chen X, Kang S, Xu X, Sun H, et al. Inosine is an alternative carbon source for cd8(+)-t-cell function under glucose restriction. *Nature metabolism*. 2020;2:635-647
88. Krystel-Whittemore M, Dileepan KN, Wood JG. Mast cell: A multi-functional master cell. *Frontiers in immunology*. 2015;6:620
89. Dahlin JS, Hallgren J. Mast cell progenitors: Origin, development and migration to tissues. *Molecular immunology*. 2015;63:9-17
90. Collington SJ, Hallgren J, Pease JE, Jones TG, Rollins BJ, Westwick J, et al. The role of the ccl2/ccr2 axis in mouse mast cell migration in vitro and in vivo. *J Immunol*. 2010;184:6114-6123
91. Arinobu Y, Iwasaki H, Gurish MF, Mizuno S, Shigematsu H, Ozawa H, et al. Developmental checkpoints of the basophil/mast cell lineages in adult murine hematopoiesis. *Proc Natl Acad Sci U S A*. 2005;102:18105-18110

92. Sonoda T, Hayashi C, Kitamura Y. Presence of mast cell precursors in the yolk sac of mice. *Developmental biology*. 1983;97:89-94
93. Li Z, Liu S, Xu J, Zhang X, Han D, Liu J, et al. Adult connective tissue-resident mast cells originate from late erythro-myeloid progenitors. *Immunity*. 2018;49:640-653.e645
94. Gentek R, Ghigo C, Hoeffel G, Bulle MJ, Msallam R, Gautier G, et al. Hemogenic endothelial fate mapping reveals dual developmental origin of mast cells. *Immunity*. 2018;48:1160-1171.e1165
95. Walker BE. Mast cell turn-over in adult mice. *Nature*. 1961;192:980-981
96. Kobayasi T, Asboe-Hansen G. Degranulation and regranulation of human mast cells. An electron microscopic study of the whealing reaction in urticaria pigmentosa. *Acta Derm Venereol*. 1969;49:369-381
97. Xiang Z, Block M, Lofman C, Nilsson G. Ige-mediated mast cell degranulation and recovery monitored by time-lapse photography. *J Allergy Clin Immunol*. 2001;108:116-121
98. Dwyer DF, Barrett NA, Austen KF, Immunological Genome Project C. Expression profiling of constitutive mast cells reveals a unique identity within the immune system. *Nat Immunol*. 2016;17:878-887
99. Kitamura Y, Go S, Hatanaka K. Decrease of mast cells in w/wv mice and their increase by bone marrow transplantation. *Blood*. 1978;52:447-452
100. Kiernan JA. Production and life span of cutaneous mast cells in young rats. *Journal of anatomy*. 1979;128:225-238
101. Kambe N, Miyachi Y. A possible mechanism of mast cell proliferation in mastocytosis. *The Journal of dermatology*. 2002;29:1-9
102. Galli SJ, Borregaard N, Wynn TA. Phenotypic and functional plasticity of cells of innate immunity: Macrophages, mast cells and neutrophils. *Nature immunology*. 2011;12:1035-1044
103. Galli SJ, Tsai M. Mast cells in allergy and infection: Versatile effector and regulatory cells in innate and adaptive immunity. *European journal of immunology*. 2010;40:1843-1851
104. McNeil HP, Gotis-Graham I. Human mast cell subsets--distinct functions in inflammation? *Inflammation research : official journal of the European Histamine Research Society ... [et al.]*. 2000;49:3-7
105. Plum T, Wang X, Rettel M, Krijgsveld J, Feyerabend TB, Rodewald HR. Human mast cell proteome reveals unique lineage, putative functions, and structural basis for cell ablation. *Immunity*. 2020;52:404-416.e405
106. Oka T, Kalesnikoff J, Starkl P, Tsai M, Galli SJ. Evidence questioning cromolyn's effectiveness and selectivity as a 'mast cell stabilizer' in mice. *Lab Invest*. 2012;92:1472-1482
107. Galli SJ, Gaudenzio N, Tsai M. Mast cells in inflammation and disease: Recent progress and ongoing concerns. *Annual review of immunology*. 2020;38:49-77
108. Bradding P, Arthur G. Mast cells in asthma--state of the art. *Clinical and experimental allergy : journal of the British Society for Allergy and Clinical Immunology*. 2016;46:194-263
109. Galli SJ, Tsai M. Ige and mast cells in allergic disease. *Nature medicine*. 2012;18:693-704
110. Sandig H, Bulfone-Paus S. Tlr signaling in mast cells: Common and unique features. *Front Immunol*. 2012;3:185
111. Bradding P, Pejler G. The controversial role of mast cells in fibrosis. *Immunol Rev*. 2018;282:198-231
112. Bowers HM, Jr., Mahapatro RC, Kennedy JW. Numbers of mast cells in the axillary lymph nodes of breast cancer patients. *Cancer*. 1979;43:568-573
113. Majorini MT, Colombo MP, Lecis D. Few, but efficient: The role of mast cells in breast cancer and other solid tumors. *Cancer research*. 2022;82:1439-1447

114. Miettinen M, Lasota J. Kit (cd117): A review on expression in normal and neoplastic tissues, and mutations and their clinicopathologic correlation. *Applied immunohistochemistry & molecular morphology : AIMM*. 2005;13:205-220
115. Ribatti D. The staining of mast cells: A historical overview. *International archives of allergy and immunology*. 2018;176:55-60
116. Newman AM, Liu CL, Green MR, Gentles AJ, Feng W, Xu Y, et al. Robust enumeration of cell subsets from tissue expression profiles. *Nature methods*. 2015;12:453-457
117. Regev A, Teichmann SA, Lander ES, Amit I, Benoist C, Birney E, et al. The human cell atlas. *Elife*. 2017;6
118. Gentles AJ, Newman AM, Liu CL, Bratman SV, Feng W, Kim D, et al. The prognostic landscape of genes and infiltrating immune cells across human cancers. *Nature medicine*. 2015;21:938-945
119. Jiang J, Pan W, Xu Y, Ni C, Xue D, Chen Z, et al. Tumour-infiltrating immune cell-based subtyping and signature gene analysis in breast cancer based on gene expression profiles. *Journal of Cancer*. 2020;11:1568-1583
120. Pizzamiglio S, Ciniselli CM, Triulzi T, Gargiuli C, De Cecco L, de Azambuja E, et al. Integrated molecular and immune phenotype of her2-positive breast cancer and response to neoadjuvant therapy: A neoaltto exploratory analysis. *Clinical cancer research : an official journal of the American Association for Cancer Research*. 2021;27:6307-6313
121. Bense RD, Sotiriou C, Piccart-Gebhart MJ, Haanen J, van Vugt M, de Vries EGE, et al. Relevance of tumor-infiltrating immune cell composition and functionality for disease outcome in breast cancer. *Journal of the National Cancer Institute*. 2017;109
122. Okano M, Oshi M, Butash AL, Katsuta E, Tachibana K, Saito K, et al. Triple-negative breast cancer with high levels of annexin a1 expression is associated with mast cell infiltration, inflammation, and angiogenesis. *International journal of molecular sciences*. 2019;20
123. Chtanova T, Newton R, Liu SM, Weininger L, Young TR, Silva DG, et al. Identification of t cell-restricted genes, and signatures for different t cell responses, using a comprehensive collection of microarray datasets. *Journal of immunology (Baltimore, Md. : 1950)*. 2005;175:7837-7847
124. Morimoto K, Shirata N, Taketomi Y, Tsuchiya S, Segi-Nishida E, Inazumi T, et al. Prostaglandin e2-ep3 signaling induces inflammatory swelling by mast cell activation. *Journal of immunology (Baltimore, Md. : 1950)*. 2014;192:1130-1137
125. Garcia-Garcia L, Olle L, Martin M, Roca-Ferrer J, Muñoz-Cano R. Adenosine signaling in mast cells and allergic diseases. *International journal of molecular sciences*. 2021;22
126. Eissmann MF, Dijkstra C, Jarnicki A, Phesse T, Brunnberg J, Poh AR, et al. Il-33-mediated mast cell activation promotes gastric cancer through macrophage mobilization. *Nature communications*. 2019;10:2735
127. Aponte-López A, Fuentes-Pananá EM, Cortes-Muñoz D, Muñoz-Cruz S. Mast cell, the neglected member of the tumor microenvironment: Role in breast cancer. *Journal of immunology research*. 2018;2018:2584243
128. Hugo HJ, Lebret S, Tomaskovic-Crook E, Ahmed N, Blick T, Newgreen DF, et al. Contribution of fibroblast and mast cell (afferent) and tumor (efferent) il-6 effects within the tumor microenvironment. *Cancer microenvironment : official journal of the International Cancer Microenvironment Society*. 2012;5:83-93
129. Legere SA, Haidl ID, Légaré JF, Marshall JS. Mast cells in cardiac fibrosis: New insights suggest opportunities for intervention. *Frontiers in immunology*. 2019;10:580
130. Overed-Sayer C, Rapley L, Mustelin T, Clarke DL. Are mast cells instrumental for fibrotic diseases? *Frontiers in pharmacology*. 2013;4:174
131. Qian N, Li X, Wang X, Wu C, Yin L, Zhi X. Tryptase promotes breast cancer angiogenesis through par-2 mediated endothelial progenitor cell activation. *Oncol Lett*. 2018;16:1513-1520

132. Lu J, Chen B, Li S, Sun Q. Tryptase inhibitor apc 366 prevents hepatic fibrosis by inhibiting collagen synthesis induced by tryptase/protease-activated receptor 2 interactions in hepatic stellate cells. *International immunopharmacology*. 2014;20:352-357
133. Mangia A, Malfettone A, Rossi R, Paradiso A, Ranieri G, Simone G, et al. Tissue remodelling in breast cancer: Human mast cell tryptase as an initiator of myofibroblast differentiation. *Histopathology*. 2011;58:1096-1106
134. Marech I, Ammendola M, Sacco R, Capriuolo GS, Patruno R, Rubini R, et al. Serum tryptase, mast cells positive to tryptase and microvascular density evaluation in early breast cancer patients: Possible translational significance. *BMC Cancer*. 2014;14:534
135. Roy A, Libard S, Weishaupt H, Gustavsson I, Uhrbom L, Hesselager G, et al. Mast cell infiltration in human brain metastases modulates the microenvironment and contributes to the metastatic potential. *Frontiers in oncology*. 2017;7:115
136. Yang Z, Zhang B, Li D, Lv M, Huang C, Shen GX, et al. Mast cells mobilize myeloid-derived suppressor cells and treg cells in tumor microenvironment via il-17 pathway in murine hepatocarcinoma model. *PloS one*. 2010;5:e8922
137. Saleem SJ, Martin RK, Morales JK, Sturgill JL, Gibb DR, Graham L, et al. Cutting edge: Mast cells critically augment myeloid-derived suppressor cell activity. *Journal of immunology (Baltimore, Md. : 1950)*. 2012;189:511-515
138. Solito S, Falisi E, Diaz-Montero CM, Doni A, Pinton L, Rosato A, et al. A human promyelocytic-like population is responsible for the immune suppression mediated by myeloid-derived suppressor cells. *Blood*. 2011;118:2254-2265
139. Lin Y, Xu J, Lan H. Tumor-associated macrophages in tumor metastasis: Biological roles and clinical therapeutic applications. *Journal of hematology & oncology*. 2019;12:76
140. Finlay CM, Cunningham KT, Doyle B, Mills KHG. Il-33-stimulated murine mast cells polarize alternatively activated macrophages, which suppress t cells that mediate experimental autoimmune encephalomyelitis. *J Immunol*. 2020;205:1909-1919
141. Liu J, Shen JX, Hu JL, Huang WH, Zhang GJ. Significance of interleukin-33 and its related cytokines in patients with breast cancers. *Frontiers in immunology*. 2014;5:141
142. Cildir G, Yip KH, Pant H, Tergaonkar V, Lopez AF, Tumes DJ. Understanding mast cell heterogeneity at single cell resolution. *Trends Immunol*. 2021;42:523-535
143. Iyengar NM, Zhou XK, Gucalp A, Morris PG, Howe LR, Giri DD, et al. Systemic correlates of white adipose tissue inflammation in early-stage breast cancer. *Clin Cancer Res*. 2016;22:2283-2289
144. Subbaramaiah K, Morris PG, Zhou XK, Morrow M, Du B, Giri D, et al. Increased levels of cox-2 and prostaglandin e2 contribute to elevated aromatase expression in inflamed breast tissue of obese women. *Cancer Discov*. 2012;2:356-365
145. Degnim AC, Hoskin TL, Arshad M, Frost MH, Winham SJ, Brahmbhatt R, et al. Alterations in the immune cell composition in premalignant breast tissue that precede breast cancer development. *Clinical cancer research : an official journal of the American Association for Cancer Research*. 2017
146. Gwak JM, Jang MH, Kim DI, Seo AN, one P-SY. Prognostic value of tumor-associated macrophages according to histologic locations and hormone receptor status in breast cancer. *PloS one*. 2015
147. Boyd NF, Guo H, Martin LJ, Sun L, Stone J, Fishell E, et al. Mammographic density and the risk and detection of breast cancer. *N Engl J Med*. 2007;356:227-236
148. Huo CW, Hill P, Chew G, Neeson PJ, Halse H, Williams ED, et al. High mammographic density in women is associated with protumor inflammation. *Breast Cancer Res*. 2018;20:92
149. Gong Y, Liu YR, Ji P, Hu X, Shao ZM. Impact of molecular subtypes on metastatic breast cancer patients: A seer population-based study. *Sci Rep*. 2017;7:45411

150. Allegrezza MJ, Rutkowski MR, Stephen TL, Svoronos N, Perales-Puchalt A, Nguyen JM, et al. Trametinib drives t-cell-dependent control of kras-mutated tumors by inhibiting pathological myelopoiesis. *Cancer Res*. 2016;76:6253-6265
151. Allegrezza MJ, Rutkowski MR, Stephen TL, Svoronos N, Tesone AJ, Perales-Puchalt A, et al. Il15 agonists overcome the immunosuppressive effects of mek inhibitors. *Cancer Res*. 2016;76:2561-2572
152. Sheen MR, Marotti JD, Allegrezza MJ, Rutkowski M, Conejo-Garcia JR, Fiering S. Constitutively activated pi3k accelerates tumor initiation and modifies histopathology of breast cancer. *Oncogenesis*. 2016;5
153. Buchta Rosean C, Bostic RR, Ferey JCM, Feng TY, Azar FN, Tung KS, et al. Pre-existing commensal dysbiosis is a host-intrinsic regulator of tissue inflammation and tumor cell dissemination in hormone receptor-positive breast cancer. *Cancer Res*. 2019
154. Terrisse S, Derosa L, Iebba V, Ghiringhelli F, Vaz-Luis I, Kroemer G, et al. Intestinal microbiota influences clinical outcome and side effects of early breast cancer treatment. *Cell Death Differ*. 2021;28:2778-2796
155. Pierce BL, Ballard-Barbash R, Bernstein L, Baumgartner RN, Neuhouser ML, Wener MH, et al. Elevated biomarkers of inflammation are associated with reduced survival among breast cancer patients. *J Clin Oncol*. 2009;27:3437-3444
156. Sun X, Glynn DJ, Hodson LJ, Huo C, Britt K, Thompson EW, et al. Ccl2-driven inflammation increases mammary gland stromal density and cancer susceptibility in a transgenic mouse model. *Breast Cancer Research*. 2017;19:4
157. Cimpean AM, Tamma R, Ruggieri S, Nico B, Toma A, Ribatti D. Mast cells in breast cancer angiogenesis. *Crit Rev Oncol Hematol*. 2017;115:23-26
158. Ribatti D, Annese T, Tamma R. Controversial role of mast cells in breast cancer tumor progression and angiogenesis. *Clin Breast Cancer*. 2021;21:486-491
159. Majorini MT, Cancila V, Rigoni A, Botti L, Dugo M, Triulzi T, et al. Infiltrating mast cell-mediated stimulation of estrogen receptor activity in breast cancer cells promotes the luminal phenotype. *Cancer Res*. 2020;80:2311-2324
160. McKee AM, Kirkup BM, Madgwick M, Fowler WJ, Price CA, Dreger SA, et al. Antibiotic-induced disturbances of the gut microbiota result in accelerated breast tumor growth. *iScience*. 2021;24:103012
161. Kitamura T, Qian BZ, Soong D, Cassetta L, Noy R, Sugano G, et al. Ccl2-induced chemokine cascade promotes breast cancer metastasis by enhancing retention of metastasis-associated macrophages. *The Journal of experimental medicine*. 2015;212:1043-1059
162. Liu M, Guo S, Stiles JK. The emerging role of cxcl10 in cancer (review). *Oncol Lett*. 2011;2:583-589
163. Morimoto K, Shirata N, Taketomi Y, Tsuchiya S, Segi-Nishida E, Inazumi T, et al. Prostaglandin e2-ep3 signaling induces inflammatory swelling by mast cell activation. *The Journal of Immunology*. 2014;192:1130-1137
164. Bos PD, Plitas G, Rudra D, Lee SY, Rudensky AY. Transient regulatory t cell ablation deters oncogene-driven breast cancer and enhances radiotherapy. *J Exp Med*. 2013;210:2435-2466
165. Cruse G, Bradding P. Mast cells in airway diseases and interstitial lung disease. *European journal of pharmacology*. 2016;778:125-138
166. Grimbaldeston MA, Chen CC, Piliponsky AM, Tsai M, Tam SY, Galli SJ. Mast cell-deficient w-sash c-kit mutant kit w-sh/w-sh mice as a model for investigating mast cell biology in vivo. *Am J Pathol*. 2005;167:835-848

167. Avagliano A, Fiume G, Ruocco MR, Martucci N, Vecchio E, Insabato L, et al. Influence of fibroblasts on mammary gland development, breast cancer microenvironment remodeling, and cancer cell dissemination. *Cancers*. 2020;12
168. Virakul S, van Steensel L, Dalm VA, Paridaens D, van Hagen PM, Dik WA. Platelet-derived growth factor: A key factor in the pathogenesis of graves' ophthalmopathy and potential target for treatment. *European thyroid journal*. 2014;3:217-226
169. Henke E, Nandigama R, Ergün S. Extracellular matrix in the tumor microenvironment and its impact on cancer therapy. *Frontiers in molecular biosciences*. 2019;6:160
170. Motakis E, Guhl S, Ishizu Y, Itoh M, Kawaji H, de Hoon M, et al. Redefinition of the human mast cell transcriptome by deep-cage sequencing. *Blood*. 2014;123:e58-67
171. Kieffer Y, Hocine HR, Gentric G, Pelon F, Bernard C, Bourachot B, et al. Single-cell analysis reveals fibroblast clusters linked to immunotherapy resistance in cancer. *Cancer Discov*. 2020;10:1330-1351
172. Aponte-López A, Fuentes-Pananá EM, Cortes-Muñoz D, Muñoz-Cruz S. Mast cell, the neglected member of the tumor microenvironment: Role in breast cancer. *Journal of Immunology Research*. 2018;2018:1-11
173. Rajput AB, Turbin DA, Cheang MC, Voduc DK, Leung S, Gelmon KA, et al. Stromal mast cells in invasive breast cancer are a marker of favourable prognosis: A study of 4,444 cases. *Breast Cancer Res Treat*. 2008;107:249-257
174. Dabiri S, Huntsman D, Makretsov N, Cheang M, Gilks B, Bajdik C, et al. The presence of stromal mast cells identifies a subset of invasive breast cancers with a favorable prognosis. *Modern pathology : an official journal of the United States and Canadian Academy of Pathology, Inc*. 2004;17:690-695
175. Dabiri S, Huntsman D, Makretsov N, Cheang M, Gilks B, Badjik C, et al. The presence of stromal mast cells identifies a subset of invasive breast cancers with a favorable prognosis. *Modern Pathology*. 2004;17:690-695
176. Keser SH, Kandemir NO, Ece D, Gecmen GG, Gul AE, Barisik NO, et al. Relationship of mast cell density with lymphangiogenesis and prognostic parameters in breast carcinoma. *Kaohsiung J Med Sci*. 2017;33:171-180
177. Marech I, Ammendola M, Leporini C, Patruno R, Luposella M, Zizzo N, et al. C-kit receptor and tryptase expressing mast cells correlate with angiogenesis in breast cancer patients. *Oncotarget*. 2018;9:7918-7927
178. Ranieri G, Ammendola M, Patruno R, Celano G, Zito FA, Montemurro S, et al. Tryptase-positive mast cells correlate with angiogenesis in early breast cancer patients. *Int J Oncol*. 2009;35:115-120
179. Somasundaram R, Connelly T, Choi R, Choi H, Samarkina A, Li L, et al. Tumor-infiltrating mast cells are associated with resistance to anti-pd-1 therapy. *Nat Commun*. 2021;12:346
180. de Souza Junior DA, Borges AC, Santana AC, Oliver C, Jamur MC. Mast cell proteases 6 and 7 stimulate angiogenesis by inducing endothelial cells to release angiogenic factors. *PLoS One*. 2015;10:e0144081
181. Jansson S, Aaltonen K, Bendahl PO, Falck AK, Karlsson M, Pietras K, et al. The pdgf pathway in breast cancer is linked to tumour aggressiveness, triple-negative subtype and early recurrence. *Breast cancer research and treatment*. 2018;169:231-241
182. Yam C, Murthy RK, Rauch GM, Murray JL, Walters RS, Valero V, et al. A phase ii study of imatinib mesylate and letrozole in patients with hormone receptor-positive metastatic breast cancer expressing c-kit or pdgfr-β. *Investigational new drugs*. 2018;36:1103-1109

183. Modi S, Seidman AD, Dickler M, Moasser M, D'Andrea G, Moynahan ME, et al. A phase ii trial of imatinib mesylate monotherapy in patients with metastatic breast cancer. *Breast cancer research and treatment*. 2005;90:157-163
184. Cristofanilli M, Morandi P, Krishnamurthy S, Reuben JM, Lee BN, Francis D, et al. Imatinib mesylate (gleevec) in advanced breast cancer-expressing c-kit or pdgfr-beta: Clinical activity and biological correlations. *Annals of oncology : official journal of the European Society for Medical Oncology*. 2008;19:1713-1719
185. Conklin MW, Eickhoff JC, Riching KM, Pehlke CA, Eliceiri KW, Provenzano PP, et al. Aligned collagen is a prognostic signature for survival in human breast carcinoma. *Am J Pathol*. 2011;178:1221-1232
186. Rutkowski MR, Allegrezza MJ, Svoronos N, Tesone AJ, Stephen TL, Perales-Puchalt A, et al. Initiation of metastatic breast carcinoma by targeting of the ductal epithelium with adenovirus-cre: A novel transgenic mouse model of breast cancer. *J Vis Exp*. 2014
187. Herschkowitz JI, Simin K, Weigman VJ, Mikaelian I, Usary J, Hu Z, et al. Identification of conserved gene expression features between murine mammary carcinoma models and human breast tumors. *Genome Biol*. 2007;8:R76
188. Pfefferle AD, Herschkowitz JI, Usary J, Harrell JC, Spike BT, Adams JR, et al. Transcriptomic classification of genetically engineered mouse models of breast cancer identifies human subtype counterparts. *Genome Biol*. 2013;14:R125
189. Fang WB, Yao M, Jokar I, Alhakamy N, Berkland C, Chen J, et al. The ccl2 chemokine is a negative regulator of autophagy and necrosis in luminal b breast cancer cells. *Breast Cancer Res Treat*. 2015;150:309-320
190. Sun X, Glynn DJ, Hodson LJ, Huo C, Britt K, Thompson EW, et al. Ccl2-driven inflammation increases mammary gland stromal density and cancer susceptibility in a transgenic mouse model. *Breast cancer research : BCR*. 2017;19:4
191. Vetizou M, Pitt JM, Daillere R, Lepage P, Waldschmitt N, Flament C, et al. Anticancer immunotherapy by ctla-4 blockade relies on the gut microbiota. *Science*. 2015;350:1079-1084
192. Iida N, Dzutsev A, Stewart CA, Smith L, Bouladoux N, Weingarten RA, et al. Commensal bacteria control cancer response to therapy by modulating the tumor microenvironment. *Science*. 2013;342:967-970
193. Wilmanski T, Diener C, Rappaport N, Patwardhan S, Wiedrick J, Lapidus J, et al. Gut microbiome pattern reflects healthy ageing and predicts survival in humans. *Nature metabolism*. 2021;3:274-286
194. Reader J, Holt D, Fulton A. Prostaglandin e2 ep receptors as therapeutic targets in breast cancer. *Cancer metastasis reviews*. 2011;30:449-463
195. Esbona K, Inman D, Saha S, Jeffery J, Schedin P, Wilke L, et al. Cox-2 modulates mammary tumor progression in response to collagen density. *Breast cancer research : BCR*. 2016;18:35
196. Kay LJ, Yeo WW, Peachell PT. Prostaglandin e2 activates ep2 receptors to inhibit human lung mast cell degranulation. *British journal of pharmacology*. 2006;147:707-713
197. Rastogi S, Willmes DM, Nassiri M, Babina M, Worm M. Pge(2) deficiency predisposes to anaphylaxis by causing mast cell hyperresponsiveness. *The Journal of allergy and clinical immunology*. 2020;146:1387-1396.e1313
198. Feng C, Beller EM, Bagga S, Boyce JA. Human mast cells express multiple ep receptors for prostaglandin e2 that differentially modulate activation responses. *Blood*. 2006;107:3243-3250
199. Niu JC, Ma N, Liu W, Wang PJ. Ep1 receptor is involved in prostaglandin e2-induced osteosarcoma growth. *Bosn J Basic Med Sci*. 2019;19:265-273

200. Chen D, Zhao J, Wang H, An N, Zhou Y, Fan J, et al. Oxytocin evokes a pulsatile pge2 release from ileum mucosa and is required for repair of intestinal epithelium after injury. *Sci Rep*. 2015;5:11731
201. Li C, Liu X, Liu Y, Zhang E, Medepalli K, Masuda K, et al. Tuberin regulates prostaglandin receptor-mediated viability, via rheb, in mtorc1-hyperactive cells. *Mol Cancer Res*. 2017;15:1318-1330
202. Albu DI, Wang Z, Huang KC, Wu J, Twine N, Leacu S, et al. Ep4 antagonism by e7046 diminishes myeloid immunosuppression and synergizes with treg-reducing il-2-diphtheria toxin fusion protein in restoring anti-tumor immunity. *Oncoimmunology*. 2017;6:e1338239
203. Noy R, Pollard JW. Tumor-associated macrophages: From mechanisms to therapy. *Immunity*. 2014;41:49-61
204. Tiainen S, Tumelius R, Rilla K, Hämäläinen K, Tammi M, Tammi R, et al. High numbers of macrophages, especially m2-like (cd163-positive), correlate with hyaluronan accumulation and poor outcome in breast cancer. *Histopathology*. 2015;66:873-883
205. Ni C, Yang L, Xu Q, Yuan H, Wang W, Xia W, et al. Cd68- and cd163-positive tumor infiltrating macrophages in non-metastatic breast cancer: A retrospective study and meta-analysis. *Journal of Cancer*. 2019;10:4463-4472
206. Nagarajah S. Exosome secretion - more than simple waste disposal? Implications for physiology, diagnostics and therapeutics. *Journal of circulating biomarkers*. 2016;5:7
207. Singh R, Pochampally R, Watabe K, Lu Z, Mo YY. Exosome-mediated transfer of mir-10b promotes cell invasion in breast cancer. *Molecular cancer*. 2014;13:256
208. Jordan KR, Hall JK, Schedin T, Borakove M, Xian JJ, Dzieciatkowska M, et al. Extracellular vesicles from young women's breast cancer patients drive increased invasion of non-malignant cells via the focal adhesion kinase pathway: A proteomic approach. *Breast cancer research : BCR*. 2020;22:128
209. Fong MY, Zhou W, Liu L, Alontaga AY, Chandra M, Ashby J, et al. Breast-cancer-secreted mir-122 reprograms glucose metabolism in premetastatic niche to promote metastasis. *Nature cell biology*. 2015;17:183-194
210. Rong L, Li R, Li S, Luo R. Immunosuppression of breast cancer cells mediated by transforming growth factor-β in exosomes from cancer cells. *Oncology letters*. 2016;11:500-504
211. Piao YJ, Kim HS, Hwang EH, Woo J, Zhang M, Moon WK. Breast cancer cell-derived exosomes and macrophage polarization are associated with lymph node metastasis. *Oncotarget*. 2018;9:7398-7410
212. Keklikoglou I, Cianciaruso C, Güç E, Squadrito ML, Spring LM, Tazzyman S, et al. Chemotherapy elicits pro-metastatic extracellular vesicles in breast cancer models. *Nature cell biology*. 2019;21:190-202
213. Felipe Lima J, Nofech-Mozes S, Bayani J, Bartlett JM. Emt in breast carcinoma-a review. *Journal of clinical medicine*. 2016;5
214. Lötvall J, Hill AF, Hochberg F, Buzás EI, Di Vizio D, Gardiner C, et al. Minimal experimental requirements for definition of extracellular vesicles and their functions: A position statement from the international society for extracellular vesicles. *Journal of extracellular vesicles*. 2014;3:26913
215. Bonneau C, Eliès A, Kieffer Y, Bourachot B, Ladoire S, Pelon F, et al. A subset of activated fibroblasts is associated with distant relapse in early luminal breast cancer. *Breast cancer research : BCR*. 2020;22:76
216. Riseberg D. Treating elderly patients with hormone receptor-positive advanced breast cancer. *Clinical Medicine Insights. Oncology*. 2015;9:65-73

217. Greten FR, Grivennikov SI. Inflammation and cancer: Triggers, mechanisms, and consequences. *Immunity*. 2019;51:27-41
218. Landskron G, De la Fuente M, Thuwajit P, Thuwajit C, Hermoso MA. Chronic inflammation and cytokines in the tumor microenvironment. *Journal of immunology research*. 2014;2014:149185
219. Zhang S, Yang X, Wang L, Zhang C. Interplay between inflammatory tumor microenvironment and cancer stem cells. *Oncology letters*. 2018;16:679-686
220. Chatterjee V, Gashev AA. Aging-associated shifts in functional status of mast cells located by adult and aged mesenteric lymphatic vessels. *American journal of physiology. Heart and circulatory physiology*. 2012;303:H693-702
221. Pilkington SM, Barron MJ, Watson REB, Griffiths CEM, Bulfone-Paus S. Aged human skin accumulates mast cells with altered functionality that localize to macrophages and vasoactive intestinal peptide-positive nerve fibres. *The British journal of dermatology*. 2019;180:849-858
222. Nelson JF, Felicio LS, Osterburg HH, Finch CE. Altered profiles of estradiol and progesterone associated with prolonged estrous cycles and persistent vaginal cornification in aging c57bl/6j mice. *Biology of reproduction*. 1981;24:784-794
223. McIntosh FM, Maison N, Holtrop G, Young P, Stevens VJ, Ince J, et al. Phylogenetic distribution of genes encoding beta-glucuronidase activity in human colonic bacteria and the impact of diet on faecal glycosidase activities. *Environ Microbiol*. 2012;14:1876-1887
224. Gadelle D, Raibaud P, Sacquet E. Beta-glucuronidase activities of intestinal bacteria determined both in vitro and in vivo in gnotobiotic rats. *Appl Environ Microbiol*. 1985;49:682-685
225. Gloux K, Berteau O, El Oumami H, Beguet F, Leclerc M, Dore J. A metagenomic beta-glucuronidase uncovers a core adaptive function of the human intestinal microbiome. *Proc Natl Acad Sci U S A*. 2011;108 Suppl 1:4539-4546
226. Adlercreutz H, Pulkkinen MO, Hamalainen EK, Korpela JT. Studies on the role of intestinal bacteria in metabolism of synthetic and natural steroid hormones. *J Steroid Biochem*. 1984;20:217-229
227. Friedman GD, Oestreicher N, Chan J, Quesenberry CP, Jr., Udaltsova N, Habel LA. Antibiotics and risk of breast cancer: Up to 9 years of follow-up of 2.1 million women. *Cancer Epidemiol Biomarkers Prev*. 2006;15:2102-2106
228. Velicer CM, Heckbert SR, Lampe JW, Potter JD, Robertson CA, Taplin SH. Antibiotic use in relation to the risk of breast cancer. *JAMA*. 2004;291:827-835
229. Goedert JJ, Jones G, Hua X, Xu X, Yu G, Flores R, et al. Investigation of the association between the fecal microbiota and breast cancer in postmenopausal women: A population-based case-control pilot study. *Journal of the National Cancer Institute*. 2015;107
230. Rao VP, Poutahidis T, Ge Z, Nambiar PR, Boussahmain C, Wang YY, et al. Innate immune inflammatory response against enteric bacteria helicobacter hepaticus induces mammary adenocarcinoma in mice. *Cancer Res*. 2006;66:7395-7400
231. Parida S, Wu S, Siddharth S, Wang G, Muniraj N, Nagalingam A, et al. A procarcinogenic colon microbe promotes breast tumorigenesis and metastatic progression and concomitantly activates notch and beta-catenin axes. *Cancer Discov*. 2021;11:1138-1157
232. Boursi B, Mamtani R, Haynes K, Yang YX. Recurrent antibiotic exposure may promote cancer formation--another step in understanding the role of the human microbiota? *European Journal of Cancer*. 2015;51:2655-2664
233. Chlebowski RT, Chen Z, Anderson GL, Rohan T, Aragaki A, Lane D, et al. Ethnicity and breast cancer: Factors influencing differences in incidence and outcome. *Journal of the National Cancer Institute*. 2005;97:439-448

234. de Andrade OF, Fontelles CC, Rosim MP. Exposure to lard-based high-fat diet during fetal and lactation periods modifies breast cancer susceptibility in adulthood in rats. *The Journal of nutritional Biochemistry*. 2014;25:613-622
235. Martin AM, Weber BL. Genetic and hormonal risk factors in breast cancer. *J Natl Cancer Inst*. 2000;92:1126-1135
236. Rutkowski MR, Stephen TL, Svoronos N, Allegrezza MJ, Tesone AJ, Perales-Puchalt A, et al. Microbially driven tlr5-dependent signaling governs distal malignant progression through tumor-promoting inflammation. *Cancer Cell*. 2015;27:27-40
237. Yu DK, Wu J, Shen ZZ, Shao MZ. Hazard of breast cancer-specific mortality among women with estrogen receptor-positive breast cancer after five years from diagnosis: Implication for extended endocrine therapy. *Journal of Clinical Endocrinology & Metabolism*. 2012;97
238. Zhao Y, Tan YS, Aupperlee MD, Langohr IM, Kirk EL, Troester MA, et al. Pubertal high fat diet: Effects on mammary cancer development. *Breast Cancer Res*. 2013;15:R100
239. Yonekura S, Terrisse S, Alves Costa Silva C, Lafarge A, Iebba V, Ferrere G, et al. Cancer induces a stress ileopathy depending on b-adrenergic receptors and promoting dysbiosis that contribute to carcinogenesis. *Cancer Discov*. 2021
240. Costa A, Kieffer Y, Scholer-Dahirel A, Pelon F, Bourachot B, Cardon M, et al. Fibroblast heterogeneity and immunosuppressive environment in human breast cancer. *Cancer cell*. 2018;33:463-479.e410
241. Tzu-Yu Feng FNA, Claire Buchta Rosean, Mitchell T. McGinty, Audrey M. Putelo, Sree Koli, Natascia Marino, Rana German, Ram Podicheti, Sally A. Dreger, Wesley J. Fowler, Stephanie Greenfield, Stephen D. Robinson, Melanie R. Rutkowski. Reciprocal interactions between the gut microbiome and mammary tissue mast cells promote metastatic dissemination of hr+ breast tumors. *bioRxiv* 2022;https://doi.org/10.1101/2021.12.23.474065
242. Lyon MF, Glenister PH. A new allele sash (wsh) at the w-locus and a spontaneous recessive lethal in mice. *Genetical research*. 1982;39:315-322
243. Berrozpe G, Timokhina I, Yukl S, Tajima Y, Ono M, Zelenetz AD, et al. The w(sh), w(57), and ph kit expression mutations define tissue-specific control elements located between -23 and -154 kb upstream of kit. *Blood*. 1999;94:2658-2666
244. Taketomi Y, Ueno N, Kojima T, Sato H, Murase R, Yamamoto K, et al. Mast cell maturation is driven via a group iii phospholipase a2-prostaglandin d2-dp1 receptor paracrine axis. *Nature immunology*. 2013;14:554-563
245. Harney AS, Arwert EN, Entenberg D, Wang Y, Guo P, Qian B-Z, et al. Real-time imaging reveals local, transient vascular permeability, and tumor cell intravasation stimulated by tie2hi macrophage–derived vegfa. *Cancer discovery*. 2015
246. Marino N, German R, Podicheti R, Rush DB, Rockey P, Huang J, et al. Aberrant epigenetic and transcriptional events associated with breast cancer risk. *bioRxiv*. 2021
247. Bolger AM, Lohse M, Usadel B. Trimmomatic: A flexible trimmer for illumina sequence data. *Bioinformatics (Oxford, England)*. 2014;30:2114-2120
248. Dobin A, Davis CA, Schlesinger F, Drenkow J, Zaleski C, Jha S, et al. Star: Ultrafast universal rna-seq aligner. *Bioinformatics*. 2013;29:15-21
249. Subramanian A, Tamayo P, Mootha VK, Mukherjee S, Ebert BL, Gillette MA, et al. Gene set enrichment analysis: A knowledge-based approach for interpreting genome-wide expression profiles. *Proceedings of the National Academy of Sciences of the United States of America*. 2005;102:15545-15550